

## Chapter 1

### Phases of one-dimensional $SU(N)$ cold atomic Fermi gases — from molecular Luttinger liquids to topological phases

S. Capponi<sup>1</sup>, P. Lecheminant<sup>2</sup>, and K. Totsuka<sup>3</sup>

<sup>1</sup> *Laboratoire de Physique Théorique, CNRS UMR 5152, Université Paul Sabatier, F-31062 Toulouse, France*

<sup>2</sup> *Laboratoire de Physique Théorique et Modélisation, CNRS UMR 8089, Université de Cergy-Pontoise, Site de Saint-Martin, F-95300 Cergy-Pontoise Cedex, France.*

<sup>3</sup> *Yukawa Institute for Theoretical Physics, Kyoto University, Kitashirakawa Oiwake-Cho, Kyoto 606-8502, Japan.*

Alkaline-earth and ytterbium cold atomic gases make it possible to simulate  $SU(N)$ -symmetric fermionic systems in a very controlled fashion. Such a high symmetry is expected to give rise to a variety of novel phenomena ranging from molecular Luttinger liquids to (symmetry-protected) topological phases. We review some of the phases that can be stabilized in a one dimensional lattice. The physics of this multi-component Fermi gas turns out to be much richer and more exotic than in the standard  $SU(2)$  case. For  $N > 2$ , the phase diagram is quite rich already in the case of the single-band model, including a molecular Luttinger liquid (with dominant superfluid instability in the  $N$ -particle channel) for incommensurate fillings, as well as various Mott-insulating phases occurring at commensurate fillings. Particular attention will be paid to the cases with additional orbital degree of freedom (which is accessible experimentally either by taking into account two atomic states or by putting atoms in the  $p$ -band levels). We introduce two microscopic models which are relevant for these cases and discuss their symmetries and strong coupling limits. More intriguing phase diagrams are then presented including, for instance, symmetry protected topological phases characterized by non-trivial edge states.

#### 1. Introduction

Symmetry lies at the heart of physics, since it is a powerful concept to classify conventional phases of matter (with broken symmetries) as well as

phase transitions within the Ginzburg-Landau paradigm. It has also been often used to idealize some physical situation, or simply to make analytical progress feasible. In high-energy physics, continuous symmetries based on the  $SU(N)$  unitary group play fundamental roles in the standard model of particle physics. For instance, an approximate  $SU(N)$  symmetry, where  $N$  is the number of species of quarks, or flavors, underlies the description of hadrons.

In realistic condensed-matter experiments, such a high continuous symmetry is rarely realized [in stark contrast to the  $SU(2)$  case] since it is not guaranteed by any fundamental principles of physics and usually requires some sort of fine-tuning of parameters. There are, however, notable exceptions where relatively simple physical situations enable the system to fine-tune itself and realize a higher symmetry group. For instance, the interplay between spin and orbital degrees of freedom can lead to the realization of an  $SU(4)$  Kondo effect using semiconductor quantum dots [1] or an  $SU(4)$  symmetry in strongly correlated electrons with orbital degeneracy [2]. Another important example is electrons in graphene which have four flavors associated with the low-energy spin and valley degrees of freedom; the fractional quantum Hall effect in graphene is governed by Coulomb interactions which are invariant under rotations of these four flavors and thus an  $SU(4)$  symmetry could also be realized. Though, weak atomic-range valley-dependent interactions might explicitly break this symmetry, it has been shown recently that an  $SO(5)$  symmetry arises in the  $\nu = 0$  quantum Hall regime of graphene [3].

On top of these examples, ultracold fermions loaded into optical lattices might be ideal systems to simulate strongly correlated electrons with a high symmetry, thanks to their great tunability (for reviews on recent development in many-body physics of cold atoms in optical lattices, see, e.g., Refs. [4–6]). In principle, ultracold atomic gases with alkali atoms with hyperfine spin  $F > 1/2$  can explore the physics with  $SO(5)$  and  $SU(3)$  symmetries [7–12]. However, alkaline-earth atoms and related ones, like ytterbium atoms, have a peculiar energy spectrum associated with the two-valence outer electrons which make them the best candidates for experimental realizations of  $SU(N)$  many-body physics [13–15]. The ground state (“ $g$ ” state) is a long-lived singlet state  $^1S_0$  and the spectrum exhibits a metastable triplet excited state (“ $e$ ” state)  $^3P_0$ . The  $g$  and  $e$  states have therefore zero electronic angular momentum, so that the nuclear spin  $I$  is almost decoupled from the electronic spin. From perturbation theory, it is expected that the nuclear-spin-dependent variation of the scattering

lengths is expected to be smaller than  $\sim 10^{-9}$  (respectively  $\sim 10^{-3}$ ) for the  $g$  (respectively  $e$ ) states [14]. As will be reviewed in Sec. 2.1.1, this decoupling of the electronic spin from the nuclear one in two-body collisions paves the way to the experimental realization of fermions with an SU( $N$ ) symmetry where  $N = 2I + 1$  ( $I$  being the nuclear spin) is the number of nuclear states.

The cooling of fermionic isotopes of these atoms below the quantum degeneracy has been achieved for strontium atoms  $^{87}\text{Sr}$  with  $I = 9/2$  [16, 17] (see Ref. [18] for a review) and for ytterbium atoms  $^{171}\text{Yb}$  and  $^{173}\text{Yb}$  respectively with  $I = 1/2$  and  $5/2$  [19, 20] (see Ref. [21] for a review). These atoms enable the experimental exploration of the physics of fermions with an SU( $N$ ) symmetry where  $N$  can be as large as 10. Several experiments have been done recently with these fermionic atoms loaded into optical lattices. An SU(6) Mott insulator has been explored from  $^{173}\text{Yb}$  atoms loaded into a three-dimensional (3D) optical lattice [22]. The experimental proof of the presence of the SU( $N$ ) symmetry has been provided in Refs. [23] and [24] by using  $^{87}\text{Sr}$  and  $^{173}\text{Yb}$ , respectively, in a 2D ( $^{87}\text{Sr}$ ) and 3D ( $^{173}\text{Yb}$ ) optical lattices. Furthermore, the specific form of the interactions between the  $g$  and  $e$  states was determined in these works. Quite recently also, a coherent spin-orbital exchange interaction has been observed using  $^{173}\text{Yb}$  loaded into a 3D optical lattice [25].

All these remarkable experiments give us confidence that there will be many more upcoming breakthroughs in the near future. Motivated by recent experiments on  $^{173}\text{Yb}$  in the one-dimensional (1D) regime [26], in this review, we will be focusing only on the 1D case in the presence of an optical lattice and will not discuss many interesting results in two and three dimensions. Therefore, as a complement to our review, we refer the readers to Ref. [15] for an recent extensive review about the realization of SU( $N$ ) symmetric fermionic gases and its physics in 2D or 3D.

More specifically, we will first discuss the zero-temperature phases that can occur in the SU( $N$ ) alkaline-earth fermions consisting only of atoms in the  $g$ -state loaded in one-dimensional optical lattices. As will be seen in Sec. 2, the low-energy properties of alkaline-earth atoms in the  $g$ -state are described by the single-band SU( $N$ ) Fermi-Hubbard model with the on-site interaction  $U$  that depends on the  $s$ -wave scattering length between two  $g$  atoms. A rich physics emerges already in this simple setting when  $N > 2$ , which is very different from that in the standard SU(2) case. At a filling of one atom per site ( $1/N$ -filling), which best avoids three-body losses, the repulsive SU( $N$ ) Fermi-Hubbard model simplifies, for large repulsive

interaction, to the  $SU(N)$  antiferromagnetic Heisenberg spin chain with the fundamental representation at each site. The latter model, the so-called Sutherland model [27], has been quite extensively studied in the context of quantum magnetism [28–30] and the underlying gapless Mott-insulating phase can be directly investigated in ongoing experiments with 1D ytterbium cold fermions. While low temperatures are difficult to achieve for fermionic gases, there is some advantage at working with several species (large  $N$ ) since some short-range features might be observed at accessible temperatures due to some entropic effect, as was computed numerically in one [31, 32] and two dimensions [33]. The Mott insulating phase at  $1/N$ -filling has been already realized experimentally with  $^{173}\text{Yb}$  ( $N = 6$ ) loaded in three-dimensional optical lattices [22].

In sharp contrast to the case of  $SU(2)$ , the  $SU(N)$  Fermi-Hubbard model displays *fully gapped* Mott-insulating phases. However, these phases exhibits bond-ordering and spontaneously break translation symmetry. Therefore, the realization of some featureless gapped exotic phases of matter requires going beyond the single-band model. In this respect, it would be interesting to consider various two-band models which, on top of the  $SU(N)$ , have an additional ‘orbital’ degree of freedom. The origin of the two orbitals could be either the two atomic states  $g$  and  $e$  ( $e$ - $g$  model), or the  $p_x$  and  $p_y$  orbital states ( $p$ -band model) of the harmonic trap.

In the two-orbital cases, the interplay between the orbital and  $SU(N)$  nuclear spin degrees of freedom will be shown to give rise to several interesting phases, including symmetry-protected topological (SPT) phases [34, 35]. The latter refer to non-degenerate fully gapped phases which do not break any symmetry and defy the characterization with local order parameters. Since any gapful phases in one dimension have short-range entanglement [36] and can be reduced to a trivial product state by a series of local unitary transformations, the presence of a symmetry (which restricts the type of possible local unitary) is necessary to protect the properties of that 1D topological phase, in particular the existence of non-trivial edge states [35, 36].

The outline of our review is as follows. In Sec. 2, we will provide a minimal introduction to  $SU(N)$  symmetry in alkaline-earth systems and then describe the known results for the single-band Hubbard model in 1D. We consider both the cases with commensurate fillings, where various Mott phases occur, and those with incommensurate fillings where low-energy properties can be described using the Luttinger-liquid theory [37, 38].

In Sec. 3, we will move on to the case of two-‘orbital’ fermions. After in-

roducing two relevant microscopic models ( $e$ - $g$  model and  $p$ -band model), which are directly relevant to experiments [23, 24], we will discuss their strong-coupling limits, i.e., the  $SU(N)$  spin chains in various representations, for which several results are known or conjectured. In particular, we will sketch the known classification of the so-called  $SU(N)$  SPT phases allowing us to understand the formation of topological states in our  $SU(N)$  fermion system as generalizations of the well-known Haldane phases in spin systems. Finally, we will present some typical numerical results to provide complete phase diagrams as well as clear signatures of the SPT phases through the direct measurements of nontrivial edge states. Conclusions will be given in Sec. 4.

## 2. Single-band Fermi-Hubbard model

### 2.1. Definition of the model

#### 2.1.1. $SU(N)$ symmetry in cold-atom systems

Like the  $SU(3)$ -symmetry in the quantum chromodynamics for the strong interactions, the existence of the multiplet of  $N$  particles and the  $SU(N)$ -symmetry that governs the dynamics of these particles have nothing to do with spins and are built in the theory from the outset in high-energy physics. In condensed-matter physics, on the other hand, such internal symmetries independent of spin may originate from, e.g., sublattice symmetry and normally fine-tuning is necessary to realize high symmetries as discussed in the introduction. In order to understand how  $SU(N)$  symmetry arises among the multiplet which originates from the angular momentum *without any fine-tuning*, consider two spin- $F$  fermionic atoms interacting with a contact interaction. Due to the rotational invariance, the two-body interaction depends *only* on the total spin  $F$ . Among all the possible values  $f = 0, 1, 2, \dots, 2F$ , only the  $(2F + 1)/2$  antisymmetric combinations  $f = 0, 2, \dots, 2F - 1$  ( $F$  is assumed to be half-odd integer) are allowed by fermionic statistics. Therefore, the most general form of rotationally [i.e.,  $SU(2)$ ] invariant interaction between two spin- $F$  objects may be written as [39]

$$V_{F,F}(\mathbf{r}, \mathbf{r}') = \delta(\mathbf{r} - \mathbf{r}') \sum_{f=0,2,\dots}^{2F-1} g_f P_f, \quad (1)$$

where  $P_f$  denotes the projection operator onto the total spin- $f$  sector and the coupling constants  $g_f$  are determined by the corresponding  $s$ -wave scat-

tering lengths  $a_f$  as ( $M$  being the mass of the atoms in question)

$$g_f = \frac{4\pi\hbar^2}{M} a_f . \quad (2)$$

In the ground state  $^1S_0$  of  $^{173}\text{Yb}$ , for instance,  $I = F = 5/2$  and we have, in principle, three coupling constants  $g_0$ ,  $g_2$ , and  $g_4$ .

In the second-quantized formulation, the above projection operators can be simply given as

$$\hat{P}_f = \sum_{m=-f}^f \hat{P}_{f,m} \equiv \sum_{m=-f}^f A_{f,m}^\dagger(\mathbf{r}) A_{f,m}(\mathbf{r}), \quad (3)$$

with the ‘pairing operators’ defined by [39]

$$\begin{aligned} A_{f,m}^\dagger(\mathbf{r}) &\equiv \sum_{\alpha,\beta=-F}^F \langle F, \alpha; F, \beta | f, m \rangle c_\alpha^\dagger(\mathbf{r}) c_\beta^\dagger(\mathbf{r}) \\ A_{f,m}(\mathbf{r}) &\equiv \sum_{\alpha,\beta=-F}^F \langle f, m | F, \alpha; F, \beta \rangle c_\beta(\mathbf{r}) c_\alpha(\mathbf{r}) . \end{aligned} \quad (4)$$

Using the definition of the pairing operators [i.e., creation/annihilation operators for a pair with a particular value of the hyperfine spin ( $F, M$ )], the interaction may be rewritten as [39, 40]

$$\begin{aligned} &\sum_{f=0,2,\dots}^{2F-1} g_f \hat{P}_f = \\ &\sum_{f=0,2,\dots}^{2F-1} g_f \sum_{m=-f}^f \sum_{\alpha_1,\beta_1=-F}^F \sum_{\alpha_2,\beta_2=-F}^F \langle F, \alpha_1; F, \beta_1 | f, m \rangle \langle f, m | F, \alpha_2; F, \beta_2 \rangle \\ &\quad \times c_{\alpha_1}^\dagger(\mathbf{r}) c_{\beta_1}^\dagger(\mathbf{r}) c_{\beta_2}(\mathbf{r}) c_{\alpha_2}(\mathbf{r}) . \end{aligned} \quad (5)$$

When the coupling constants (or, the scattering lengths) do not depend on

$f$  (i.e.,  $g_f = g$ ), the above simplifies to the following expression

$$\begin{aligned}
g \sum_{f=0,2,\dots}^{2F-1} \hat{P}_f &= g \sum_{f=0,2,\dots}^{2F-1} \sum_{m=-f}^f A_{f,m}^\dagger(\mathbf{r}) A_{f,m}(\mathbf{r}) \\
&= g \sum_{\alpha_1, \beta_1 = -F}^F \sum_{\alpha_2, \beta_2 = -F}^F \\
&\times \underbrace{\left\{ \sum_{f=0,2,\dots}^{2F-1} \sum_{m=-f}^f \langle F, \alpha_1; F, \beta_1 | f, m \rangle \langle f, m | F, \alpha_2; F, \beta_2 \rangle \right\}}_{=\delta_{\alpha_1, \alpha_2} \delta_{\beta_1, \beta_2}} \\
&\times c_{\alpha_1}^\dagger(\mathbf{r}) c_{\beta_1}^\dagger(\mathbf{r}) c_{\beta_2}(\mathbf{r}) c_{\alpha_2}(\mathbf{r}) \\
&= g \sum_{\alpha, \beta = -F}^F c_\alpha^\dagger(\mathbf{r}) c_\beta^\dagger(\mathbf{r}) c_\beta(\mathbf{r}) c_\alpha(\mathbf{r}) = g : n(\mathbf{r}) n(\mathbf{r}) : ,
\end{aligned} \tag{6}$$

where  $n(\mathbf{r}) = \sum_\alpha c_\alpha^\dagger(\mathbf{r}) c_\alpha(\mathbf{r})$  is the density operator which is invariant under  $SU(N)$  symmetry with  $N = 2F + 1$ . Therefore, when  $g_f$  do not depend on  $f$ , i.e., when the fine-tuning of the scattering lengths  $a_0 = a_2 = \dots = a_{2F-1}$  occurs, the original  $SU(2)$ -symmetry of the atom-atom interaction gets enlarged to  $SU(N)$  with  $N = 2F + 1$ <sup>a</sup>.

A natural question to ask then is when and in which system this fine tuning happens? The collision among neutral atoms are mainly governed by short-range van der Waals interaction that depends only on the electronic wave functions of the two colliding atoms. The nuclear-spin degrees of freedom can participate in the collisional processes only through the hyperfine interaction. In alkali cold atoms with hyperfine  $F = 3/2$  spin, an enlarged continuous  $Sp(4) \sim SO(5)$  symmetry arises without fine-tuning<sup>b</sup>, i.e., with two independent scattering lengths  $a_0, a_2$ . [7, 10] The physical properties of this model in one dimension have been extensively

<sup>a</sup>Even when the fine-tuning is incomplete, we may have other extended symmetries. See Ref. [41] for the discussion of the phase structure of these cases.

<sup>b</sup>In order to understand this, we first identify the two quartets  $\mathbf{4}$  of the two colliding  $F = 3/2$  atoms with two 4-dimensional spinor representations ( $\mathbf{4}_{SO(5)}$ ) of  $SO(5)$ . Then, the states of the two atoms may be decomposed, in terms of  $SO(5)$ , as

$$(F = 3/2) \otimes (F = 3/2) \Leftrightarrow \mathbf{4}_{SO(5)} \otimes \mathbf{4}_{SO(5)} \simeq \mathbf{1}_{SO(5)} \oplus \mathbf{5}_{SO(5)} \oplus \mathbf{10}_{SO(5)} ,$$

among which the last one (symmetric  $\mathbf{10}_{SO(5)}$ ) must be discarded by the Fermi statistics (for the  $s$ -wave scattering). The remaining two ( $\mathbf{1}_{SO(5)}$  and  $\mathbf{5}_{SO(5)}$ ) may be identified with the singlet ( $f = 0$ ) and the quintet ( $f = 2$ ) of  $SU(2)$  [see Eq. (1)]. Therefore, the scattering of two fermionic  $F = 3/2$  atoms can be rephrased in terms of  $SO(5)$ .

investigated over the years by means of various analytical and numerical approaches [9, 41–52]. The fine-tuning of the scattering lengths  $a_0 = a_2$  to achieve a higher SU(4) symmetry is not easy to realize experimentally with these alkali atoms. In contrast, if the hyperfine interaction is quenched for some reasons, the scattering processes are independent of the nuclear spin  $f$ :  $g_0 = g_2 = \dots = g_{2f-1}$ . As the total electron angular momentum vanishes (and so does the hyperfine interaction) in the ground state  $^1S_0$  of alkaline-earth and Yb atoms, these atoms are the best candidates of systems that realize SU( $N$ ) symmetry without any fine-tuning [13–15].

### 2.1.2. SU( $N$ ) Hubbard model

In order to derive a lattice Hamiltonian that describes low-energy physics of an  $N$ -component Fermi gas with the SU( $N$ ) symmetry moving on 1D optical lattices, let us begin with the single-particle problem:

$$\mathcal{H}_0 = \left\{ -\frac{\hbar^2}{2M} \partial_z^2 + V_{\text{per}}(z) \right\} \equiv \mathcal{H}_{//}(z), \quad (7)$$

where  $V_{\text{per}}(z)$  is a periodic potential that introduces a lattice structure along the chain (i.e.  $z$ ) direction. Also we have assumed that the confining potential in the other directions (i.e.,  $x$  and  $y$ ) is so strong that we are able to neglect the motion in the  $xy$ -direction and set  $x = y = 0$ . If the chain is translationally invariant in the  $z$ -direction, the single-particle state is given by the Bloch function  $\varphi_{k_z}^{(n)}(z)$  ( $n$  being the band index) satisfying:

$$\mathcal{H}_{//}(z) \varphi_{k_z}^{(n)}(z) = \varepsilon^{(n)}(k_z) \varphi_{k_z}^{(n)}(z). \quad (8)$$

To derive an effective Hubbard-like Hamiltonian [53, 54], it is convenient to move from the Bloch function  $\varphi_{k_z}^{(n)}(z)$  to the Wannier function defined by

$$w_R^{(n)}(z) \equiv \frac{1}{\sqrt{N_{\text{cell}}}} \sum_{k_z} e^{-ik_z R} \varphi_{k_z}^{(n)}(z) \quad (9)$$

(the index  $R$  labels the center of the Wannier function and  $N_{\text{cell}}$  is the number of unit cells in the  $z$ -direction) and introduce the fermion operators in the Wannier basis  $\{c_{\alpha,R}^{(n)}\}$ :

$$c_{\alpha}(z) = \sum_R \sum_n w_R^{(n)}(z) c_{\alpha,R}^{(n)}, \quad c_{\alpha}^{\dagger}(z) = \sum_R \sum_n w_R^{(n)*}(z) c_{\alpha,R}^{(n)\dagger} \quad (10)$$

$(\alpha = 1, \dots, N).$



We use these operators to rewrite the  $SU(N)$ -invariant two-body interaction (6) as

$$\begin{aligned} & g \sum_{\alpha, \beta = -F}^F c_{\alpha}^{\dagger}(z) c_{\beta}^{\dagger}(z) c_{\beta}(z) c_{\alpha}(z) \\ &= \frac{1}{2} \sum_{\alpha, \beta = 1}^N \sum_{\{R_i, n_i\}} V_{(R_1, R_2; R_3, R_4)}^{(n_1, n_2; n_3, n_4)} c_{\alpha, R_1}^{(n_1)\dagger} c_{\beta, R_2}^{(n_2)\dagger} c_{\beta, R_3}^{(n_3)} c_{\alpha, R_4}^{(n_4)}, \end{aligned} \quad (11)$$

where

$$V_{(\mathbf{R}_1, \mathbf{R}_2; \mathbf{R}_3, \mathbf{R}_4)}^{(n_1, n_2; n_3, n_4)} \equiv g \int d\mathbf{r} w_{\mathbf{R}_1}^{(n_1)*}(\mathbf{r}) w_{\mathbf{R}_2}^{(n_2)*}(\mathbf{r}) w_{\mathbf{R}_3}^{(n_3)}(\mathbf{r}) w_{\mathbf{R}_4}^{(n_4)}(\mathbf{r}) \quad (12)$$

and we have re-labelled  $\alpha = -F, \dots, F \Rightarrow \alpha = 1, \dots, N$  ( $N = 2F + 1$ ). As usual [53, 54], we keep only the most relevant band (denoted by  $n_1 = n_2 = n_3 = n_4 = n_0$ ) and the on-site term  $\mathbf{R}_1 = \mathbf{R}_2 = \mathbf{R}_3 = \mathbf{R}_4 = \mathbf{R}_i$  to obtain the so-called Hubbard interaction:

$$\begin{aligned} & \frac{1}{2} V_{(\mathbf{R}_i, \mathbf{R}_i; \mathbf{R}_i, \mathbf{R}_i)}^{(n_0, n_0; n_0, n_0)} \sum_{\alpha, \beta = 1}^N \sum_i c_{\alpha, i}^{\dagger} c_{\beta, i}^{\dagger} c_{\beta, i} c_{\alpha, i} \\ & \equiv \frac{1}{2} U \sum_{\alpha, \beta = 1}^N \sum_i c_{\alpha, i}^{\dagger} c_{\beta, i}^{\dagger} c_{\beta, i} c_{\alpha, i} = \frac{1}{2} U \sum_i n_i (n_i - 1). \end{aligned} \quad (13)$$

In the above, we have introduced a short-hand notations

$$c_{\alpha, i} \equiv c_{\alpha, \mathbf{R}_i}, \quad \sum_i \equiv \sum_{\mathbf{R}_i}, \quad (14)$$

and  $n_i = \sum_{\alpha} c_{\alpha, i}^{\dagger} c_{\alpha, i}$  is the density operator on site  $i$ .

When second-quantized, the single-particle part reads as

$$\begin{aligned} & \sum_{\alpha=1}^N \int dz c_{\alpha}^{\dagger}(z) \mathcal{H}_{//}(z) c_{\alpha}(z) \\ &= \sum_{\alpha=1}^N \sum_{\{R_i, n_i\}} \left\{ \int dz w_{R_1}^{(n_1)*}(z) \mathcal{H}_{//}(z) w_{R_2}^{(n_2)}(z) \right\} c_{\alpha, R_1}^{(n_1)\dagger} c_{\alpha, R_2}^{(n_2)}. \end{aligned} \quad (15)$$

This may be further rewritten using the hopping amplitudes:

$$\begin{aligned}
& \int dz w_{R_1}^{(n_1)*}(z) \mathcal{H}_{//}(z) w_{R_2}^{(n_2)}(z) \\
&= \frac{1}{N_{\text{cell}}} \sum_{k_z} \sum_{k'_z} e^{ik_z R_1} e^{-ik'_z R_2} \left\{ \int dz \varphi_{k_z}^{(n_1)*}(z) \mathcal{H}_{//}(z) \varphi_{k'_z}^{(n_2)}(z) \right\} \\
&= \delta_{n_1 n_2} \left\{ \frac{1}{N_{\text{cell}}} \sum_{k_z} \epsilon_{k_z}^{(n_1)} e^{ik_z (R_1 - R_2)} \right\} \equiv -\delta_{n_1 n_2} t^{(n_1)}(R_1 - R_2),
\end{aligned} \tag{16}$$

and we finally obtain the kinetic term

$$-\sum_{\alpha=1}^N \sum_{n \in \text{bands}} \sum_{R_1, R_2} t^{(n)}(R_1 - R_2) c_{\alpha, R_1}^{(n)\dagger} c_{\alpha, R_2}^{(n)}. \tag{17}$$

Retaining only the terms with  $n = n_0$  and  $|R_1 - R_2| = 1$  in the above and combining it with Eq. (13), we arrive at the  $SU(N)$  generalization of the famous Fermi-Hubbard model:

$$\mathcal{H}_{SU(N)} = -t \sum_i \sum_{\alpha=1}^N \left( c_{\alpha, i}^\dagger c_{\alpha, i+1} + \text{H.c.} \right) + \frac{U}{2} \sum_i n_i (n_i - 1). \tag{18}$$

The model (18) is invariant under the global  $U(1)$  symmetry:  $c_{\alpha, i} \mapsto e^{i\theta} c_{\alpha, i}$ , which implies the conservation of the total number of atoms. In the rest of this chapter, we frequently use the terminology ‘charge’ to denote the degree of freedom associated with this symmetry, although we are dealing with neutral atoms *without* electric charge. All the parameters in the model (18) are independent from the nuclear-spin states ( $\alpha = 1, \dots, N$ ) and an extended  $SU(N)$  symmetry arises:  $c_{\alpha, i} \mapsto \sum_{\beta} U_{\alpha\beta} c_{\beta, i}$ ,  $U$  being an  $SU(N)$  matrix. The actual continuous symmetry group of the Hamiltonian (18) is then  $U(N) = U(1) \times SU(N)$  but the model  $\mathcal{H}_{SU(N)}$  is often called the  $SU(N)$  Fermi-Hubbard model to put the emphasis on its non-trivial  $SU(N)$  hyperfine-spin rotational invariance.

## 2.2. Sutherland model and its low-energy physics

The model (18) describes alkaline-earth atoms in the  $g$  state (i.e., ground state  $^1S_0$ ) loaded into the lowest band of the optical lattice. The interaction parameter  $U$  is directly related to the  $s$ -wave scattering length associated with the collision between two atoms in the  $g$  state [see Eqs. (12) and (13)]. When  $N = 2$ , the model (18) is the famous  $SU(2)$  Hubbard chain which is exactly solvable by means of the Bethe ansatz [55]. The physical properties

of the model have been discussed in great detail over the years and are reviewed in the book [56]. However, for  $N > 2$ , the Hamiltonian (18) is not integrable for arbitrary  $U$  and filling  $n$ . Although it is possible to formally generalize the Lieb-Wu Bethe ansatz equation [55] to fermions with internal  $SU(N)$  symmetry, it is believed that it describes a non-local variant of the  $SU(N)$  Hubbard model [57]. In the absence of a lattice, the model is again integrable and its properties have been described in a recent review [58].

The situation becomes much simpler in the limit of large repulsive  $U$  for a filling  $n = 1/N$  with one atom per site which best avoids three-body losses. In that case, the model (18) reduces to the  $SU(N)$  Heisenberg antiferromagnetic spin chain with the  $SU(N)$  fundamental representation (represented by the Young diagram  $\square$ ; for a pedagogical explanation of the representation theory of  $SU(N)$  and the Young diagrams, see, e.g., Ref. [59]) on each site (*Sutherland model* [27]):

$$\mathcal{H} = J \sum_i P_{i,i+1}, \quad (19)$$

where  $J = 2t^2/U$  is the antiferromagnetic spin exchange and  $P_{i,i+1}$  is the operator which permutes the  $SU(N)$  hyperfine states on the sites  $i$  and  $i+1$ . For the fundamental representation ( $\square$ ),  $P_{i,i+1}$  is compactly written, in terms of the  $SU(N)$  generators that are normalized to be  $\text{Tr } \mathcal{S}_i^A \mathcal{S}_i^B = \delta^{AB}$ , as [SU( $N$ ) generalization of the *Dirac identity*]

$$P_{i,i+1} = \frac{1}{N} + \sum_{A=1}^{N^2-1} \mathcal{S}_i^A \mathcal{S}_{i+1}^A. \quad (20)$$

It is known that the ‘spin’ model (19) well describes the low-energy sector of the original Hubbard model (18) for  $U/t \gtrsim 12$  [60].

In contrast to the original fermionic model (18), the large- $U$  effective Hamiltonian (19) can be solved exactly by the Bethe ansatz [27]. The low-energy spectrum is gapless with  $N - 1$  relativistic modes with the same velocity  $v_s = 2\pi J/N$ . The critical theory has been identified by Affleck [28, 29] as described by the level-1  $SU(N)$  Wess-Zumino-Witten [ $SU(N)_1$  WZW] conformal field theory [61–63]. This conformal field theory (CFT) has a central charge  $c = N - 1$  and the low-temperature specific heat (per volume) scales as: [64, 65]  $C(T) \simeq k_B^2 N(N - 1)T/(6\hbar J)$  (with  $k_B$  denoting the Boltzmann constant). The latter result has been confirmed by the thermodynamic Bethe ansatz [66] (see Ref. [30] for the determination of  $c$  by finite-size corrections) and quantum Monte-Carlo calculations (QMC) [32, 67]. The gapless behavior in the  $SU(N)$  Mott-insulating phase with

one atom per site manifests itself in the spin-spin correlation functions which exhibit a universal power-law decay in the long-distance limit at zero temperature [28, 29]:

$$\langle \mathcal{S}^A(\tau, x) \mathcal{S}^B(0, 0) \rangle \sim \delta^{AB} (-1)^{x/a_0} \frac{\log^{2/N^2} (x^2 + v_s^2 \tau^2)}{(x^2 + v_s^2 \tau^2)^{1-1/N}}, \quad (21)$$

where  $\tau$  is the Euclidean time,  $a_0$  is the lattice spacing, and  $A, B = 1, \dots, N^2 - 1$  are the components of the  $SU(N)$  spin operator. The logarithm corrections in Eq. (21) stems from the existence of a marginal operator in the low-energy effective field theory describing the model (19) [68, 69]. The thermodynamics properties of the Sutherland model (19) have been investigated numerically in Refs. [31, 32]. In particular, it has been shown that characteristic short-range correlations develop at low temperature as a precursor of the ground state algebraic correlations (21). The first sign of short-range order appears at an entropy per particle which increases with  $N$ , leading to observable qualitative effects in ongoing ultracold atom experiments with alkaline-earth fermions.

### 2.3. Phase structure

Since the  $SU(N)$  Fermi-Hubbard model (18) with  $N > 2$  is, in general, not exactly solvable, one has to resort to approximate but powerful techniques available in one dimension to map out its zero-temperature phase diagram: field theory, strong-coupling, and numerical approaches. In this section, we sketch the phase diagram of the model (18) for both incommensurate (Sec. 2.3.1) and commensurate fillings (Secs. 2.3.2–2.3.4). The main results of Sec. 2.3 are summarized in Table 1.

#### 2.3.1. Incommensurate fillings

We first consider the  $SU(N)$  Fermi-Hubbard model (18) for incommensurate fillings. In this respect, there is no umklapp processes which opens a gap for the charge degrees of freedom [or, the  $U(1)$  sector corresponding to the continuous symmetry of Eq. (18)]. A metallic state is then formed whose nature strongly depends on the sign of the coupling constant  $U$ .

When  $U > 0$ , all modes are gapless and a metallic Luttinger-liquid phase emerges [37, 38]. The hallmark of this  $N$ -component Luttinger liquid phase is the  $2k_F$  oscillations in the density-density and the spin-spin correlation functions decaying with non-universal power-law exponents [29, 60, 70]. For

instance, the leading asymptotics of  $SU(N)$  spin-spin correlation functions (21) reads now in the metallic phase as:

$$\langle \mathcal{S}^A(\tau, x) \mathcal{S}^B(0, 0) \rangle \sim \delta^{AB} \frac{\cos(2k_F x)}{(x^2 + v_c^2 \tau^2)^{K/N} (x^2 + v_s^2 \tau^2)^{1-1/N}}, \quad (22)$$

where  $K$  and  $v_c$  are respectively the Luttinger parameter and the characteristic velocity of the charge excitation which depend on the interaction and density [37, 38]. In particular,  $K$  determines the singularity in the momentum distribution around the Fermi point  $k_F$ :  $n(k) \sim n(k_F) + \text{const. sign}(k - k_F) |k - k_F|^\alpha$  with  $\alpha = (1 - K)^2 / (2NK)$  [70]. This power-law singularity at the Fermi level is inherent in Luttinger liquids unlike in the standard Fermi liquid [37, 38]. Similarly, the single-particle density of states also has an anomalous power-law behavior for any finite value of  $N$ :  $\rho(\omega) \sim |\omega|^\alpha$ .

On the other hand, the physics is very different in the attractive case ( $U < 0$ ); there is a spin gap for the  $SU(N)$  degrees of freedom and the only remaining gapless mode is the charge one. The metallic phase is then characterized by a CFT with the central charge  $c = 1$ , i.e., a single bosonic gapless mode. The resulting spin-gap phase is the Luther-Emery phase [37, 38, 71], which turns out to be very exotic when  $N > 2$  at sufficiently low density [46, 72]. In the  $N = 2$  case, the Luther-Emery phase describes the competition between a charge-density wave (CDW) instability and a superconducting one [37, 38]. For the attractive  $SU(2)$  Hubbard model, the leading instability is the superconducting one. When  $N > 2$ , on the other hand, the  $SU(N)$  symmetry plays an important role in one dimension by preventing any pairing between fermions: there is no way to form an  $SU(N)$  singlet with only *two* fermions. When  $N > 2$ , the usual pairing instability is then completely suppressed with exponential-decaying correlation functions in stark contrast to the  $N = 2$  case. The only possible gapless fluctuation corresponding to the superfluid instability is a molecular one where  $N$  fermions form  $SU(N)$  singlet (an analog of baryons in high-energy physics):  $\mathcal{M}_i = c_{1,i}^\dagger c_{2,i}^\dagger \dots c_{N,i}^\dagger$ , i.e., *trionic* and *quartetting* superfluid instabilities when  $N = 3$  and  $N = 4$ , respectively. The Luther-Emery phase of the model (18) with  $U < 0$  is then governed by the competition between the instability toward this molecular superfluid (MS) and the one toward CDW. The leading instability of this region corresponds to the order parameter that exhibits the slowest power-law decaying correlations at zero temperature. The equal-time correlation functions of these order

parameters have been determined by means of bosonization [9, 45, 72]:

$$\begin{aligned} \langle n_i n_{i+x} \rangle &\sim \cos(2k_F x) x^{-2K/N} \\ \langle \mathcal{M}_i \mathcal{M}_{i+x}^\dagger \rangle &\sim \begin{cases} x^{-N/2K} & \text{for } N \text{ even} \\ \sin(k_F x) x^{-(K+N^2/K)/2N} & \text{for } N \text{ odd.} \end{cases} \end{aligned} \quad (23)$$

Either CDW or MS instability thus dominates depending on the value of the Luttinger parameter  $K$ ; dominant MS instability requires  $K > N/\sqrt{3}$  (respectively  $K > N/2$ ) when  $N$  is odd (respectively even). At issue is the value of the the Luttinger parameter  $K$ . Its expression as a function of  $U$  and the density  $n$  has been numerically determined in Ref. [72] and is reproduced in Fig. 1 for  $N = 3$ . In the low-density regime, the MS phase, characterized by a bound state made of  $N$  fermions, exists for a wide range of attractive  $U$  (the shaded region in Fig. 1). The latter phase might also be viewed as a ‘molecular’ Luttinger liquid with molecules of  $N$  atoms and the confinement of Cooper pairs. In the high-density regime (the lower part of Fig. 1), the dominant instability for  $U < 0$  is a standard CDW.

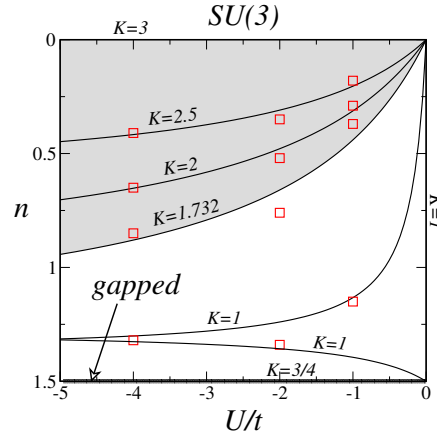


Fig. 1. (Color online) The Luttinger parameter  $K$  as function of  $U$  and the density  $n$  for the  $SU(3)$  Fermi-Hubbard model with attractive interaction ( $U < 0$ ). Grey region marks the onset of the MS phase. The  $n = 3/2$  line corresponds to the half-filled case where a fully gapped Mott-insulating phase occurs as discussed in Sec. 2.3.3. From Ref. [72].

### 2.3.2. Mott transition

For commensurate fillings, umklapp processes might become strongly relevant perturbations and open a spectral gap for the charge degrees of freedom. The nature of the resulting Mott-insulating phase depends crucially on the filling  $n$  [73]. In the case of one atom per site (i.e.,  $n = 1/N$  filling), the Mott-insulating phase is gapless in the large  $U$  limit and is described by the Sutherland model (19) and its physical properties were discussed already in Sec. 2.2. In the  $N = 2$  case, it is well-known from the exact Bethe-ansatz solution that there is no (finite- $U$ ) Mott transition and a charge gap opens as soon as  $U > 0$  [55]. A gapless Mott-insulating phase with central charge  $c = 1$ , described by the  $SU(2)$  Heisenberg spin model, emerges thus for  $U > 0$ .

Again, the situation might be very different when  $N > 2$  as advocated in Ref. [70]. In the weak-coupling ( $U \ll t$ ) limit, the umklapp operator appearing in the low-energy effective Hamiltonian has the scaling dimension  $\Delta = NK$  [70], which becomes a relevant perturbation when the Luttinger parameter is sufficiently small:  $K < 2/N$ . When  $N = 2$ , this is always the case since  $K < 1$  as soon as a repulsive interaction is switched on [37, 38]. In stark contrast, the umklapp operator is always *irrelevant* when  $N > 2$  for sufficiently weak  $U$  and a Mott-transition at finite  $U$  is thus expected toward the large- $U$  gapless  $SU(N)$  phase with a charge gap described by the  $SU(N)$  Sutherland model (19) [70]. This problem has been investigated numerically by various different techniques [60, 70, 74, 75]. The determination of the position of the Mott-transition turned out to be a difficult numerical problem due to the smallness of the charge gap. The QMC simulations of Ref. [70] found a critical value  $U_c \simeq 2.2t$  for  $N = 3$  and  $U_c \simeq 2.8t$  for  $N = 4$ . Density matrix renormalization group (DMRG) [76] calculations done in Ref. [60] reported smaller values:  $U_c \simeq 1.1t$  for  $N = 3$  and  $U_c \simeq 2.1t$  for  $N = 4$  while those in Ref. [75] concluded the absence of a Mott-transition for  $N > 2$ :  $U_c = 0$ . The physical properties of the metallic phase when  $U < U_c$  are described by the multi-component Luttinger liquid with  $N$  gapless channels (see Sec. 2.3.1). Above the critical value  $U > U_c$ , there is a charge gap and we are left with  $N - 1$  gapless spin modes whose physical properties are governed by the Sutherland model (19). The Mott-transition is argued [70] to be of the Berezinskii-Kosterlitz-Thouless universality class [77, 78].

### 2.3.3. Half-filled case

We now consider the half-filled case with  $k_F = \pi/2a_0$  ( $N/2$  fermions per site;  $n = 1/2$ ). For  $N = 2$ , it corresponds to the situation where we have one atom per site and reduces to the case considered already in Sec. 2.2; the physics for  $U > 0$  is governed by the Heisenberg model with a gapless  $c = 1$  behavior (corresponding to the level-1  $SU(2)$  WZW CFT). On the attractive side  $U < 0$ , we can apply a transformation (*Shiba transformation* [79, 80]), that interchanges spin and charge while flipping the sign of  $U$ , to show that now a gap opens in the spin sector while the charge sector remains gapless (Luther-Emery liquid).

In contrast, when  $N > 2$ , all degrees of freedom are fully gapped for *any* values of  $U$  (whether positive or negative) due to the absence of spin-charge separation in the low-energy limit [41, 75]. The resulting fully gapped Mott-insulating phase is two-fold degenerate as the result of the spontaneous breakdown of the one-step translation symmetry [41]. The physical nature of the Mott-insulating phase depends on the sign of  $U$ .

In the attractive case ( $U < 0$ ), long-range ordering of period-2 CDW emerges [41, 81, 82]. In the strong-coupling region ( $|U| \gg t$ ), the picture of the CDW formation is simple;  $SU(N)$ -singlet molecules ( $N$ -mers) of  $N$  atoms are formed first and then the preformed  $N$ -mers organize themselves into period-2 crystalline structures in such a way that they optimize the  $O(t^2/|U|)$  repulsive interaction generated by virtual hopping [81, 82]. To illustrate the crystalline pattern of  $N$ -mers, we show, in the left panel of Fig. 2, the spatial profile of physical quantities (local fermion density and kinetic-energy density) obtained by DMRG for the half-filled  $SU(4)$  Hubbard model at  $U/t = -8$ . The local fermion density clearly shows period-two oscillation indicative of CDW of tetramers (the maxima of the density is close to 4), while the kinetic energy does not exhibit any special feature. A typical wave function of the CDW phase is shown in Fig. 3(a).

When  $U > 0$ , on the other hand, it has been shown that a gapful dimerized [or spin-Peierls (SP)] phase with bond ordering [see Fig. 3(b) for an intuitive picture of the ground state] appears as soon as a weak repulsive interaction is switched on [41, 75]. In this respect, the situation is very different from the  $N = 2$  case where, at half-filling (one atom per site), a Mott-insulating phase with gapless spin excitations is stabilized when  $U > 0$ . It has been shown numerically (by means of QMC and DMRG) for  $N = 4$  that there is adiabatic continuity from weak to strong coupling and that the SP phase occurs for all  $U > 0$  [41, 83]. In the large- $U$  limit,



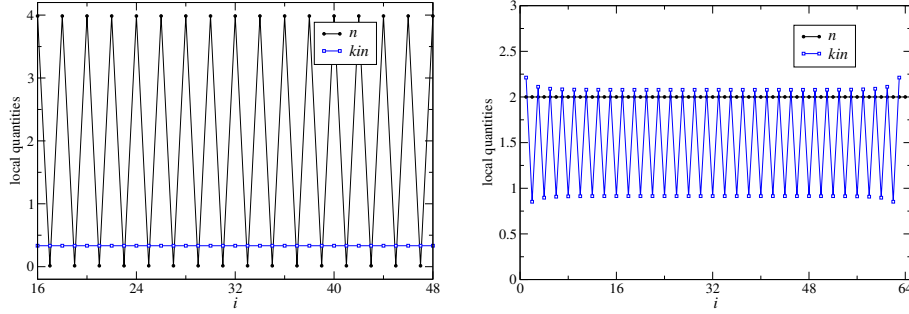


Fig. 2. (Color online) Local density  $n_i$  and kinetic bond energy for the fermionic  $SU(4)$  model with two particles per site at  $U/t = -8$  (left, data are only shown in the bulk) and  $U/t = 8$  (right) on a  $L = 64$  chain computed by DMRG. Data strongly indicate CDW and SP phase respectively.

the existence of this SP phase can be simply understood from the fact that the half-filled  $SU(4)$  Fermi-Hubbard model becomes equivalent to an  $SU(4)$  Heisenberg spin chain in the antisymmetric self-conjugate representation  $(\square)$  of  $SU(4)$ ; the latter model is known to display, at zero-temperature, a dimerized phase with two-fold ground-state degeneracy [84–86]. In the right panel of Fig. 2, we also present the plot of the local fermion density and the kinetic-energy density for the SP phase obtained by direct DMRG simulations of the  $SU(4)$  Hubbard model at  $U/t = 8$ . As can be clearly seen, there is a period-two oscillation in the profile of the kinetic energy, whereas the local-density profile is completely flat.

#### 2.3.4. Others commensurate fillings

The nature of  $SU(N)$  Mott-insulating phases for general commensurate fillings  $n = p/q$  ( $p$  and  $q$  being relatively primes) has been investigated with combined use of bosonization and DMRG simulations [73]. For  $N = 2$ , there is no Mott transition and the charge sector remains gapless for any commensurate fillings other than half-filling [38]. Again, for  $N > 2$ , the physics turns out to be much richer. If  $q > N$ , umklapp processes are irrelevant and a metallic  $N$ -component Luttinger-liquid phase is stabilized with  $N$  gapless degrees of freedom [1 for charge and  $N - 1$  for  $SU(N)$  spin], i.e., with the central charge  $c = N$ . When  $q = N$ , spin-charge separation occurs and a charge gap opens for finite  $U > 0$ . A gapless Mott-insulating phase emerges with  $N - 1$  bosonic modes. The physics is then

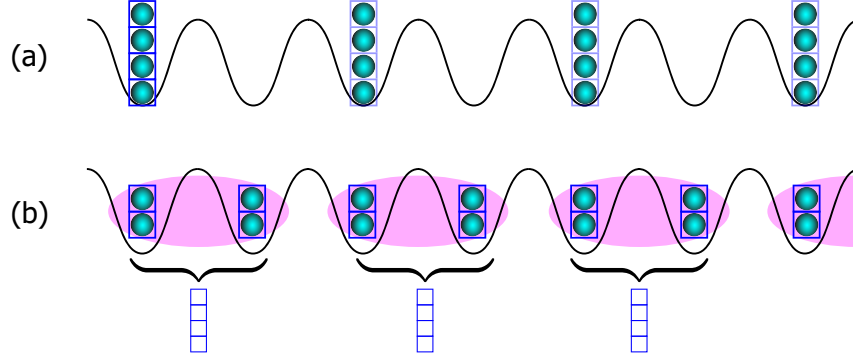


Fig. 3. (Color online) (a) Charge density wave (CDW) and (b) spin-Peierls (SP) phases of SU(4) Hubbard model. In both SU(4)-singlet phases, translation symmetry is broken. In CDW [(a)],  $N$ -mers ( $N = 4$ , here), that are each SU( $N$ )-singlet, form (period-2) crystalline structures. In SP [(b)], a six-dimensional representation ( $\mathbf{6}$ ) is formed at each site and then it is combined with another  $\mathbf{6}$  on the adjacent site to form an SU(4)-singlet.

quite similar to the one discussed above (Sec. 2.2) for the Sutherland model for the  $1/N$ -filling (i.e., one atom per site). Last, when  $q < N$ , umklapp processes are strongly relevant perturbation that couple charge and spin degrees of freedom. As a consequence, fully gapped Mott-insulating phases are obtained which break spontaneously the one-step translation symmetry. In particular, bond-ordered dimerized, trimerized, or tetramerized phases are found depending on the filling [73]. For instance, a trimerized phase with a three-fold ground-state degeneracy can be stabilized in the SU(6) Hubbard model with two particles per site ( $n = 1/3$ ). In Fig. 4 we provide complementary DMRG data showing the emergence of this phase.

For filling  $n = m/N$  ( $m = 1, \dots, N - 1$ ), a Mott insulator with  $m$  atoms per site is formed in the large- $U$  limit. Then, one can perform a strong-coupling expansion to derive an effective spin model for the remaining SU( $N$ ) low-energy degrees of freedom. The resulting magnet takes the form of the SU( $N$ ) antiferromagnetic Heisenberg chain with the Hamiltonian [29]:

$$\mathcal{H} = J \sum_i \sum_{A=1}^{N^2-1} \mathcal{S}_i^A \mathcal{S}_{i+1}^A, \quad (24)$$

where  $\mathcal{S}_i^A$  is the SU( $N$ ) spin operators at site  $i$  which transform in the

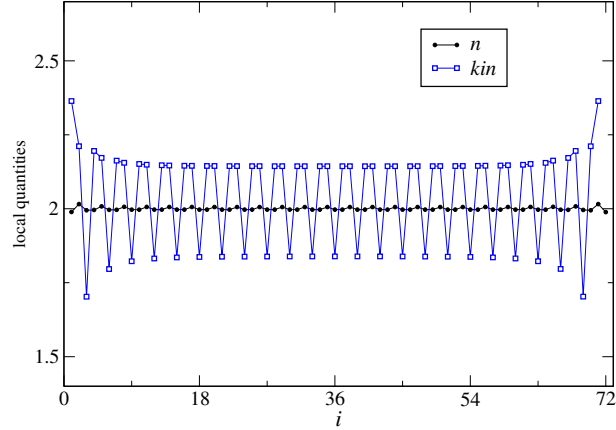


Fig. 4. (Color online) Local density  $n_i$  and kinetic bond energy for the fermionic  $SU(6)$  model with two particles per site at  $U/t = 8$  on a  $L = 72$  chain computed by DMRG. There is a strong trimerization pattern with a three-periodicity.

antisymmetric  $m$ -tensor representation of  $SU(N)$ :

$$m \left\{ \begin{array}{c} \square \\ \square \\ \square \\ \square \end{array} \right\} . \tag{25}$$

For  $m = 1$  and  $m = N - 1$ , one recovers the Sutherland model (19) with a gapless behavior described by  $SU(N)_1$  WZW CFT [29]. The physical properties of model (24) for other values of  $m$  have been investigated by a CFT approach [29, 87] and variational QMC calculations [88]; when  $m$  and  $N$  have no common divisor, a gapless  $SU(N)_1$  WZW quantum criticality occurs<sup>c</sup>. If  $N$  is divisible by  $m$  (i.e.,  $N = mp$ ), on the other hand, either a fully gapped bond-ordered phase with  $p$ -fold ground-state degeneracy or the  $SU(N)_1$  quantum critical phase realizes depending on whether the underlying umklapp operator is relevant or (marginally) irrelevant [29, 88]. The latter case corresponds to situations when  $N(m - 1) \geq 2m^2$  [29]. These predictions have been checked with a great accuracy recently by variational QMC calculations [88]. When  $m$  and  $N$  have a common divisor, one observes that these results are not in agreement with the  $SU(N)$  generalization of the Haldane conjecture proposed in Ref. [89] (see Sec. 3.2.4 for

<sup>c</sup>From the effective-field-theory point of view, whether  $N$  and  $m$  have a common divisor or not affects the selection rule for the relevant perturbations allowed at the level-1  $SU(N)$  WZW fixed point and thereby governs the ground-state properties [29].

more details of the conjecture).

Table 1. Phases of single-band  $SU(N)$  Hubbard chain (18) for various fillings. The notation  $Cm_cSm_s$  ( $m_c = 0, 1$ ,  $m_s = 0, \dots, N - 1$ ) denotes a phase with  $m_c$  ( $m_s$ ) gapless charge [ $SU(N)$ ] degrees of freedom.

filling $n$	$N = 2$	$N \geq 3$
incommensurate	C1S1	C1S( $N - 1$ ) for $U > 0$ , C1S0 for $U < 0$ (MS or CDW) <sup>a</sup>
$1/N$	C0S1 for $U > 0$ , C1S0 for $U < 0$	C1S( $N - 1$ ) for $0 < U \leq U_c$ , C0S( $N - 1$ ) <sup>b</sup> for $U_c < U$
$1/2$ (half-filling)	same as $n = 1/N$	C0S0 [dimerized (SP) for $U > 0$ , period-2 CDW for $U < 0$ ] <sup>c</sup>
generic $p/q$ ( $p, q$ : coprime)	C1S1	C1S( $N - 1$ ) when $q > N$ , C0S( $N - 1$ ) <sup>b</sup> when $q = N$ ( $U > U_c$ ), C0S0 with broken translation or C0S( $N - 1$ ) when $q < N$

<sup>a</sup> molecular superfluid (MS) of  $N$ -mers at low densities or  $2k_F$ -CDW (see, e.g., Fig. 1).

<sup>b</sup> low-energy physics described by Sutherland model (19) or level-1  $SU(N)$  WZW CFT.

<sup>c</sup> see Fig. 3.

### 3. Two-orbital fermionic Hubbard models

#### 3.1. Various physical realizations

In this review, we describe two different ways to introduce additional ‘orbital’ degree of freedom. One is to use two atomic states, the ground state ‘ $g$ ’ ( $^1S_0$ ) and a metastable excited state ‘ $e$ ’ ( $^3P_0$ ) of the alkaline-earth fermions [14]. Although we use the terminology ‘orbital’ here, it is in fact related to an additional internal degree of freedom and has nothing to do with the real orbital. The highly suppressed internal conversion  $^1S_0 \leftrightarrow ^3P_0$  guarantees separate conservation of the number of fermions in the  $g$  and  $e$  states leading to nearly perfect  $U(1)$  symmetry in the orbital sector.

The other uses the two degenerate  $p$ -bands of a 1D optical lattice. Let us consider a 1D optical lattice (running in the  $z$ -direction) with moderate strength of the harmonic confining potential  $V_{\perp}(x, y) = \frac{1}{2}m\omega_{xy}^2(x^2 + y^2)$  in the direction (i.e.  $xy$ ) perpendicular to the chain. The two degenerate  $p$ -bands are formed by the two degenerate first excited states of the above two-dimensional harmonic oscillator and we use them to introduce the orbital degree of freedom. In this scheme, the two orbital states originate from

the two symmetry-related excited states with specific spatial structures. For this reason, we obtain a slightly different effective Hamiltonian for the latter case (in particular, we have much less degree of freedom in the effective Hamiltonian).

### 3.1.1. $g$ - $e$ model

Since both  $g$  ( $^1S_0$ ) and  $e$  ( $^3P_0$ ) states have vanishing total electron angular momentum, the same mechanism as in Sec. 2.1.1 leads to the  $SU(N)$ -symmetry in the two-body scattering processes. Even if the scattering lengths for the two atoms in the same state do not depend on the total  $f$ , they may be different for different combinations of the atomic states (e.g.,  $g$ - $g$  and  $e$ - $e$ ). In general, the scattering length may differ for the following four combinations of the two colliding particles:

$$\begin{aligned} |gg\rangle &\equiv |g\rangle_1|g\rangle_2, \quad |ee\rangle \equiv |e\rangle_1|e\rangle_2, \\ |ge^\pm\rangle &\equiv \frac{1}{\sqrt{2}}(|g\rangle_1|e\rangle_2 \pm |e\rangle_1|g\rangle_2). \end{aligned} \quad (26)$$

Then, the interaction is characterized by the four  $s$ -wave scattering lengths  $a_X$  ( $X = gg, ee, ge^+, ge^-$ ), which determine the four interaction parameters as

$$g_X = \frac{4\pi\hbar^2}{M} a_X. \quad (27)$$

The scattering lengths  $a_{gg}$ ,  $a_{ee}$  and  $a_{ge}^\pm$  are for two atoms in the electronic state  $|gg\rangle$ ,  $|ee\rangle$  and  $|ge^\pm\rangle$ , respectively. The known values of the scattering length  $a_X$  for  $^{173}\text{Yb}$  and  $^{87}\text{Sr}$  are summarized in Table 2.

Table 2. Values of scattering length  $a_X$  ( $X = gg, ee, ge^+, ge^-$ ) known from experiments.

	$^{173}\text{Yb}$ ( $I = 5/2$ )	$^{87}\text{Sr}$ ( $I = 9/2$ )
$a_{gg}$	10.55 [nm] (Ref. [90])	5.09 [nm] (Refs. [91, 92])
$a_{ee}$	$16.2 \pm 0.55$ [nm] (Ref. [24])	$9.31 \pm 0.58$ [nm] (Ref. [23])
$a_{ge}^+$	$11.6 \pm 0.1$ [nm] (Ref. [24])	$8.94 \pm 0.42$ [nm] (Ref. [23])
$a_{ge}^-$	$\begin{cases} 115 \pm 10$ [nm] (Ref. [24]) \\ $175 \pm 16$ [nm] (Ref. [25]), \end{cases}	$3.60 \pm 1.16$ [nm] (Ref. [23])

When the two-body interaction  $\hat{V}$  is independent of the nuclear spin (this is the case to a good approximation in alkaline-earth atoms), the

most general form of  $\hat{V}$  may be given by the following contact interaction:

$$\begin{aligned} \hat{V}(\mathbf{r} - \mathbf{r}') &= \{g_{gg}|gg\rangle\langle gg| + g_{ee}|ee\rangle\langle ee| + g_{ge}^+|ge^+\rangle\langle ge^+| + g_{ge}^-|ge^-\rangle\langle ge^-|\} \delta(\mathbf{r} - \mathbf{r}') . \\ & \end{aligned} \quad (28)$$

Note that all the four couplings  $g_{gg}$ ,  $g_{ee}$ , and  $g_{ge}^\pm$  are independent of the nuclear-spin states of the colliding atoms (see the discussion of Sec. 2.1.1). From (28), the orbital-dependent part of the matrix elements is calculated easily:

$$\begin{aligned} \langle a, b | \hat{V} | m, n \rangle &= \left\{ g_{gg} \delta_{a,g} \delta_{b,g} \delta_{m,g} \delta_{n,g} + g_{ee} \delta_{a,e} \delta_{b,e} \delta_{m,e} \delta_{n,e} \right. \\ & \quad + \frac{1}{2} (g_{ge}^+ + g_{ge}^-) (\delta_{a,g} \delta_{b,e} \delta_{m,g} \delta_{n,e} + \delta_{a,e} \delta_{b,g} \delta_{m,e} \delta_{n,g}) \\ & \quad \left. + \frac{1}{2} (g_{ge}^+ - g_{ge}^-) (\delta_{a,g} \delta_{b,e} \delta_{m,e} \delta_{n,g} - \delta_{a,e} \delta_{b,g} \delta_{m,g} \delta_{n,e}) \right\} \delta(\mathbf{r} - \mathbf{r}') \\ & \quad (a, b, m, n = e, g) . \end{aligned} \quad (29)$$

The derivation of the lattice Hamiltonian for the case of two orbitals closely follows that described in Sec. 2.1.2 for the single-band case except that now we have two species of fermions and the corresponding Wannier functions:

$$\begin{aligned} c_{m\alpha}(z) &= \sum_R \sum_{n \in \text{bands}} w_{m,R}^{(n)}(z) c_{m\alpha,R}^{(n)} , \quad c_{m\alpha}^\dagger(z) = \sum_{\mathbf{R}_0} \sum_n w_{m,R}^{(n)*}(z) c_{m\alpha,R}^{(n)\dagger} \\ w_{m,R}^{(n)}(z) &\equiv \frac{1}{\sqrt{N_{\text{cell}}}} \sum_{k_z} e^{-ik_z R} \varphi_{m,k_z}^{(n)}(z) \quad (m = e, g; \alpha = 1, \dots, N) . \end{aligned} \quad (30)$$

We use these operators to rewrite the two-body interaction

$$\frac{1}{2} \sum_{\alpha, \beta=1}^N \sum_{a, b, m, n=e, g} \int dz \int dz' c_{a\alpha}^\dagger(z) c_{b\beta}^\dagger(z') \langle a, b | \hat{V} | m, n \rangle c_{n\beta}(z') c_{m\alpha}(z) . \quad (31)$$

In contrast to the single-band case where we have obtained only the Hubbard- $U$  interactions, we now have the following four different types

of interactions:

$$\begin{aligned}
& \frac{1}{2} \sum_{\alpha, \beta=1}^N \sum_{\{R_i, n_i\}} V_{gg}^{(n_1, n_2; n_3, n_4)} c_{g\alpha, R_1}^{(n_1)\dagger} c_{g\beta, R_2}^{(n_2)\dagger} c_{g\beta, R_3}^{(n_3)} c_{g\alpha, R_4}^{(n_4)} \\
& + \frac{1}{2} \sum_{\alpha, \beta=1}^N \sum_{\{R_i, n_i\}} V_{ee}^{(n_1, n_2; n_3, n_4)} c_{e\alpha, R_1}^{(n_1)\dagger} c_{e\beta, R_2}^{(n_2)\dagger} c_{e\beta, R_3}^{(n_3)} c_{e\alpha, R_4}^{(n_4)} \\
& + \frac{1}{2} \sum_{\alpha, \beta=1}^N \sum_{\{R_i, n_i\}} V_{ge}^+{}^{(n_1, n_2; n_3, n_4)} c_{g\alpha, R_1}^{(n_1)\dagger} c_{e\beta, R_2}^{(n_2)\dagger} c_{e\beta, R_3}^{(n_3)} c_{g\alpha, R_4}^{(n_4)} \\
& + \frac{1}{2} \sum_{\alpha, \beta=1}^N \sum_{\{R_i, n_i\}} V_{ge}^-{}^{(n_1, n_2; n_3, n_4)} c_{g\alpha, R_1}^{(n_1)\dagger} c_{e\beta, R_2}^{(n_2)\dagger} c_{g\beta, R_3}^{(n_3)} c_{e\alpha, R_4}^{(n_4)}.
\end{aligned} \tag{32}$$

In the above, the interactions are given in terms of the Wannier basis as

$$\begin{aligned}
V_{mm}^{(n_1, n_2; n_3, n_4)} & \equiv g_{aa} \int dz w_{a, R_1}^{(n_1)*}(z) w_{a, R_2}^{(n_2)*}(z) w_{a, R_3}^{(n_3)}(z) w_{a, R_4}^{(n_4)}(z) \quad (m = g, e) \\
V_{ge}^+{}^{(n_1, n_2; n_3, n_4)} & \equiv (g_{ge}^+ + g_{ge}^-) \int dz w_{g, R_1}^{(n_1)*}(z) w_{e, R_2}^{(n_2)*}(z) w_{e, R_3}^{(n_3)}(z) w_{g, R_4}^{(n_4)}(z) \\
V_{ge}^-{}^{(n_1, n_2; n_3, n_4)} & \equiv (g_{ge}^+ - g_{ge}^-) \int dz w_{g, R_1}^{(n_1)*}(z) w_{e, R_2}^{(n_2)*}(z) w_{g, R_3}^{(n_3)}(z) w_{e, R_4}^{(n_4)}(z),
\end{aligned} \tag{33}$$

and the coupling constants  $g_{gg}$ ,  $g_{ee}$ , and  $g_{ge}^\pm$  are calculated from the scattering lengths as Eq. (27). The first two terms in Eq. (32) describe the density-density interactions between the fermions in the same orbital, while the third and the fourth ones correspond to fermions from different orbitals. Specifically, the third one is just the density-density interaction of a pair of fermions on different orbitals and the last one is the orbital exchange interaction (or, the Hund coupling). Here it should be noted that there is no special relation among the four couplings  $V_{gg}$ ,  $V_{ee}$ ,  $V_{ge}^\pm$  as the Wannier functions for the two orbitals  $w_{g/e, R_i}^{(n)}(z)$  are *not* symmetry-related to each other<sup>d</sup>. As before, we restrict ourselves only to the same band  $n_1 = n_2 = n_3 = n_4 = n_0$  and keep only the onsite terms  $R_1 = R_2 = R_3 = R_4 = i$  to obtain the fol-

<sup>d</sup>This is not the case for the  $p$ -band model where the two orbitals are related to each other by  $C_4$ -symmetry.

lowing Hamiltonian ( $g$ - $e$  model) [14]:

$$\begin{aligned} \mathcal{H}_{g-e} = & - \sum_{m=g,e} t_m \sum_i \sum_{\alpha=1}^N \left( c_{m\alpha,i}^\dagger c_{m\alpha,i+1} + \text{H.c.} \right) \\ & - \sum_{m=g,e} \mu^{(m)} \sum_i n_{m,i} + \sum_{m=g,e} \frac{U_{mm}}{2} \sum_i n_{m,i} (n_{m,i} - 1) \\ & + V \sum_i n_{g,i} n_{e,i} + V_{\text{ex}}^{g-e} \sum_{i,\alpha\beta} c_{g\alpha,i}^\dagger c_{e\beta,i}^\dagger c_{g\beta,i} c_{e\alpha,i}, \end{aligned} \quad (34)$$

where the index  $\alpha$  labels the nuclear-spin multiplet and the orbital indices  $m = g$  and  $e$  label the two atomic states  $^1S_0$  and  $^3P_0$ , respectively. We have also introduced the number of  $m$ -fermion at each site

$$n_{m,i} \equiv \sum_{\alpha=1}^N c_{m\alpha,i}^\dagger c_{m\alpha,i} \quad (m = g, e) \quad (35)$$

and suppressed the common band index  $n_0$ . The coupling constants are given in terms of  $V_{gg}$ ,  $V_{ee}$ , and  $V_{ge}^\pm$  as [see Eq. (33)]

$$U_{mm} = V_{mm} \binom{n_0, n_0; n_0, n_0}{R_i, R_i; R_i, R_i}, \quad V = V_{ge}^+ \binom{n_0, n_0; n_0, n_0}{R_i, R_i; R_i, R_i}, \quad V_{\text{ex}}^{g-e} = V_{ge}^- \binom{n_0, n_0; n_0, n_0}{R_i, R_i; R_i, R_i}, \quad (36a)$$

while the hopping  $t_m$  and the chemical potential  $\mu^{(m)}$  are given by the Bloch energy as

$$\begin{aligned} t_m & \equiv t_m(1), \quad \mu^{(m)} \equiv t_m(0) \\ t_m(j-j') & \equiv -\frac{1}{N_{\text{cell}}} \sum_{k_z} \varepsilon_m^{(n)}(k_z) e^{ik_z(j-j')} \quad (m = g, e). \end{aligned} \quad (36b)$$

In order to understand the physical processes contained in this Hamiltonian, it is helpful to represent it as two coupled (single-band)  $SU(N)$  Hubbard chains (see Fig. 5). On each chain, we have the standard hopping  $t_m$  along each chain and the Hubbard-type interaction  $U_{mm}$ , and the two are coupled to each other by the nearest-neighbor Coulomb interaction  $V$  and the  $g$ - $e$  exchange process  $V_{\text{ex}}^{g-e}$ . On top of the obvious  $SU(N)$ -symmetry, the Hamiltonian is invariant under the following  $U(1)$ -symmetry

$$c_{g\alpha,i} \mapsto e^{i\theta_0} c_{g\alpha,i}, \quad c_{e\alpha,i} \mapsto e^{-i\theta_0} c_{e\alpha,i}. \quad (37)$$

This is a consequence of the fact that the total fermion numbers for  $g$  and  $e$  are conserved *separately*.<sup>e</sup>

<sup>e</sup>This breaks down when there is transition (i.e., ‘hopping’) between the two atomic states  $g$  and  $e$ .



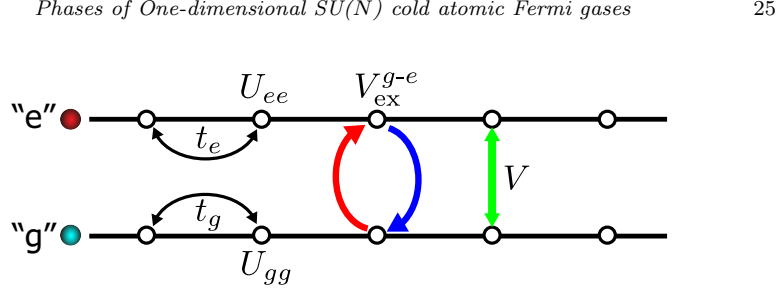


Fig. 5. (Color online) Two-leg ladder representation of the  $g$ - $e$  Hamiltonian (34).

To understand the global phase structure, it is useful to rewrite the exchange interaction  $V_{\text{ex}}^{g-e}$  in two different ways. First, we introduce the second-quantized  $SU(N)$  generators of each orbital as

$$\hat{S}_{m,i}^A = \sum_{\alpha,\beta=1}^N c_{m\alpha,i}^\dagger (\mathcal{S}^A)_{\alpha\beta} c_{m\beta,i} \quad (m = g, e). \quad (38)$$

If we normalize the  $SU(N)$  generators  $\{\mathcal{S}^A\}$  as<sup>f</sup>

$$\text{Tr}(\mathcal{S}^A \mathcal{S}^B) = \delta^{AB}, \quad (39)$$

they satisfy the following identity:

$$\sum_{A=1}^{N^2-1} (\mathcal{S}^A)_{\alpha\beta} (\mathcal{S}^A)_{\gamma\delta} = \left( \delta_{\alpha\delta} \delta_{\beta\gamma} - \frac{1}{N} \delta_{\alpha\beta} \delta_{\gamma\delta} \right). \quad (40)$$

Then, it is straightforward to show that the orbital-exchange interaction  $V_{\text{ex}}^{g-e}$  can be written as the ‘Hund coupling’ between the  $SU(N)$  ‘spins’ of the two orbitals

$$\sum_{i,\alpha\beta} c_{g\alpha,i}^\dagger c_{e\beta,i}^\dagger c_{g\beta,i} c_{e\alpha,i} = - \sum_i \left( \sum_{A=1}^{N^2-1} \hat{S}_{g,i}^A \hat{S}_{e,i}^A \right) - \frac{1}{N} \sum_i n_{g,i} n_{e,i}. \quad (41)$$

The fermionic anti-commutation is crucial in obtaining the minus sign in front of the Hund coupling. The above expression enables us to rewrite the

<sup>f</sup>This corresponds to, e.g., using the  $SU(2)$  generators  $\sigma^a/\sqrt{2}$  ( $a = x, y, z$ ) instead of the standard ones  $\sigma^a/2$ .

original  $g$ - $e$  Hamiltonian (34) as [93]

$$\begin{aligned} \mathcal{H}_{g-e} = & - \sum_i \sum_{m=g,e} t_m \sum_{\alpha=1}^N \left( c_{m\alpha,i}^\dagger c_{m\alpha,i+1} + \text{H.c.} \right) \\ & - \sum_{m=g,e} \mu^{(m)} \sum_i n_{m,i} + \sum_i \sum_{m=g,e} \frac{U_{mm}}{2} n_{m,i} (n_{m,i} - 1) \\ & + \left( V - \frac{1}{N} V_{\text{ex}}^{g-e} \right) \sum_i n_{g,i} n_{e,i} - V_{\text{ex}}^{g-e} \underbrace{\sum_i \left( \sum_{A=1}^{N^2-1} \hat{S}_{g,i}^A \hat{S}_{e,i}^A \right)}_{\text{Hund}}. \end{aligned} \quad (42)$$

From this, one readily sees that positive  $V_{\text{ex}}^{g-e}$  leads to *ferromagnetic* coupling between the two  $\text{SU}(N)$  spins on the  $g$  and  $e$  orbitals.

To derive the second form, we introduce the *orbital pseudo-spin*

$$\begin{aligned} \hat{T}_i^a = & \frac{1}{2} \sum_{\alpha=1}^N \sum_{m,n=g,e} c_{m\alpha,i}^\dagger \sigma_{mn}^a c_{n\alpha,i} \equiv \sum_{\alpha=1}^N \hat{T}_{\alpha,i}^a \\ & (a = x, y, z; m, n = g, e; \sigma^a : \text{Pauli matrices}). \end{aligned} \quad (43)$$

Clearly, the  $\text{U}(1)$ -symmetry (37) is generated by  $\sum_i \hat{T}_i^z$  and, in the following, we call it  $\text{U}(1)_o$ . Using these pseudo-spin operators, we obtain the third form of the  $g$ - $e$  Hamiltonian [93]

$$\begin{aligned} \mathcal{H}_{g-e} = & - \sum_i \sum_{m=g,e} t_m \sum_{\alpha=1}^N \left( c_{m\alpha,i}^\dagger c_{m\alpha,i+1} + \text{H.c.} \right) \\ & - \sum_{m=g,e} \left( \mu^{(m)} + 3V_{\text{ex}}^{g-e}/4 \right) \sum_i n_{m,i} \\ & + \sum_i \sum_{m=g,e} \frac{U_{mm} - V_{\text{ex}}^{g-e}/2}{2} n_{m,i} (n_{m,i} - 1) \\ & + (V + V_{\text{ex}}^{g-e}/2) \sum_i n_{g,i} n_{e,i} + V_{\text{ex}}^{g-e} \underbrace{\sum_i (\hat{T}_i)^2}_{\text{Hund}}. \end{aligned} \quad (44)$$

This expression, which is equivalent to (42), represents the exchange interaction  $V_{\text{ex}}^{g-e}$  in terms of the orbital  $\text{SU}(2)$  pseudo-spin  $\mathbf{T}$ . It is important to note that the sign of  $V_{\text{ex}}^{g-e}$  is opposite to the one in Eq. (42); positive (negative)  $V_{\text{ex}}^{g-e}$  tends to quench (maximize) the orbital pseudo-spin and maximize (quench) the  $\text{SU}(N)$  spin. This dual nature of the orbital pseudo-spin  $\mathbf{T}$

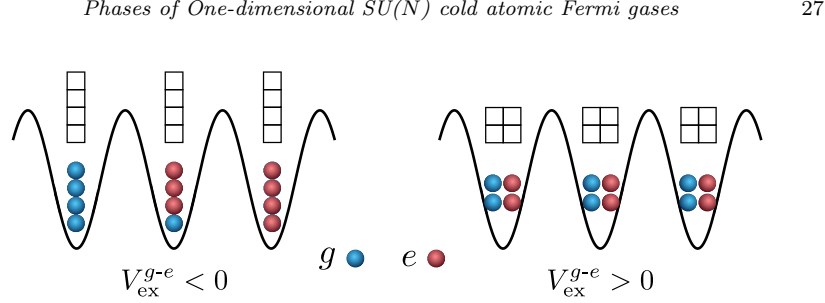


Fig. 6. (Color online) Typical strong-coupling ground states for SU(4)  $g$ - $e$  Hamiltonian (42) with  $t_m = 0$ . The SU( $N$ ) ‘magnetic moment’ that appears at each site in the Mott-insulating limit is shown by Young diagrams. For  $V_{\text{ex}}^{g-e} < 0$ , SU( $N$ )-spin at each site is quenched [see Eq. (42)], while orbital pseudo-spin  $\hat{T}$  is quenched (and hence SU( $N$ ) spin is maximized) for  $V_{\text{ex}}^{g-e} > 0$ .

and the SU( $N$ ) spin is the key to understand the structure of the phase diagram.

Before concluding this subsection, let us give another useful form of the  $g$ - $e$  Hamiltonian [93]:

$$\begin{aligned}
 \mathcal{H}_{g-e} = & - \sum_i \sum_{m=g,e} \sum_{\alpha=1}^N t_m \left( c_{m\alpha, i}^\dagger c_{m\alpha, i+1} + \text{H.c.} \right) \\
 & - \frac{1}{2} (\mu_e + \mu_g) \sum_i n_i + \frac{U}{2} \sum_i n_i^2 \\
 & + J \sum_i \left\{ (\hat{T}_i^x)^2 + (\hat{T}_i^y)^2 \right\} + J_z \sum_i (\hat{T}_i^z)^2 - (\mu_g - \mu_e) \sum_i \hat{T}_i^z \\
 & + U_{\text{diff}} \sum_i \hat{T}_i^z n_i,
 \end{aligned} \tag{45}$$

where a set of the new coupling constants are given in terms of those in Eq. (34)

$$\begin{aligned}
 U &= \frac{1}{4} (U_{gg} + U_{ee} + 2V), \quad U_{\text{diff}} = \frac{1}{2} (U_{gg} - U_{ee}), \\
 J &= V_{\text{ex}}^{g-e}, \quad J_z = \frac{1}{2} (U_{gg} + U_{ee} - 2V), \\
 \mu_g &= \frac{1}{2} (2\mu^{(g)} + U_{gg} + V_{\text{ex}}^{g-e}), \quad \mu_e = \frac{1}{2} (2\mu^{(e)} + U_{ee} + V_{\text{ex}}^{g-e}).
 \end{aligned} \tag{46}$$

The model (45) with  $U_{gg} = U_{ee}$ ,  $\mu^{(g)} = \mu^{(e)}$  is dubbed the generalized Hund model and has been studied extensively for  $N = 2$  in the cold-fermion context [94, 95]. It is obvious that, when  $t_g = t_e$ ,  $J = J_z = U_{\text{diff}} = 0$ ,  $\mu_g = \mu_e$ , the Hamiltonian  $\mathcal{H}_{g-e}$  is U( $2N$ )-invariant and the orbital part ( $J$

and  $J_z$ ) breaks it down to the generic symmetry  $U(1)_c \times SU(N)_s \times U(1)_o$ :

$$\begin{aligned} U(2N) &\xrightarrow[U_{\text{diff}=0}]{J=J_z(\neq 0)} U(1)_c \times SU(N)_s \times SU(2)_o \\ &\xrightarrow[\text{or } U_{\text{diff}\neq 0}]{J\neq J_z} U(1)_c \times SU(N)_s \times U(1)_o . \end{aligned} \quad (47)$$

### 3.1.2. $p$ -band model

In the second scheme, we use only the  $g$ -state ( $^1S_1$ ) and, to implement the orbital degree of freedom, introduce the two degenerate  $p$ -bands of a 1D optical lattice. Let us consider a 1D optical lattice (running in the  $z$ -direction) with moderate strength of (harmonic) confining potential  $V_\perp(x, y) = \frac{1}{2}M\omega_{xy}^2(x^2 + y^2)$  in the direction (i.e.  $xy$ ) perpendicular to the chain. Then, the single-particle part of the Hamiltonian reads as

$$\begin{aligned} \mathcal{H}_0 &= \left\{ -\frac{\hbar^2}{2M}\partial_z^2 + V_{\text{per}}(z) \right\} + \left\{ -\frac{\hbar^2}{2M}(\partial_x^2 + \partial_y^2) + V_\perp(x, y) \right\} \\ &\equiv \mathcal{H}_{//}(z) + \mathcal{H}_\perp(x, y) , \end{aligned} \quad (48)$$

where  $V_{\text{per}}(z)$  is a periodic potential that introduces a lattice structure along the chain (i.e.  $z$ ) direction. If the chain is infinite in the  $z$ -direction, the single-particle state is given by the following Bloch function:

$$\psi_{n_x, n_y, k_z}^{(n)}(x, y, z) = \phi_{n_x, n_y}(x, y)\varphi_{k_z}^{(n)}(z) , \quad (49)$$

where the two functions  $\varphi_{k_z}^{(n)}(z)$  and  $\phi_{n_x, n_y}(x, y)$  respectively are the eigenfunctions of  $\mathcal{H}_{//}(z)$  and  $\mathcal{H}_\perp(x, y)$  (see Fig. 7):

$$\mathcal{H}_{//}(z)\varphi_{k_z}^{(n)}(z) = \varepsilon^{(n)}(k_z)\varphi_{k_z}^{(n)}(z) \quad (50a)$$

$$\mathcal{H}_\perp(x, y)\phi_{n_x, n_y}(x, y) = \epsilon_{(n_x, n_y)}\phi_{n_x, n_y}(x, y) . \quad (50b)$$

with

$$\epsilon_{(n_x, n_y)} = (n_x + n_y + 1)\hbar\omega_{xy} \quad (n_x, n_y = 0, 1, 2, \dots) . \quad (50c)$$

This implies that due to the motion perpendicular to the chain, each Bloch band specified by  $n$  splits into subbands labeled by  $(n_x, n_y)$ :

$$E_{(n_x, n_y)}^{(n)}(k_z) = \varepsilon^{(n)}(k_z) + \epsilon_{(n_x, n_y)} . \quad (51)$$

We call, for a given main band index  $n$ , the subbands with  $(n_x, n_y) = (0, 0)$ ,  $(1, 0)$ , and  $(0, 1)$  as ‘ $s$ ’, ‘ $p_x$ ’ and ‘ $p_y$ ’, respectively.

Now let us suppose that only the  $n = 0$  bands are occupied, and that, among them, the lowest one (the  $s$ -band) is completely filled. Then, it is

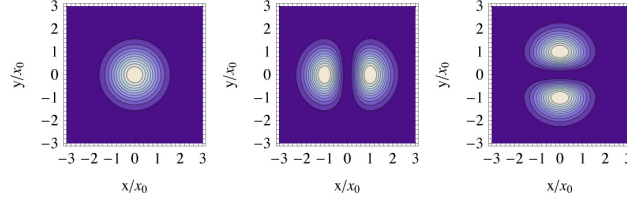


Fig. 7. (Color online) Contour plots of squared wave functions  $|\phi_{n_x, n_y}|^2$  for three orbitals  $(n_x, n_y) = (0, 0), (1, 0)$  and  $(0, 1)$ . From Ref. [93]

legitimate to keep the next two bands  $p_x$  and  $p_y$  in the effective Hamiltonian in describing the low-energy physics [96, 97]. The argument goes almost in the same way except that now we have to take into account the motion in the perpendicular (i.e.,  $xy$ ) directions. Now the Wannier function

$$w_{(n_x, n_y); R}^{(n)}(x, y, z) \equiv \frac{1}{\sqrt{N_{\text{cell}}}} \phi_{(n_x, n_y)}(x, y) \sum_{k_z} e^{-ik_z R} \varphi_{k_z}^{(n)}(z) \quad (52)$$

( $R$  labels the center of the Wannier function and  $N_{\text{cell}}$  is the number of unit cells) is used instead to expand the Fermi operators:

$$c_{\alpha}(\mathbf{r}) = \sum_R \sum_{n=\text{bands}} \sum_{(n_x, n_y)} w_{(n_x, n_y); R}^{(n)}(x, y, z) c_{(n_x, n_y), \alpha, R}^{(n)} \quad (\alpha = 1, \dots, N). \quad (53)$$

We plug them into the two-body (contact) interaction for atoms in the  $g$  state

$$\frac{1}{2} \sum_{\alpha, \beta=1}^N \int d\mathbf{r} \int d\mathbf{r}' c_{\alpha}^{\dagger}(\mathbf{r}) c_{\beta}^{\dagger}(\mathbf{r}') V(\mathbf{r} - \mathbf{r}') c_{\beta}(\mathbf{r}') c_{\alpha}(\mathbf{r}) \quad (54)$$

with

$$V(\mathbf{r} - \mathbf{r}') = g_{gg} \delta(\mathbf{r} - \mathbf{r}'). \quad (55)$$

Retaining only the terms with  $R_1 = R_2 = R_3 = R_4 = i$ ,  $n_1 = n_2 = n_3 =$

$n_4 = 0$ ,  $(n_x, n_y) = (1, 0), (0, 1)$ , we obtain

$$\begin{aligned} & \frac{1}{2} \sum_R \sum_{\alpha, \beta=1}^N \left\{ \sum_{a=p_x, p_y} U_{aaaa} c_{a, \alpha, R}^\dagger c_{a, \beta, R}^\dagger c_{a, \beta, R} c_{a, \alpha, R} \right. \\ & + \sum_{\substack{a \neq b \\ =p_x, p_y}} U_{aabb} c_{a, \alpha, R}^\dagger c_{a, \beta, R}^\dagger c_{b, \beta, R} c_{b, \alpha, R} + \sum_{\substack{a \neq b \\ =p_x, p_y}} U_{abba} c_{a, \alpha, R}^\dagger c_{b, \beta, R}^\dagger c_{b, \beta, R} c_{a, \alpha, R} \\ & \left. + \sum_{\substack{a \neq b \\ =p_x, p_y}} U_{abab} c_{a, \alpha, R}^\dagger c_{b, \beta, R}^\dagger c_{a, \beta, R} c_{b, \alpha, R} \right\}, \end{aligned} \quad (56)$$

where the superscript ‘(0)’ for the fermion operators of the lowest Bloch band has been suppressed. We have also introduced a short-hand notation  $m = p_x, p_y$  with  $p_x = (n_x, n_y) = (1, 0)$  and  $p_y = (n_x, n_y) = (0, 1)$ .

As the Wannier functions  $w_{a;R}^{(0)}$  are related to each other by the  $C_4$ -symmetry, the coupling constants  $U_{abcd}$  defined by

$$U_{abcd} \equiv g_{gg} \int d\mathbf{r} w_{a;R}^{(0)*}(\mathbf{r}) w_{b;R}^{(0)*}(\mathbf{r}) w_{c;R}^{(0)}(\mathbf{r}) w_{d;R}^{(0)}(\mathbf{r}) \quad (a, b, c, d = p_x, p_y) \quad (57)$$

obey the following relation:

$$\begin{aligned} U_1 & \equiv U_{p_x p_x p_x p_x} = U_{p_y p_y p_y p_y} \\ U_2 & \\ & \equiv U_{p_x p_x p_y p_y} = U_{p_y p_y p_x p_x} = U_{p_x p_y p_y p_x} = U_{p_y p_x p_x p_y} = U_{p_x p_y p_x p_y} = U_{p_y p_x p_y p_x}. \end{aligned} \quad (58)$$

Therefore, in contrast to the case of the  $g$ - $e$  model, we have only two independent couplings  $U_1$  and  $U_2$  for any  $C_4$ -symmetric potentials. In fact, further simplification occurs for axially-symmetric potentials like the harmonic one used here. In these cases,  $\phi_{n_x, n_y}(x, y)$  in Eq. (52) is replaced by

$$f(r) \cos \theta \quad \text{for } p_x, \quad f(r) \sin \theta \quad \text{for } p_y \quad (r = \sqrt{x^2 + y^2}) \quad (59)$$

with some real-valued function  $f(r)$  depending the choice of the potential. Carrying out the integration in Eq. (57), we obtain

$$U_1 = \frac{3\pi}{4} \mathcal{I}_{r,z}, \quad U_2 = \frac{\pi}{4} \mathcal{I}_{r,z}, \quad (60)$$

where  $\mathcal{I}_{r,z}$  is the result of the integration over  $r$  and  $z$  that is common to all  $U_{abcd}$ . This implies that  $(U_1, U_2)$  are bound to satisfy a relation

$$U_1 = 3U_2 \quad (61)$$

for *any* axially-symmetric potentials  $V_{\perp}(x, y) = f(\sqrt{x^2 + y^2})$ . That is, as far as we use axially-symmetric traps, there is only one free parameter for the interactions. One possible way to deviate from the line  $U_1 = 3U_2$  is to use such ( $C_4$ -symmetric) anharmonic potentials as [93]:

$$V_{\perp}(x, y) = \frac{1}{2}M\omega_{xy}^2(x^2 + y^2) + \frac{1}{2}\beta(x^4 + y^4) \quad (\beta \geq 0) \quad (62)$$

(see Fig. 3 of Ref. [93] for the ratio  $U_1/U_2$  obtained for the above  $V_{\perp}$ ).

As the single-particle energy  $E_{(n_x, n_y)}^{(n)}(k_z)$  [Eq. (51)] is the same for the two  $p$ -bands, we have the same hopping amplitude and the chemical potential for  $p_x$  and  $p_y$ . Summing up all these, we obtain the following form of the  $p$ -band model [93, 96, 97]:

$$\begin{aligned} \mathcal{H}_{p\text{-band}} = & -t_p \sum_i \sum_{m=p_x, p_y} (c_{m\alpha, i}^{\dagger} c_{m\alpha, i+1} + \text{H.c.}) \\ & - \mu_p \sum_i \sum_{m=p_x, p_y} n_{m, i} + \frac{1}{2}U_1 \sum_i \sum_{m=p_x, p_y} n_{m, i}(n_{m, i} - 1) \\ & + U_2 \sum_i n_{p_x, i} n_{p_y, i} + U_2 \sum_i c_{p_x\alpha, i}^{\dagger} c_{p_y\beta, i}^{\dagger} c_{p_x\beta, i} c_{p_y\alpha, i} \\ & + \frac{1}{2}U_2 \sum_i \sum_{\alpha, \beta=1}^N \sum_{\substack{m \neq n \\ =p_x, p_y}} c_{m\alpha, i}^{\dagger} c_{m\beta, i}^{\dagger} c_{n\beta, i} c_{n\alpha, i}, \end{aligned} \quad (63)$$

where the hopping  $t_p$  and the chemical potential  $\mu_p$  are given by the single-particle energy

$$t_p = -\frac{1}{N_{\text{cell}}} \sum_{k_z} E_{(1,0)}^{(n)}(k_z) e^{ik_z}, \quad \mu_p = -\frac{1}{N_{\text{cell}}} \sum_{k_z} E_{(1,0)}^{(n)}(k_z). \quad (64)$$

The last term of Eq. (63) comes from the pair-hopping between the two orbitals, which is not allowed for the setting of the  $g$ - $e$  model, and breaks  $U(1)_o$ -symmetry in general, while the other five terms already existed in the  $g$ - $e$  model (34). In fact, except for the last term,  $\mathcal{H}_{p\text{-band}}$  coincides with the Hamiltonian  $\mathcal{H}_{g-e}$  [(34)] after the identification (see Fig. 8)

$$\begin{aligned} t_g = t_e = t_p, \quad \mu^{(g)} = \mu^{(e)} = \mu_p, \\ U_{gg} = U_{ee} = U_1, \quad V = U_2, \quad V_{\text{ex}}^{g-e} = U_2. \end{aligned} \quad (65)$$

Due to the pair-hopping between the two orbitals, the  $p$ -band Hamiltonian (63) appears to break the  $U(1)_o$ -symmetry. However, this is not always the case and, in fact, there is a *hidden*  $U(1)_o$  symmetry in the case of axially-symmetric traps ( $U_1 = 3U_2$ ). To see this, we rewrite (63) using the orbital

pseudo-spin:

$$\begin{aligned}
\mathcal{H}_{p\text{-band}} = & -t_p \sum_i \sum_{m=p_x, p_y} \left( c_{m\alpha, i}^\dagger c_{m\alpha, i+1} + \text{H.c.} \right) \\
& - \mu_p \sum_i n_i + \frac{1}{4} (U_1 + U_2) \sum_i n_i^2 \\
& + \sum_i \left\{ 2U_2 (\hat{T}_i^x)^2 + (U_1 - U_2) (\hat{T}_i^z)^2 \right\},
\end{aligned} \tag{66}$$

which is to be compared with Eq. (45). As can be easily seen, the last two terms break  $U(1)_o$ . Therefore, the generic symmetry of the  $p$ -band model is

$$U(1)_c \times SU(N)_s \times \mathbb{Z}_{2,o}. \tag{67}$$

However, for *any* axially-symmetric  $V_\perp(x, y)$  where the relation  $U_1 = 3U_2$  holds [see Eq. (61)], the orbital part assumes a fully  $U(1)$ -symmetric form:  $2U_2 \{ (T_j^x)^2 + (T_j^z)^2 \}$  and  $\mathcal{H}_{p\text{-band}}$  reduces to a special case of  $\mathcal{H}_{g-e}$  [Eq. (45)] (with  $\mu_g = \mu_e$ ,  $U_{\text{diff}} = 0$ ) after the redefinition  $T_i^y \leftrightarrow T_i^z$ ,  $T_i^z \rightarrow -T_i^y$ .<sup>§</sup>

A few remarks are in order here about the special points where great simplification or enhanced symmetries emerge. When  $U_2 = 0$  since it decouples into two non-interacting copies of  $U(N)$  Hubbard chains, we can borrow the results from Sec. 2. Moreover, along the line  $U_1 = U_2$ , the  $p$ -band model (66) is identical to the above  $U_2 = 0$  case after the redefinition  $T_i^x \leftrightarrow T_i^z$ ,  $U_1 \rightarrow U_1/2$ . Finally, in the  $N = 2$  case, the  $p$ -band model can be recast in the following form [97]:

$$\begin{aligned}
\mathcal{H}_{p\text{-band}} = & -t_p \sum_{\alpha=\uparrow, \downarrow} \sum_{m=p_x, p_y} \sum_j (c_{m\alpha, j}^\dagger c_{m\alpha, j+1} + \text{H.c.}) \\
& - \mu_p \sum_i n_i - \frac{2}{3} U_1 \sum_i \sum_{m=p_x, p_y} (\hat{\mathbf{S}}_{m, i})^2 \\
& - 2U_2 \sum_i \hat{\mathbf{S}}_{p_x, i} \cdot \hat{\mathbf{S}}_{p_y, i} + 2U_2 \sum_i \hat{\mathbf{K}}_{p_x, i} \cdot \hat{\mathbf{K}}_{p_y, i}
\end{aligned} \tag{68}$$

<sup>§</sup>This is in a sense an artifact of the choice of the basis ( $p_x$  and  $p_y$ ). In fact, if we had chosen the orbital-angular-momentum (along the  $z$ -axis) basis, the  $U(1)_o$ -symmetry would have been explicit.



using the following two sets of spin operators [98]:

$$\hat{S}_{m,i}^a = \frac{1}{2} c_{m\alpha,i}^\dagger \sigma_{\alpha\beta}^a c_{m\beta,i} \quad (a = x, y, z; m = p_x, p_y) \quad (69a)$$

$$\begin{aligned} \hat{K}_{m,i}^+ &\equiv (-1)^i c_{m\uparrow,i}^\dagger c_{m\downarrow,i}^\dagger, & \hat{K}_{m,i}^- &\equiv (-1)^i c_{m\downarrow,i} c_{m\uparrow,i}, \\ \hat{K}_{m,i}^z &\equiv \frac{1}{2} (n_{m\uparrow,i} + n_{m\downarrow,i} - 1) = \frac{1}{2} (n_{m,i} - 1). \end{aligned} \quad (69b)$$

From this, we can see that the  $N = 2$   $p$ -band model at half-filling enjoys an enlarged  $SU(2)_{\text{spin}} \times SU(2)_{\text{charge}} \sim SO(4)$  symmetry for *all*  $U_1, U_2$  which stems from an additional  $SU(2)$  symmetry for the charge degrees of freedom at half-filling [97].

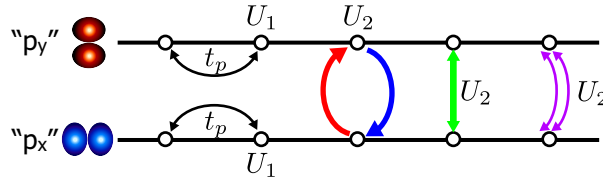


Fig. 8. (Color online) The two-leg ladder representation of the  $p$ -band model (63). On top of the interactions included already in the  $g$ - $e$  model, pair-hopping processes between the two orbitals are allowed.

### 3.2. Results known for Mott-insulating limits

As in the usual Hubbard Hamiltonian, when we have an integer number of particles at each site, the system becomes a Mott insulator in the limit

$$U = \frac{1}{4} (U_{gg} + U_{ee} + 2V) \rightarrow \infty \quad (70)$$

[see Eq. (45)]. Depending on  $N$  and the number of fermions at each site, we have a variety of  $SU(N)$  spins emerging at each site in the Mott-insulating limits (see, e.g., Fig. 6).

#### 3.2.1. Low-energy degrees of freedom in Mott phases

To find the  $SU(N)$  and the orbital  $SU(2)$  content, we first note that when  $J = V_{\text{ex}}^{g-e} = 0$ ,  $J_z = 0$ ,  $U_{\text{diff}} = 0$ , the system attains the maximal symmetry  $U(2N)$  [see (47)]. In this limit, for a given number of fermions per site (say,

$n$ ), we can uniquely assign the following  $U(2N)$  irreducible representation:

$$n \left\{ \begin{array}{c} \square \\ \square \\ \square \\ \square \end{array} \right\} \quad (0 \leq n \leq 2N) . \quad (71)$$

Formally, the  $\frac{(2N)!}{n!(2N-n)!}$  states in the above representations may be decomposed in terms of the direct product of  $SU(N)$  and the orbital  $SU(2)$ . This problem is explicitly worked out in Ref. [99] (see also Appendix A of Ref. [93] for a concise explanation in the context of the  $SU(N)$  Hubbard model). As a simplest example, let us consider the  $n = 1$  case. Then the  $2N$  singly-occupied states at each site are decomposed as

$$\underbrace{\square}_{SU(2N)} \sim \left( \underbrace{\square}_{SU(N)}, \underbrace{\square}_{SU(2)} \right) = (\mathbf{N}, T = 1/2) . \quad (72)$$

Therefore, the low-energy physics of the highly degenerate ground-state manifold is described by the composite of the  $SU(N)$  ‘spins’ in the fundamental representation ( $\square$ ) and the orbital pseudo-spins  $T = 1/2$  [14].

Different results are obtained when we consider the case of half filling. For instance, the 70 half-filled states of the  $SU(4)$   $g$ - $e$  model (i.e.,  $N = 4$ ,  $n = 4$ ) may be decomposed as

$$n = 4 \left\{ \begin{array}{c} \square \\ \square \\ \square \\ \square \end{array} \right\} \sim \left( \underbrace{\begin{array}{cc} \square & \square \\ \square & \square \end{array}}_{SU(4)}, \underbrace{\bullet}_{SU(2)} \right) \oplus \left( \begin{array}{c} \square \square \\ \square \\ \square \end{array}, \square \square \right) \oplus (\bullet, \square \square \square \square) \quad (73)$$

$$= (\mathbf{20}, T = 0) \oplus (\mathbf{15}, T = 1) \oplus (\mathbf{1}, T = 2)$$

(with  $\bullet$  being the singlet). Note that the Fermi statistics dictates the possible combinations of  $SU(N)$  and orbital. The Hund coupling  $V_{\text{ex}}^{g-e}$

$$-V_{\text{ex}}^{g-e} \sum_i \left( \sum_{A=1}^{N^2-1} \mathcal{S}_{g,i}^A \mathcal{S}_{e,i}^A \right) = +V_{\text{ex}}^{g-e} \sum_i (\mathbf{T}_i)^2 + (\text{density-density interaction}) \quad (74)$$

[see Eqs. (42) and (44)] then selects one of the irreducible representations appearing on the right-hand side:

$$\begin{aligned} & \left( \begin{array}{cc} \square & \square \\ \square & \square \end{array}, \bullet \right) && \text{for } V_{\text{ex}}^{g-e} > 0 \\ & (\bullet, \square \square \square \square) && \text{for } V_{\text{ex}}^{g-e} < 0 . \end{aligned} \quad (75)$$

That is, when the  $SU(N)$  spin is maximized (quenched), the orbital pseudo-spin  $\mathbf{T}$  is quenched (maximized). This dual nature of the  $SU(N)$  and the orbital is common to all  $SU(N)$   $g$ - $e$  models with even  $N$ .

For odd- $N$ , on the other hand, we have different decompositions. For instance, for  $N = 3$  and  $n = 3$  (half-filling), the decomposition in terms of  $SU(3) \times SU(2)$  reads as

$$\begin{aligned}
 n = 3 \left\{ \begin{array}{|c|} \hline \square \\ \hline \square \\ \hline \square \\ \hline \end{array} \right. &\sim \left( \begin{array}{|c|c|} \hline \square & \square \\ \hline \square & \square \\ \hline \end{array}, \begin{array}{|c|} \hline \square \\ \hline \square \\ \hline \end{array} \right) \oplus (\bullet, \begin{array}{|c|c|c|c|} \hline \square & \square & \square & \square \\ \hline \end{array}) \\
 &= (\mathbf{8}, T = 1/2) \oplus (\mathbf{1}, T = 3/2) .
 \end{aligned} \tag{76}$$

Therefore, the situation on the  $V_{\text{ex}}^{g-e} > 0$  side is rather different for  $N$ -even and  $N$ -odd. Specifically, the low-energy degrees of freedom in the half-filled Mott insulator for  $N$ -even are the *pure*  $SU(N)$  spins, while those for  $N$ -odd are the composite of  $SU(N)$  spins [with  $(N + 1)/2$  boxes in the first column and  $(N - 1)/2$  boxes in the second] and orbital pseudo-spins  $T = 1/2$ .

### 3.2.2. Strong-coupling limits

In the previous section, we have seen that different low-energy degrees of freedom emerge depending on  $N$ , filling  $n(\in \mathbb{Z})$ , and the sign of  $V_{\text{ex}}^{g-e}$ . Therefore, when the hopping amplitudes vanish (atomic limit), i.e.  $t_g = t_e = 0$  or  $t_p = 0$  depending on the model, the ground state has extensive degeneracy. This degeneracy is lifted when the hopping  $t_m$  is taken into account. Clearly,  $t_m$  changes the fermion number  $n$  at each site and non-trivial matrix elements require at least  $t_m^2$  processes.

For the clarity of the argument, we restrict ourselves to the case of half-filling (i.e., the number of fermions per site  $n = N$ ) in the following. Let us begin with the case where  $N = \text{even}$ ,  $V_{\text{ex}}^{g-e} > 0$ . Then, in the atomic-limit ground state, we have

$$N/2 \left\{ \begin{array}{|c|c|} \hline \square & \square \\ \hline \square & \square \\ \hline \square & \square \\ \hline \end{array} \right. \tag{77}$$

with the orbital pseudo-spin quenched ( $\mathbf{T} = \mathbf{0}$ ). The resulting effective Hamiltonian is obtained by the second-order perturbation and reads as

follows [93]

$$\mathcal{H}_{\text{SU}(N)} = J_{\text{SU}(N)} \sum_{A=1}^{N^2-1} \mathcal{S}_i^A \mathcal{S}_{i+1}^A + \text{const.}, \quad (78)$$

where the exchange coupling  $J_{\text{SU}(N)}$  is  $N$ -independent:

$$J_{\text{SU}(N)} \equiv \frac{1}{2} \left\{ \frac{t_g^2}{U + U_{\text{diff}} + J + \frac{J_z}{2}} + \frac{t_e^2}{U - U_{\text{diff}} + J + \frac{J_z}{2}} \right\} \quad (79)$$

and the  $\text{SU}(N)$  spins  $\{\mathcal{S}_i\}$  transform under the representation (77) [see Eq. (75)]. As  $\mathbf{T}$  is quenched, we obtain a pure ‘spin’ Hamiltonian (as we have seen above, this is not the case when  $N = \text{odd}$ ).

In the case of  $\mathcal{H}_{p\text{-band}}$ , the condition  $V_{\text{ex}}^{g-e} > 0$  translates to  $U_2 > 0$ . However,  $T^z$  is not conserved in general and we cannot use the argument in Sec. 3.2.1 as it is. However, we found that when  $U_1 > U_2 (> 0)$  the lowest-energy state is  $T = 0$  singlet that enables us to follow exactly the same steps and obtain [93]

$$\mathcal{H}_{\text{SU}(N)} = \frac{t_p^2}{U_1 + U_2} \sum_{A=1}^{N^2-1} \mathcal{S}_i^A \mathcal{S}_{i+1}^A + \text{const.} \quad (80)$$

In Sec. 3.3, we will show that the  $\text{SU}(N)$  spin Hamiltonians (78) and (80) host a topological phase in quite a large region of the parameter space.

When  $V_{\text{ex}}^{g-e} < 0$  (or  $U_2 < 0$ ), on the other hand, the low-energy degree of freedom is the orbital pseudo-spin transforming like a  $T = N/2$  spin [Eq. (75)]

$$\underbrace{\square \square \square}_{N \text{ boxes } (T=N/2)} \quad (81)$$

and the  $\text{SU}(N)$  ‘spins’ are quenched. The resulting effective Hamiltonian is rather different for the  $g$ - $e$  Hamiltonian and the  $p$ -band Hamiltonian. For the  $g$ - $e$  Hamiltonian, we obtain the following  $T = N/2$  Hamiltonian:

$$\begin{aligned} \mathcal{H}_{\text{orbital}} = & \sum_i \{ \mathcal{J}_{xy} (T_i^x T_{i+1}^x + T_i^y T_{i+1}^y) + \mathcal{J}_z T_i^z T_{i+1}^z - (J - J_z) (T_i^z)^2 \} \\ & + \sum_i \{ N U_{\text{diff}} - (\mu_g - \mu_e) \} T_i^z \end{aligned} \quad (82)$$

with the *easy-axis* exchange coupling [93]

$$\begin{aligned}\mathcal{J}_{xy} &\equiv \frac{4t_g t_e}{N \left\{ U + |J| \left( N + \frac{1}{2} \right) \right\}} \\ \mathcal{J}_z &\equiv \frac{2 \{ t_g^2 + t_e^2 \}}{N \left\{ U + |J| \left( N + \frac{1}{2} \right) \right\}} \quad (\mathcal{J}_{xy} \leq \mathcal{J}_z).\end{aligned}\tag{83}$$

In the ideal situation where the two orbitals are symmetric, the model reduces to the spin  $T = N/2$  Heisenberg model ( $\mathcal{J}_{xy} = \mathcal{J}_z$ ) with the single-ion  $D$ -term, for which much is known (see, e.g. Refs. [100–102] and references cited therein). When  $|J_z| \ll |J|$  ( $J < 0$ ), the system has *easy-plane* anisotropy and, if  $N$  is even<sup>h</sup> and  $|J|$  is large enough compared with  $\mathcal{J}_{xy}$  and  $\mathcal{J}_z$ , the ground state is in the so-called large- $D$  phase, which, in its extreme case, is a product of  $T^z = 0$  states. In the fermionic language, it is a state where there are  $N/2$  fermions on each orbital (and hence  $T_i^z = 0$ ) and these  $N$  fermions form total  $SU(N)$ -singlet at each site.

When  $J_z$  takes a large negative value (this is the case typically for large  $V$ ), the  $D$ -term is of easy-axis-type and the ground state is Ising-like:  $T^z = \dots, -N/2, N/2, -N/2, N/2, \dots$ . This is the  $2k_F (= \pi)$  density wave of the *orbital* pseudo-spin and we call it *orbital density wave* (ODW).

In the case of the  $p$ -band model, physics of the orbital sector is even more involved. Since the condition  $V_{\text{ex}}^{g-e} = J < 0$  translates to  $U_2 < 0$  in the  $p$ -band model [see Eq. (65)], the interaction is attractive  $U_1 + U_2 < 0$  in the physical region  $U_1 \simeq 3U_2$  and we have to take into account several different values of  $n_i$ . Therefore, the physics here is quite different from the usual Mott physics described above. For instance, at  $\mu = -N|U_1 + U_2|$ , we have two degenerate  $SU(N)$ -singlet states  $n_i = 0$  ( $T = 0$ ) and  $n_i = 2N$  ( $T = 0$ ) which feel a repulsive interaction coming from  $t^2$ -processes thereby stabilizing the  $2k_F$ -CDW<sup>i</sup> in a region around the line  $U_1 = 3U_2 (< 0)$  for  $N \geq 3$  (see, e.g., Fig. 21 of Ref. [93]).

Last, the case with  $V_{\text{ex}}^{g-e} = J = 0$  is slightly different. This region is most conveniently investigated in the limit  $U = U_{gg} = U_{ee} = V \gg t$ ,  $\mu^{(g)} = \mu^{(e)}$ . Then the  $g$ - $e$  model (45) reduces to the *single-band*  $SU(2N)$  Hubbard model at half-filling discussed in Sec. 2.3.3; the ground state is a dimerized SP state (see Fig. 3). This highlights the importance of the orbital degree of freedom and the exchange interaction  $V_{\text{ex}}^{g-e}$  between the

<sup>h</sup>When  $N$  is odd, the large- $D$  limit is not very trivial and the effective Hamiltonian is given by the  $S = 1/2$  XXZ chain.

<sup>i</sup>The basic mechanism underlying the CDW here is the same as the CDW in the case of the half-filled single-band  $SU(N)$  Hubbard chain discussed in Sec. 2.3.3.

two orbital states in realizing topological phases.

### 3.2.3. Sigma-model mapping

Some insights into the nature of the ground states may be gained by mapping the problems onto the sigma model with the  $\theta$ -term. Generalizing the semi-classical sigma-model mapping [53, 103] à la Haldane of the usual spin chains, Read and Sachdev [104–106] considered a family of  $SU(N)$  ‘spin systems’ where an irreducible representation  $\mathcal{R}$  (specified by a rectangular Young diagram with  $m$  rows and  $n_c$  columns) and its conjugate  $\bar{\mathcal{R}}$  are assigned respectively on the two sublattices of a  $D$ -dimensional bipartite lattice.

$$\mathcal{R} = \left. \begin{array}{|c|c|c|c|c|} \hline & & & & \\ \hline & & & & \\ \hline & & & & \\ \hline & & & & \\ \hline \end{array} \right\} m \quad \bar{\mathcal{R}} = \left. \begin{array}{|c|c|c|c|c|} \hline & & & & \\ \hline & & & & \\ \hline & & & & \\ \hline & & & & \\ \hline \end{array} \right\} N - m \quad (84)$$

$n_c$   $n_c$

If we represent the state (84) in terms of  $n_c$  copies of  $SU(N)$  fermions, these states are in fact invariant under  $U(N - m) \times U(m)$ . Therefore, the coherent state, generated from the reference state (84) by applying any elements of  $U(N)$ , represents  $\frac{U(N)}{U(N - m) \times U(m)}$  [105]. This is closely parallel to that the Bloch spin coherent state generated from the spin state polarized in the  $z$ -direction is isomorphic to  $\frac{SU(2)}{U(1)} \simeq \frac{U(2)}{U(1) \times U(1)} = \mathbb{C}P^1 \simeq S^2$ . The role of the expectation value  $\langle \mathbf{S} \rangle$  of spins in the usual spin path integral is now played by an  $N \times N$  hermitian matrix  $Q$  ( $Q^2 = \mathbf{1}$ ). Since the number of columns  $n_c$  controls the semi-classical limit as the spin  $S$  does in the  $SU(2)$  case, we may expect that an  $SU(N)$  analogue of Néel ordering occurs in the limit  $n_c \rightarrow \infty$ . The order parameter is the staggered component  $\Omega$  of the matrix  $Q$  and its low-energy fluctuations are governed by the following (finite-temperature) effective action [105]:

$$\begin{aligned} \mathcal{S}_E = & \frac{1}{2} \chi_s \int_0^{\beta\hbar} d\tau \int d^D \mathbf{r} \int d^D \mathbf{r}' \text{Tr} \{ \partial_\tau \Omega(\tau, \mathbf{r}) \}^2 \\ & + \frac{1}{2} \int_0^{\beta\hbar} d\tau \int d^D \mathbf{r} \sum_{\mu, \nu=1}^D \rho_s(\mathbf{r})_{\mu\nu} \text{Tr} \{ \partial_\mu \Omega(\tau, \mathbf{r}) \partial_\nu \Omega(\tau, \mathbf{r}) \} , \end{aligned} \quad (85)$$

where the two phenomenological parameters  $\chi_s$  and  $\rho_s(\mathbf{r})_{\mu\nu}$  respectively are the transverse susceptibility and the spin stiffness<sup>j</sup> [105, 107]. In one

<sup>j</sup>For the nearest-neighbor Heisenberg  $SU(N)$  magnets on a hypercubic lattice in  $D$  di-

dimension ( $D = 1$ ), this action is supplemented by the  $\theta$ -term<sup>k</sup> associated with  $\Pi_2 \left( \frac{U(N)}{U(N-m) \times U(m)} \right) = \mathbb{Z}$ :

$$\mathcal{S}_\theta = -\frac{\Theta_{\text{top}}}{16\pi} \int_0^{\beta\hbar} d\tau \int dx \epsilon_{\mu\nu} \text{Tr} \{ \Omega(\tau, x) \partial_\mu \Omega(\tau, x) \partial_\nu \Omega(\tau, x) \} \quad (87)$$

$(\epsilon_{\tau x} = +1, \Theta_{\text{top}} = n_c \pi) .$

Following the same line of argument as the one first used by Haldane [108, 109], we may conclude, for  $D = 1$ , that when the number of columns  $n_c$  is even for which the  $\theta$ -term is irrelevant to bulk properties, the system is in a featureless gapped phase [105, 106]. On the other hand, when  $n_c$  is odd, the system spontaneously dimerizes. In the context of our  $SU(N)$  Hubbard model, the case  $n_c = 1$  corresponds to the Mott-insulating phase discussed in Sec. 2.3.3 (the single-band  $SU(N)$  Hubbard model at half-filling)<sup>l</sup> and the model with  $n_c = 2$  describes the half-filled 2-orbital system (Sec. 3) deep in the Mott-insulating region. For instance, the appearance of the SP phase in the single-band model [41, 75] discussed in Sec. 2.3.3 is consistent with the above field-theory prediction. In Sec. 3.3, we will argue that the featureless phase predicted by the model (85) is in fact topological by explicitly constructing the model wave function.

### 3.2.4. Lieb-Schultz-Mattis argument and generalized Haldane conjecture

The simple argument first used by Lieb, Schultz, and Mattis [110] is quite general but sometimes can give strong constraints on the nature of the ground state and the low-energy spectrum over it. In fact, Affleck and Lieb [111] extended the argument in Ref. [110] to include the case of self-conjugate representations of  $SU(N)$ . Specifically, they showed for  $SU(N)$  ( $N = \text{even}$ ) chains based on the self-conjugate representation with  $N/2$  rows and  $n_c$  columns that (i) if  $n_c = 1$  [anti-symmetric  $(N/2)$ -tensor representation], the finite-size ground state is unique. Furthermore, assuming

$$\rho_s(\mathbf{r})_{\mu\nu} = \left( \frac{n_c}{2} \right)^2 \frac{J}{N} a_0^{2-D} \delta_{\mu\nu}, \quad \chi_s = \frac{N}{16DJ a_0^D} \quad (86)$$

(with  $a_0$  being the lattice constant).

<sup>k</sup>In contrast to the corresponding expression for the  $O(3)$  non-linear sigma model, an extra factor  $i$  is not necessary here as the integral itself is pure imaginary. In the case of the  $O(3)$  non-linear sigma model, we express the matrix field by a unit vector  $\mathbf{n}$  as  $\Omega = \mathbf{n} \cdot \boldsymbol{\sigma}$  to recover the factor  $i$  in the  $\theta$ -term.

<sup>l</sup>As we are dealing in this chapter with the translationally invariant systems,  $\mathcal{R} = \bar{\mathcal{R}}$ , i.e.,  $m = N/2$ .

the uniqueness of the ground state, they showed that (ii) for *any* translationally invariant choice of representations<sup>m</sup> (i.e., the same representation  $\mathcal{R}$  is assigned for all sites), the  $SU(N)$  chain harbors low-lying excitations of the order of  $1/L$  ( $L$  being the system size) provided that the number of boxes  $n_Y$  in the Young diagram representing  $\mathcal{R}$  is *not* divisible by  $N$ . In other words, except for the cases of  $n_Y = 0 \pmod{N}$  [including the one with  $N/2$  ( $N = \text{even}$ ) rows and two columns which is relevant to our spin chain], this statement excludes the possibility of gapped topological ground states. Remarkably, this is perfectly consistent with the recent group-cohomology classification of the gapped topological phases in 1D [112] (see Sec. 3.3.2 for the detail).

In the context of the  $SU(N)$  ( $N = \text{even}$ ) spin chains based on the representation with  $N/2$  rows and  $n_c$  columns (self-conjugate representation; the model (78) obtained in Sec. 3.2.2 corresponds to  $n_c = 2$ ), this means the existence of gapless low-lying excited states unless  $N \times n_c / (2N) \equiv 0 \pmod{1}$ , i.e.,  $n_c = \text{even}$ . This is consistent with the argument in the previous section since the sigma-model mapping tells us that when  $\Theta_{\text{top}} = n_c \pi \equiv 0 \pmod{2\pi}$  the ground state is unique and gapped.

There is an  $SU(4)$  spin model with exact charge-conjugation (or translation) breaking ground states [113]. According to the Lieb-Schultz-Mattis argument [111], the physical spin  $\square$  ( $n_Y \neq 0 \pmod{4}$ ) at each site implies that the (thermodynamic-limit) ground state is either gapless or (at least two-fold) degenerate. The existence of the two degenerate ground states means that the second possibility realizes here.

All the above statements concern 1D systems. In the  $SU(2)$  cases, the higher-dimensional extension of the Lieb-Schultz-Mattis argument is known [114, 115]. A similar extension for the  $SU(N)$  cases would be intriguing in view of the proposal of exotic spin liquids in two dimensions [116, 117].

Last, we mention a generalization of the Haldane's conjecture for  $SU(2)$  spin chains to  $SU(N)$  proposed in Ref. [89] (see also Ref. [118]). Three different cases (type-I, II, and III) have been introduced there depending on  $N$  and  $n_Y$ . Type I concerns the case when  $N$  and  $n_Y$  have no common divisor and an  $SU(N)_1$  quantum criticality with central charge  $c = N - 1$  is expected. When  $n_Y$  is divisible by  $N$  (type-II), a Haldane-gap phase is expected in general (note that this case is *not* covered by the theorem of Ref. [111]). The last category (type-III) corresponds to the case when  $n_Y$

<sup>m</sup>The proof of the existence of low-lying states works regardless of whether the ground state is unique or not. However, unless the (finite-size) ground state is unique, the proof does not tell anything about the *excited* states.



and  $N$  have a common divisor different from  $N$ . For short-range interactions, an  $SU(N)_1$  quantum critical behavior is expected. In this respect, some DMRG calculations for  $N = 4$  and  $n_Y = 2$ , i.e. type III behavior, have found an  $SU(4)_1$  criticality [89]. As already noticed in Sec. 2.3.4, however, this conjecture is not consistent with the known results that  $SU(N)$  Heisenberg spin chain in self-conjugate antisymmetric representations (i.e., type III case) have a spectral and a ground-state degeneracy.

### 3.3. *Symmetry-protected topological phases*

In this section, we try to characterize the nature of the ground state of the  $SU(N)$  spin chain (78) obtained deep in the Mott-insulating phase. Specifically, we show that the ground state of the model (78) shares essentially the same properties with that of the solvable valence bond solids (VBS) models in Sec. 3.3.3 and that it is in fact in one of the symmetry-protected topological (SPT) phases. The concept of SPT phases is a generalization of topological insulators [119] to a class of interacting states of matter that are characterized by short-range entanglement and are well-defined *only* in the presence of certain symmetries (called protecting symmetries) [34, 36]. Being topological, this class of topological phases defies the traditional characterization with symmetry and the corresponding local order parameters; two phases are distinguished not by the symmetry they possess but by the presence of quantum phase transitions that separate them [36]. One way is to use the *physical* edge states to distinguish between topological phases from trivial ones. However, this approach is not quite satisfactory in the following respects. First, even topologically trivial states may have certain structures around the edges of the system, as, e.g., in the spin-2 Heisenberg chain [120, 121]. Second, in order to see the edge excitations, it is necessary to consider the excitation spectrum, while the topological properties are intrinsic to the ground state itself and should be seen only by examining the ground-state wave function.

Recently, the use of the entanglement spectrum, which is defined as the logarithm of the spectrum of the reduced density matrix, in characterizing topological phases has been suggested in Ref. [122]. This is based on the observation that the entanglement spectrum *resembles* the spectrum of the physical edge excitations. The idea has been successfully applied to various 1D systems [123–129] and enabled us to characterize topological phases and quantum phase transitions among them. In this section, we present a clear evidence from the entanglement spectrum that the ground state of

the SU(4) Heisenberg model (78) is indeed in an SPT phase protected by SU(4) [projective unitary group PSU(4), precisely<sup>n</sup>] symmetry.

### 3.3.1. Haldane phase –the simplest example

To understand the structure of topological phases in the case of SU( $N$ ) symmetry, it is convenient to begin with the simplest prototypical case  $N = 2$ . Since Haldane’s conjecture, we know that the ground-state properties of the spin- $S$  Heisenberg chain are qualitatively different depending on the parity of  $2S$  [108, 109]; when  $2S = \text{even}$ , the ground state is in a featureless non-magnetic phase (*Haldane phase*) with the gapped triplon ( $S = 1$ ) excitations in the bulk, while, for odd  $2S$ , we have a gapless (i.e., algebraic) ground state with spinon ( $S = 1/2$ ) excitations. This conjecture has been later confirmed both by the construction of a rigorous example (see below) [130, 131] and by extensive numerical simulations [132–134]. Soon after, it has been pointed out that the featureless gapped ground state of the integer- $S$  spin chains may have a *hidden* “topological” order characterized by non-local order parameters [135–138] *at least* when  $S$  is an odd integer [139]. However, it was not until the concept of SPT phases was established that the true meaning of “topological order” in the Haldane phase was fully understood [34]. Now it is realized that the gapped phases in integer-spin chains with some protecting symmetry (e.g., time-reversal, reflection) are further categorized into topological phases or trivial ones.

To understand the properties of the Haldane phase of integer-spin antiferromagnets, it is convenient to consider the spin-1 VBS state introduced by Affleck, Kennedy, Lieb, and Tasaki [130, 131]. The basic idea of construction is to first decompose an  $S = 1$  at each site into a pair of  $S = 1/2$ s, then form uniform tiling of dimer singlets (hence ‘valence-bond solid’) among neighboring sites, and fuse the  $S = 1/2$  pairs at the same site back to the original spin-1s (see Fig. 9). One of the most convenient ways of representing the VBS state is the matrix-product-state (MPS) representation [140–142]<sup>o</sup>:

$$\begin{aligned} |S = 1 \text{ VBS}\rangle_{\alpha,\beta} &= \bigotimes_i \mathcal{A}_i \\ &= \sum_{m_i=x,y,z} \{A(m_1) \cdots A(m_i) \cdots A(m_L)\}_{\alpha,\beta} |m_1\rangle \otimes |m_2\rangle \otimes \cdots |m_L\rangle, \end{aligned} \quad (88)$$

<sup>n</sup>The difference between SU( $N$ ) and PSU( $N$ ) may become clear below.

<sup>o</sup>The symbol  $\bigotimes_i$  implies both the matrix multiplication and the tensor product of the local (spin-1) Hilbert spaces.

where  $\{|x\rangle, |y\rangle, |z\rangle\}$  are defined by

$$|x\rangle_i = -\frac{1}{\sqrt{2}}(|+1\rangle_i - |-1\rangle_i) \quad (89a)$$

$$|y\rangle_i = \frac{i}{\sqrt{2}}(|+1\rangle_i + |-1\rangle_i) \quad (89b)$$

$$|z\rangle_i = |0\rangle_i \quad (89c)$$

and the matrices  $\mathcal{A}_i$  and  $A(a)$  ( $a = x, y, z$ ) are given in terms of the Pauli matrices:

$$\begin{aligned} A(a) &= \sigma^a \quad (a = x, y, z) \\ \mathcal{A}_i &= \sum_{a=x,y,z} A(a)|a\rangle_i = \sigma^x|x\rangle_i + \sigma^y|y\rangle_i + \sigma^z|z\rangle_i. \end{aligned} \quad (90)$$

Remarkably, it can be shown [130, 131] that this quantum many-body state (88) is the unique ground state of the following simple spin-1 Hamiltonian<sup>P</sup> (*VBS model*):

$$\mathcal{H}_{\text{VBS}}^{N=2} = \sum_i \left\{ \mathbf{S}_i \cdot \mathbf{S}_{i+1} + \frac{1}{3} (\mathbf{S}_i \cdot \mathbf{S}_{i+1})^2 \right\}. \quad (91)$$

It is easy to see that the VBS state (88) describes a non-magnetic short-range phase with an excitation gap. To see whether the state is topologically non-trivial or not, it is useful to consider how the state (88) transforms under the symmetry operation. Being non-magnetic, *the bulk* does not respond to the symmetry operation but the edges do. As the consequence, the symmetry operation gets *fractionalized* into two pieces; one acts on the left edge and the other on the right. For instance, the ground state of the spin-1 AKLT model (91)  $|S = 1 \text{ VBS}\rangle_{\alpha,\beta}$  hosts two *emergent*  $S = \frac{1}{2}$  spins (i.e.,  $\alpha, \beta = \uparrow, \downarrow$ ) on both edges and hence transforms under the  $SO(3)$  rotation as

$$|S = 1 \text{ VBS}\rangle_{\alpha,\beta} \xrightarrow{SO(3)} \sum_{\alpha',\beta'} U_{\alpha,\alpha'}^\dagger U_{\beta,\beta'} |S = 1 \text{ VBS}\rangle_{\alpha',\beta'}, \quad (92)$$

where  $U$  is the  $S = \frac{1}{2}$  rotation matrix of  $SU(2)$ . Putting it another way,  $U$  serves as the mathematical labeling of the physical edge states. It is important to note that  $U$  appearing in Eq. (92), in general, may be a projective representation of  $SO(3)$  as both  $U^\dagger$  and  $U$  appear in the equation. Since in the VBS state (88)  $U$  belongs to a non-trivial projective representation that is intrinsically different from any irreducible representations of the original

<sup>P</sup>It is unique in a periodic system or in the thermodynamic limit. On a finite open system, the ground state is four-fold degenerate because of the edge modes [131].

SO(3), one sees that  $|S = 1 \text{ VBS}\rangle_{\alpha,\beta}$  is in a non-trivial topological phase with emergent edge states.

On the other hand, one can construct another model state of a spin-1 chain:

$$|S = 1 \text{ VBS-II}\rangle_{\alpha,\beta} = \bigotimes_i \mathcal{B}_i \tag{93}$$

with the following  $3 \times 3$  matrices  $\mathcal{B}_i$ :

$$\begin{aligned} \mathcal{B}_i &= S^x|x\rangle_i + S^y|y\rangle_i + S^z|z\rangle_i \\ S^x &= \begin{pmatrix} 0 & 0 & 0 \\ 0 & 0 & -i \\ 0 & i & 0 \end{pmatrix}, \quad S^y = \begin{pmatrix} 0 & 0 & i \\ 0 & 0 & 0 \\ -i & 0 & 0 \end{pmatrix}, \quad S^z = \begin{pmatrix} 0 & -i & 0 \\ i & 0 & 0 \\ 0 & 0 & 0 \end{pmatrix}. \end{aligned} \tag{94}$$

By construction, it is obvious that the above state also exhibits edge states with spin-1, and one may suspect that it describes a SPT state. Using  $[S^a]_{bc} = -i\epsilon^{abc}$ , one can easily see that the state (93) transforms as before [see Eq. (92)] but with  $U$  now belonging to the spin-1 representation. Since the spin-1 representation is trivial in the sense of projective representation of SO(3), one can eliminate the would-be edge states by continuously deforming the Hamiltonian [124] and this ground state is in a trivial phase. This reasoning may be readily generalized; when  $U$  transforms like a half-odd-integer spin, the phase is topological, while when  $U$  transforms in an integer-spin representation [i.e., linear representation of SO(3)], the system is in a trivial phase.

For later convenience, we rephrase the situation in terms of Young diagrams. The spin- $S$  representation of SU(2) is represented by the following Young diagram made of  $2S$  boxes:

$$\underbrace{\square \square \cdots \square}_{2S \text{ boxes}}. \tag{95}$$

Then, the above result may be summarized as follows; when  $U$  belongs to the representations

$$\square, \square \square \square, \dots, \tag{96}$$

the state represented by the corresponding MPS is topologically non-trivial as we cannot annihilate these “emergent” edge spins by fusing physical integer spins on neighboring sites.

On the other hand, the phase is trivial when

$$\square \square, \square \square \square \square, \dots \tag{97}$$

That is, the number of boxes (mod 2) in the Young diagram for the representation to which  $U$  belongs labels the topological classes protected by  $SO(3)$  and leads to the  $\mathbb{Z}_2$  classification of the  $SO(3)$  SPT phases [143, 144]<sup>a</sup>. As will be seen in Sec. 3.4, the  $N = 2$  models (both  $g$ - $e$  and  $p$ -band) host several different Haldane phases (in the spin, orbital, and charge sectors) in their phase diagrams.

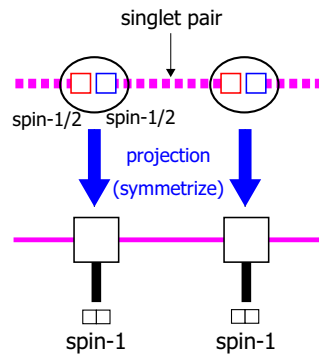


Fig. 9. (Color online) Valence-bond construction of the spin-1 VBS states (88). Two  $S = 1/2$  spins (ancillary qubits) at each site are symmetrized to obtain physical spin-1. If we replace the spin-1/2s with spin-1s and apply the anti-symmetrization at each site, we obtain the state (93).

### 3.3.2. $SU(N)$ topological phases

Using the MPS representation [145] of the gapped ground state in one dimension, the above “physical” idea can be generalized and made mathematically precise. In fact, when a given ground state that is represented by an MPS

$$\sum_{\{m_i\}} A(m_1)A(m_2)\cdots A(m_L)|m_1\rangle\otimes\cdots\otimes|m_L\rangle \quad (98)$$

is invariant under some symmetry  $G$ , a  $D$ -dimensional unitary matrix  $U_g$  ( $g \in G$ ) exists such that [146]

$$A(m_i) \xrightarrow{G} e^{i\phi_g} U_g^\dagger A(m_i) U_g, \quad (99)$$

<sup>a</sup>In the argument presented here, the Haldane phase is protected by the on-site symmetry  $SO(3)$  [not  $SU(2)$ ]. However, it is known that other discrete symmetries, e.g., time-reversal and  $\mathbb{Z}_2 \times \mathbb{Z}_2$  can also protect the Haldane phase [123, 124].

where  $A(m_i)$  denotes the  $D \times D$  MPS matrices corresponding to the local state  $|m_i\rangle$  and  $e^{i\phi_G}$  is a phase that depends on  $G$ . As has been mentioned above, the unitary matrix  $U_g$  is in fact a projective representation of the symmetry  $G$ , that corresponds to the physical edge states [123]. Therefore, the enumeration of topologically stable phases in the presence of symmetry  $G$  boils down to counting the possible (non-trivial) projective representations of  $G$ . [143] This problem was solved for  $SU(N)$  and other Lie groups in Ref. [112] and the picture in the previous section basically generalizes to the case of  $SU(N)$  with some mathematical complications.

Now the role of  $SO(3)$  in the previous section is played by  $PSU(N) \simeq SU(N)/\mathbb{Z}_N$  [note  $SO(3) \simeq PSU(2)$ ]. Considering  $PSU(N)$ , instead of  $SU(N)$ , amounts to restricting ourselves only to the irreducible representations of  $SU(N)$  specified by Young diagrams with the number of boxes  $n_Y$  divisible by  $N$  [i.e.,  $n_Y = Nk$  ( $k = 0, 1, \dots$ )]<sup>r</sup>. This subset of irreducible representations roughly corresponds to the integer-spin ones in the  $SU(2)$  case. In view of the results of the Lieb-Schultz-Mattis argument presented in Sec 3.2.4, considering the symmetry  $PSU(N)$  is quite reasonable for the hunt for gapped topological phases in one dimension, where no genuine topological phase with topologically degenerate ground states exists [36].

As in the previous section, the topological class of a given ground state (typically written as an MPS) is determined by looking at to which projective representation the unitary  $U_g$  of the state belongs. Since inequivalent projective representations of  $PSU(N)$  are labeled by  $n_Y \pmod{N}$  [112], there are  $N - 1$  non-trivial topological classes specified by the  $\mathbb{Z}_N$  label  $n_{\text{top}} = n_Y \pmod{N}$ . In the following, we use the name “class- $n_{\text{top}}$ ” for these topological classes (the class-0 corresponds to trivial phases).

We can think of other protecting symmetries associated with  $SU(N)$  [112]. For instance, when we take  $SU(4)/\mathbb{Z}_2 \simeq SO(6)$ , we consider only the  $SU(4)$  irreducible representations with  $n_Y = 0 \pmod{2}$ , which may be viewed as the linear representations of  $SO(6)$  (containing no spinor representation). In this case, we are led to a  $\mathbb{Z}_2$ -classification.

A remark is in order about the definition of the topological class. In contrast to the  $SU(2)$  case where all the irreducible representations are self-conjugate, we must distinguish between an irreducible representation and its conjugate in  $SU(N)$  (see Fig. 10). The relation (99) suggests that if we have the edge state transforming under the projective representation  $\mathcal{R}$  [of  $PSU(N)$ ] on the right edge, we necessarily have its conjugate  $\bar{\mathcal{R}}$  on the left.

<sup>r</sup>We refer the readers who want to know more about the mathematical details to Sections II and III of Ref. [112]

This means that when we talk about the topological class we must first fix which edge state we use to label the topological phases. Throughout this chapter, we define the topological class by the *right edge state* [i.e., by  $U_g$  acting from the right in Eq. (99)]. We will see, in the next section, that the  $SU(N)$  VBS states to be discussed in Sec. 3.3.3 belongs to class- $N/2$ .

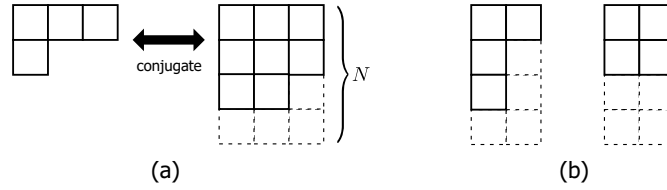


Fig. 10. (a) Young diagrams for an  $SU(N)$  representation and its conjugate for  $N = 4$ . (b) Examples of self-conjugate representations ( $N = 4$ ).

### 3.3.3. VBS construction of the model wave functions

In the previous section, we have seen that there are  $N$  topologically distinct phases in the presence of  $PSU(N) (\simeq SU(N)/\mathbb{Z}_N)$  symmetry [112]. To understand their physical properties, it is convenient to analyze the corresponding ‘fixed-point’ states that are easy to analyze. In the Haldane phase of integer-spin antiferromagnets, the spin-1 VBS state (88) discussed in Sec. 3.3.1 does the job.

A similar strategy applies to  $SU(N)$  ( $N$ : even,  $N \geq 4$ ; see Fig. 11) to construct the  $SU(N)$  generalization of the VBS state. For instance, we use a pair of six-dimensional representations ( $\square$ ) to build the  $SU(4)$  VBS state shown in Fig. 11(a) [93, 147]. At the last stage of the construction, we project the tensor product  $\square \otimes \square$  onto the 20-dimensional representation  $\square$  to obtain the physical Hilbert space. The resulting state may be conveniently expressed in the form of the MPS (98) using  $6 \times 6$  matrices  $A(m)$  [148]. The parent Hamiltonian of this  $SU(4)$  VBS state reads as<sup>s</sup> [93, 147]

$$\mathcal{H}_{\text{VBS}}^{N=4} = \sum_i \left\{ \mathcal{S}_i \cdot \mathcal{S}_{i+1} + \frac{13}{108} (\mathcal{S}_i \cdot \mathcal{S}_{i+1})^2 + \frac{1}{216} (\mathcal{S}_i \cdot \mathcal{S}_{i+1})^3 \right\}, \quad (100)$$

where we have introduced a short-hand notation  $\mathcal{S}_i \cdot \mathcal{S}_{i+1} \equiv \sum_{A=1}^{N^2-1} \mathcal{S}_i^A \mathcal{S}_{i+1}^A$ .

<sup>s</sup>In fact, the parent Hamiltonian contains two free parameters aside from the overall factor. Requiring that  $(\mathcal{S}_i \cdot \mathcal{S}_{i+1})^4$  and  $(\mathcal{S}_i \cdot \mathcal{S}_{i+1})^5$  should not appear, we obtain Eq. (100).

Similarly, from a pair of 20-dimensional representations  $\begin{smallmatrix} \square \\ \square \end{smallmatrix}$  of  $SU(6)$ , we can construct the VBS ground state of the following Hamiltonian [with  $\mathcal{S}_i$  belonging to the 175-dimensional representation  $\begin{smallmatrix} \square & \square \\ \square & \square \end{smallmatrix}$ ; see Fig. 11(b)] [148]<sup>†</sup>

$$\mathcal{H}_{\text{VBS}}^{N=6} = \sum_i \left\{ \mathcal{S}_i \cdot \mathcal{S}_{i+1} + \frac{47}{508} (\mathcal{S}_i \cdot \mathcal{S}_{i+1})^2 + \frac{17}{4572} (\mathcal{S}_i \cdot \mathcal{S}_{i+1})^3 + \frac{1}{18288} (\mathcal{S}_i \cdot \mathcal{S}_{i+1})^4 \right\}. \quad (101)$$

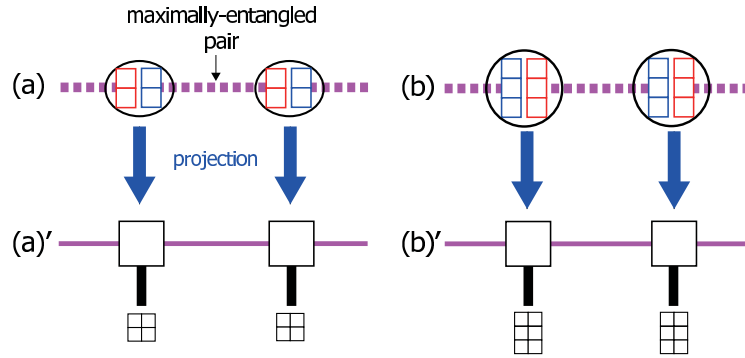


Fig. 11. (Color online) Valence-bond construction of the topological VBS states. (a) and (a)': class-2  $SU(4)$  VBS state. (b) and (b)': class-3  $SU(6)$  VBS state. From Ref. [93].

To be specific, let us restrict ourselves to the case of  $SU(4)$  to summarize the main features of the VBS wave function. Most of the properties are carried over to general  $SU(N)$  ( $N$ : even) with due modifications. The ground state is  $SU(4)$ -symmetric and featureless *in the bulk*, and has the 'spin-spin' correlation functions [93]

$$\langle \mathcal{S}_j^A \mathcal{S}_{j+n}^A \rangle = \begin{cases} \frac{12}{5} \left(-\frac{1}{5}\right)^n & n \neq 0 \\ \frac{4}{5} & n = 0 \end{cases} \quad (102)$$

that are exponentially decaying with a very short correlation length  $1/\ln 5 \approx 0.6213$ . Nevertheless, the system hosts emergent edge states near the boundaries. In fact, if one measures  $\langle \mathcal{S}_i^A \rangle$  (with  $\mathcal{S}_i^A$  being any three

<sup>†</sup>After completing this chapter, we were informed that T. Quella et al. had independently obtained similar results in their unpublished work [149].



commuting generators of  $SU(4)$ , or equivalently, independent linear combinations of local fermion densities  $n_{\alpha,i} = c_{g\alpha,i}^\dagger c_{g\alpha,i} + c_{e\alpha,i}^\dagger c_{e\alpha,i}$ , one can clearly see the structure localized around the two edges (Fig. 12. See also the bottom panel of Fig. 20 for a similar plot for the original fermionic model). At each edge, there are six different states (i.e.,  $\boxplus$ ) distinguished by the value of the set of the three generators  $\langle S_i^A \rangle$ . This implies that  $U_g$  in Eq. (99) transforms like  $\boxplus$ , telling us that the ground state of the VBS Hamiltonian (100) falls into the class-2 topological phase protected by the on-site  $PSU(4)$  symmetry.

Corresponding to the physical edge states, the entanglement spectrum exhibits a particular degeneracy structure. In fact, the entanglement spectrum of the  $SU(4)$  VBS state consists of a *single* six-fold degenerate level, which leads to the von Neumann (bipartite) entanglement entropy  $S_{vN} = \ln 6$ .<sup>u</sup> This extremely simple structure is peculiar to the solvable VBS model (100) and, for a generic  $SU(4)$  Hamiltonian in the same class-2 topological phase, we expect the degeneracy structure compatible with the  $SU(4)$  irreducible representations having  $n_Y = 2$  boxes. Fig. 13 is the plot of the entanglement spectrum of the pure  $SU(4)$  Heisenberg model (79) obtained [148] by infinite time-evolving block decimation (iTEBD) method [150, 151]. One can clearly see that the level structure is totally consistent with the topological class-2. By linearly interpolating between the VBS model (100) and the pure Heisenberg model (79), we can show [148] that the overall structure of the entanglement spectrum is maintained indicating that both models belong to the same unique SPT phase.

Before concluding the discussion of the  $SU(N)$  SPT phases, a few remarks are in order. One is about the other topological phases. The group-cohomology classification tells us that there are two more topological classes in  $PSU(4)$ -invariant systems [112]. In fact, the VBS states studied in Refs. [131, 152–154] correspond to these two. The entanglement spectra calculated for these VBS states agree with those expected from the class-1 and 3 topological phases. Quite recently, the phases of  $SU(3)$ -invariant spin chains, including the  $SU(3)$ -counterpart of the above two phases were investigated in Ref. [155].

Also interesting is the characterization of these topological phases with non-local order parameters. It has been known that the Haldane phase of  $SU(2)$  spin chains is characterized by a pair of non-local order parameters (*string order parameters*) [135, 137–139, 156]. These non-local order

<sup>u</sup>By construction, it is obvious that for general  $N$  (even), the single entanglement level of the VBS state (Fig. 11) is  $N!/[(N/2)!]^2$ -fold degenerate.

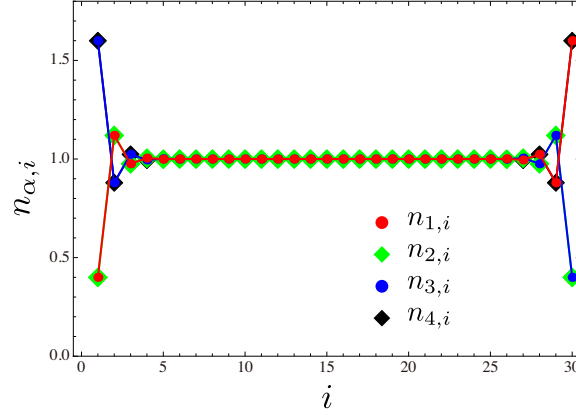


Fig. 12. (Color online) Local fermion density  $n_{\alpha,i} = c_{g\alpha,i}^\dagger c_{g\alpha,i} + c_{e\alpha,i}^\dagger c_{e\alpha,i}$  calculated for one of the 36-fold degenerate SU(4) VBS states on a finite open chain with 30 sites. There are six edge states as two of the four  $n_{\alpha,i}$  take the same value (and so do the other two) around the edge. Note that the local constraint  $\sum_{\alpha=1}^4 n_{\alpha,i} = 4$  is satisfied at each site.

parameters are not only useful as ‘working indicators’ of the topological Haldane phase but also have intimate connection to the modern characterization of the 1D SPT phases in terms of the projective representation  $U_g$  [see Eq. (99)] [157, 158].

This concept can be generalized to other symmetries [159–161]. For instance, a set of  $2(N-1)$  non-local ‘string’ order parameters distinguish between the  $N$  topologically distinct phases predicted by group cohomology [148]. The characterization of the SPT phases by non-local correlation functions seem quite interesting in view of the recent development in real-space imaging techniques [162] as some of the string order parameters are written only in terms of fermion densities which are, in principle, detectable in experiments.

Last, we comment on the relation between the trap potentials and the edge states characteristic of SPT phases. In the usual setting of harmonic potentials, it is known [163, 164] that an island of Mott insulating region (*Mott core*), that is surrounded by a compressible metallic region, is formed around the center of the trap; the above argument for SPT phases holds only within the Mott core. Due to the interaction between the Mott core and the metallic region surrounding it, the structures around the (smeared) edges may be substantially reduced<sup>v</sup> [96, 97]. However, thanks to the recent

<sup>v</sup>Especially in the case of, e.g., the CH phase where the edge states directly couple to

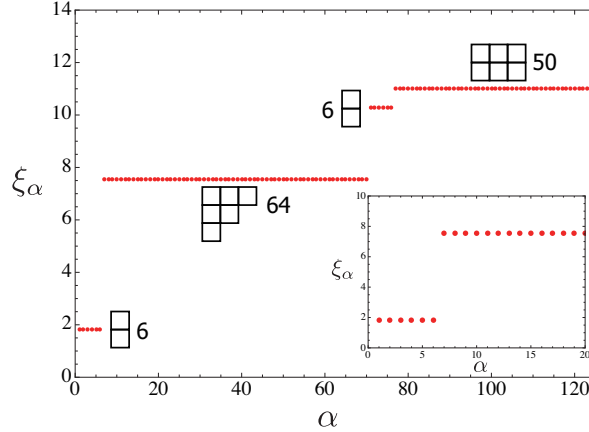


Fig. 13. (Color online) Entanglement spectrum of the  $SU(4)$  Heisenberg model (78). From Ref. [148]

success in creating a box trap [165], one may resolve this problem. Combining the box trap and the technology of single-site detection (see [166] for a recent review), quantum simulation of various SPT phases [including our  $SU(N)$  ones] will become feasible in the near future.

### 3.4. Example of phase diagrams

We will now turn to the presentation of some numerical phase diagrams that were obtained using DMRG simulations on finite chains of length  $L$  with open boundary conditions. Since we focus on particular phases occurring at fixed densities, we do not consider the (harmonic) trapping potential. In real experiments, detection could be achieved using local quantities. Let us emphasize that we will discuss mostly gapped phases, so that they are stable with respect to small perturbations and should be more robust for observation. As to the simulations, let us simply mention that we have only implemented the  $N$   $U(1)$  quantum numbers corresponding to the separate conservation of the fermion numbers of each color, though it should be possible to ease simulations by implementing the full  $SU(N)$  symmetry of the models [167]. We refer to Ref. [93] for more technical details.

For the sake of clarity, in this section, we restrict ourselves to the half-filled cases which already exhibit a rich variety of phases, including topological phases. The inhomogeneity of the potential causes destructive effects.

logical ones. Away from half-filling, one expects on general grounds the occurrence of gapless Luttinger liquid-like phases with density or superconducting (i.e. off-diagonal) correlations or degenerate Mott phases for some other commensurate fillings [168, 169].

For simplicity, when considering the  $g$ - $e$  model (34), we will assume that both orbitals are equivalent, so that they have identical hoppings  $t_g = t_e = t$ , chemical potentials  $\mu_g = \mu_e = \mu$ , and interactions  $U_{gg} = U_{ee} = U_{mm}$ . Therefore, we will consider neither the case with spin-imbalance where spin-polarization effects may dominate [97] and give rise to FFLO physics, nor the strongly anisotropic case where one of the orbitals would be much more localized than the other (e.g.,  $t_e \ll t_g$ ) hence giving rise to  $SU(N)$  Kondo lattice model physics [14, 170–173].

#### 3.4.1. $N = 2$ $g$ - $e$ model

We present in Fig. 14 some phase diagrams of the  $g$ - $e$  model (34) with  $N = 2$  which exhibit a large variety of phases: (i) charge density wave (CDW), (ii) orbital density wave (ODW), (iii) spin-Peierls (SP), (iv) charge Haldane (CH), (v) orbital Haldane (OH), (vi) spin Haldane (SH), and (vii) rung singlet (RS) (see Table 3). The CH phase is the collective Haldane state formed by the charge pseudo-spin-1 states:<sup>w</sup>  $c_{g1}^\dagger c_{g2}^\dagger c_{e1}^\dagger c_{e2}^\dagger |0\rangle$  ( $n = 4$ ),  $c_{g1}^\dagger c_{g2}^\dagger |0\rangle + c_{e1}^\dagger c_{e2}^\dagger |0\rangle$  ( $n = 2$ ), and  $|0\rangle$  ( $n = 0$ ) [see Eq. (69b) for the definition of the charge pseudo-spin]. As it is an insulating state with a charge gap, though not a Mott insulator, it, together with its bosonic counterpart, is also dubbed *Haldane insulator* in literatures [174]. To give a simple picture of these phases, we provide, respectively in Figs. 15 and 16, a cartoon of the two-fold degenerate possible density waves (CDW and ODW) and the non-degenerate Mott phases (SH, CH, and RS) that we have found.

These very rich phase diagrams are in rather good agreement with the low-energy predictions, and they were already discussed in Refs. [93, 95]. In Fig. 14, one notices that the phases concerning the charge sector (CDW and CH) and those concerning the orbital sector (ODW and OH) appear in a very symmetric manner. In fact, this is quite natural since the  $N = 2$   $g$ - $e$  model possesses the following symmetry [93]:

$$\begin{aligned} V &\rightarrow -V + V_{\text{ex}}^{g-e} \\ V_{\text{ex}}^{g-e} &\rightarrow V_{\text{ex}}^{g-e}, \quad U_{mm} \rightarrow U_{mm}, \end{aligned} \quad (103)$$

<sup>w</sup>Related ‘charge’-Haldane states have been found in the study of similar multi-component fermions [41, 47, 97].

Phases of One-dimensional  $SU(N)$  cold atomic Fermi gases

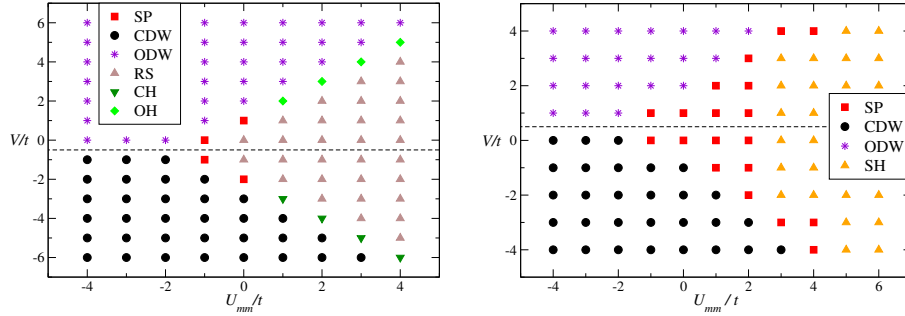


Fig. 14. (Color online) Phase diagram of the  $g$ - $e$  model with  $N = 2$  at half-filling. Left and right panels correspond respectively to  $V_{\text{ex}}^{g-e}/t = -1$  and  $V_{\text{ex}}^{g-e}/t = 1$ , which allows to realize various phases: spin-Peierls (SP), charge/orbital density waves (CDW/ODW), rung singlet (RS), charge-Haldane (CH), orbital-Haldane (OH) and spin-Haldane (SH).

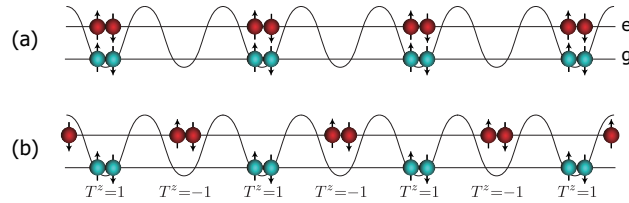


Fig. 15. (Color online) Two density-wave states for  $N = 2$ . In-phase and out-of-phase combinations of two density waves in  $g$  and  $e$  orbitals respectively form (a) CDW and (b) ODW. Adapted from Ref. [93].

that swaps a phase related to charge and the corresponding orbital phase.

3.4.2.  $N = 2$   $p$ -band model

We present here some data for the  $p$ -band model (63) with  $N = 2$  at half-filling. We refer to Ref. [93] for the full phase diagram. We focus here along the line  $U_1 = 3U_2$  which could be realized using the harmonic trapping [precisely, traps that are axially symmetric with respect to the chain direction; see Eq.(60)] and we simply plot some local quantities, that would be most easily measured experimentally using the existing quantum-

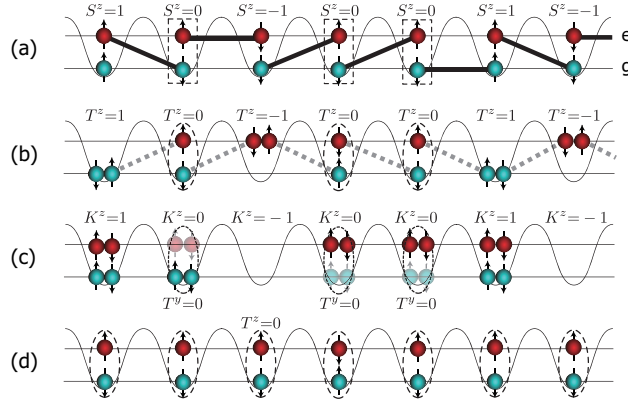


Fig. 16. (Color online) Four translationally invariant Mott states for  $N = 2$ . (a) spin Haldane (SH), (b) orbital Haldane (OH), (c) charge Haldane (CH), and (d) rung-singlet (RS) phases. Singlet bonds formed between spins (orbital pseudo-spins) are shown by thick solid (dashed) lines (singlet bonds are not shown in (c)). Charge pseudo-spin is defined as  $K_i^z = n_i/2 - 1$  and the  $K^z = 0$  state is a linear superposition of  $c_{g\uparrow}^\dagger c_{g\downarrow}^\dagger |0\rangle$  and  $c_{e\uparrow}^\dagger c_{e\downarrow}^\dagger |0\rangle$  (state with  $T^y = 0$ ). Dashed ovals (rectangles) denote spin-singlets (triplets). Adapted from Ref. [93].

optical techniques, namely: local densities and kinetic energy

$$\begin{aligned}
 n_\alpha(i) &= \left\langle \sum_{m=p_x, p_y} c_{m\alpha, i}^\dagger c_{m\alpha, i} \right\rangle \\
 E_{\text{kin}}(i) &= \left\langle \sum_{\alpha=\uparrow, \downarrow} \sum_{m=p_x, p_y} c_{m\alpha, i}^\dagger c_{m\alpha, i+1} + \text{H.c.} \right\rangle.
 \end{aligned} \tag{104}$$

In Fig. 17, one can clearly identify the edge states both for repulsive ( $U_1 = 3U_2 > 0$ ) and attractive ( $U_1 = 3U_2 < 0$ ) interactions. They correspond respectively to spin/charge Haldane phase (see Fig. 16) and are simple manifestations of their topological properties (see the discussion in Sec. 3.3). The existence of the CH phase in fermionic systems was pointed out in Refs. [41, 47] for a related but different system. The CH phase in the  $p$ -band model was first found in Ref. [97].

Let us remind the readers that, for this model, the sign of the interaction can be flipped formally using spin-charge interchange transformation [97] similar to the one used in Sec. 2.3.3 to discuss the attractive ( $U < 0$ ) side of the half-filled single-band  $SU(2)$  Hubbard chain.

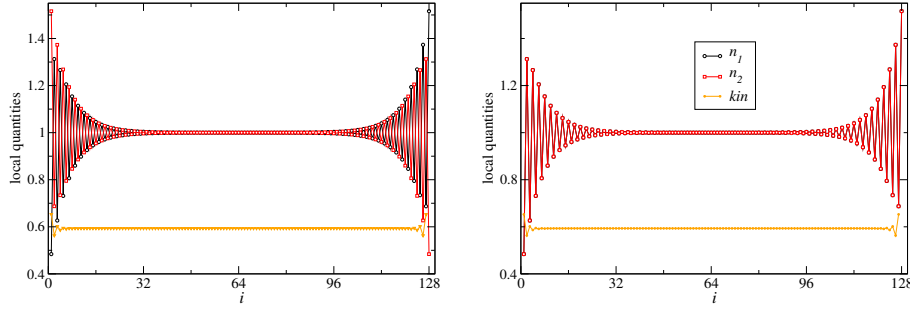


Fig. 17. (Color online) Local quantities (fermion density and kinetic energy) for the  $p$ -band model at half-filling with  $N = 2$  obtained on  $L = 128$  chain using DMRG. Left panel:  $(U_1/t, U_2/t) = (12, 4)$  exhibits spin edge states characteristics of SH phase. Right panel:  $(U_1/t, U_2/t) = (-12, -4)$  exhibits charge edge states characteristics of CH phase.

### 3.4.3. $N = 4$ $g$ - $e$ model

We now turn to the  $N = 4$   $g$ - $e$  model (34) and present some phase diagrams for some fixed values of  $V_{\text{ex}}^{g-e}/t$  in Fig. 18.

In the weak-coupling regime, we only find conventional degenerate phases, namely CDW, ODW and SP, that are in good agreement with the low-energy predictions [93]. However, in the intermediate and strong-coupling regions, one can stabilize the  $SU(4)$  topological phase as has been predicted by the strong-coupling argument (see Secs. 3.2.2 and 3.3.3). Its signatures are again given by the existence of non-trivial edge states [see Fig. 15(a) of Ref. [93], which looks similar to Fig. 20(c)] or could also be probed by computing the degeneracy of the entanglement spectrum [148], see Fig. 13. There is thus a quantum phase transition between (weak-coupling) SP and the  $SU(4)$  topological phase (class-2 SPT phase) in the strong-coupling region. The nature of the universality class of the transition is, however, difficult to determine numerically. In Ref. [147], it was conjectured that the quantum phase transition is governed by an  $SU(4)_2$  CFT with the central charge  $c = 5$ . The high value of the central charge calls for large-scale numerical simulations.

### 3.4.4. $N = 4$ $p$ -band model

When considering the  $N = 4$   $p$ -band model, we restrict ourselves to the case with half-filling and the harmonic trapping scheme that fixes  $U_1 =$

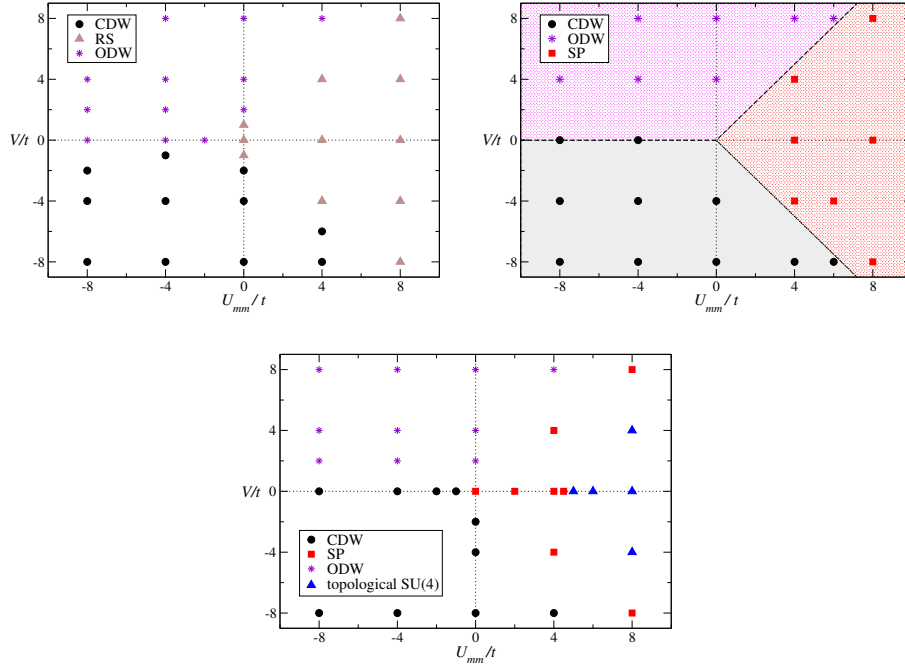


Fig. 18. (Color online) Phase diagram of the  $g$ - $e$  model with  $N = 4$  at half-filling. From top-left to bottom, we have fixed  $V_{ex}^{g-e}/t = -1, 0$  and  $1$ , which allows to realize conventional phases (SP, CDW and ODW) as well as the topological SU(4) one. The symmetry with respect to  $V = 0$  in the second plot is a direct consequence of the orbital-charge interchange that maps CDW into ODW.

$3U_2$ . The full phase diagram can be found in [93] and here we only plot relevant local quantities (local fermion densities and kinetic-energy density) in Fig. 20. Definitions are similar to Eq. (104) with the only difference that  $\alpha = 1, \dots, 4$  for  $N = 4$ . At weak-coupling, Figs. 20(a,b) indicate the existence of CDW phase for attractive interactions ( $U_1 < 0$ ) and SP in the repulsive ( $U_1 > 0$ ) case, as predicted using the low-energy field theories [93]. For strong repulsive interactions, Fig. 20(c) shows a different behavior since non-trivial edge states appear, and they are in agreement with the proposed topological SU(4) phase (see Fig. 12). Indeed, each edge state is 6-fold degenerate as it results from choosing 2 colors among 4, and this degeneracy can be directly seen in the entanglement spectrum (data not shown). As in the  $N = 4$   $g$ - $e$  model, we expect a quantum phase transition in the  $SU(4)_2$  universality class between SP and SU(4) topological phases.



Phases of One-dimensional  $SU(N)$  cold atomic Fermi gases

57

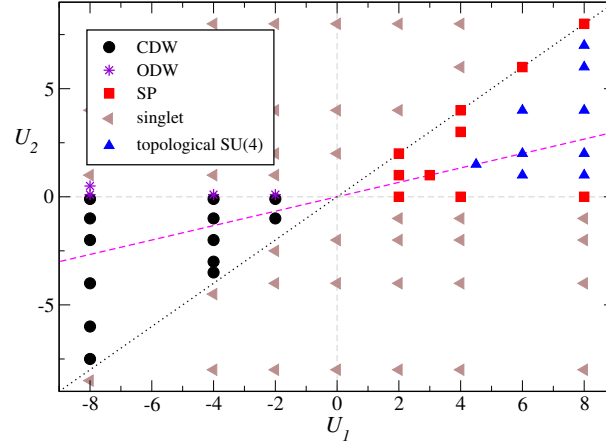


Fig. 19. (Color online) Phase diagram for half-filled  $N = 4$   $p$ -band model (63) obtained by DMRG on  $L = 32$ . Dashed line corresponds to the condition  $U_1 = 3U_2$  satisfied for an axially symmetric trap.  $U_2 = 0$  correspond to two decoupled  $SU(4)$  Hubbard. Adapted from Ref. [93].

Table 3. List of dominant phases and their abbreviations. Local  $SU(N)$ /orbital degrees of freedom are shown, too. (see also Fig. 16)

phases	abbreviation	$SU(N)$	orbital ( $T$ )
spin-Haldane <sup>a</sup>	SH	$S = 1$	local singlet
orbital-Haldane	OH	local singlet	$N/2$
charge-Haldane <sup>a</sup>	CH	local singlet	—
orbital large- $D_{x,y}$	OLD $_{x,y}$	local singlet	$N/2$
rung-singlet (OLD $_z$ ) <sup>b</sup>	RS	local singlet	$N/2$
spin-Peierls	SP	—	$N/2$
charge-density wave	CDW	local singlet	local singlet
orbital-density wave <sup>c</sup>	ODW	local singlet	$N/2$

<sup>a</sup>Only in  $N = 2$ .

<sup>b</sup>Product of  $T^z = 0$  states (large- $D$  state) of  $T = N/2$ .

<sup>c</sup>‘Néel-ordered’ state of orbital pseudo-spin  $T = N/2$ .

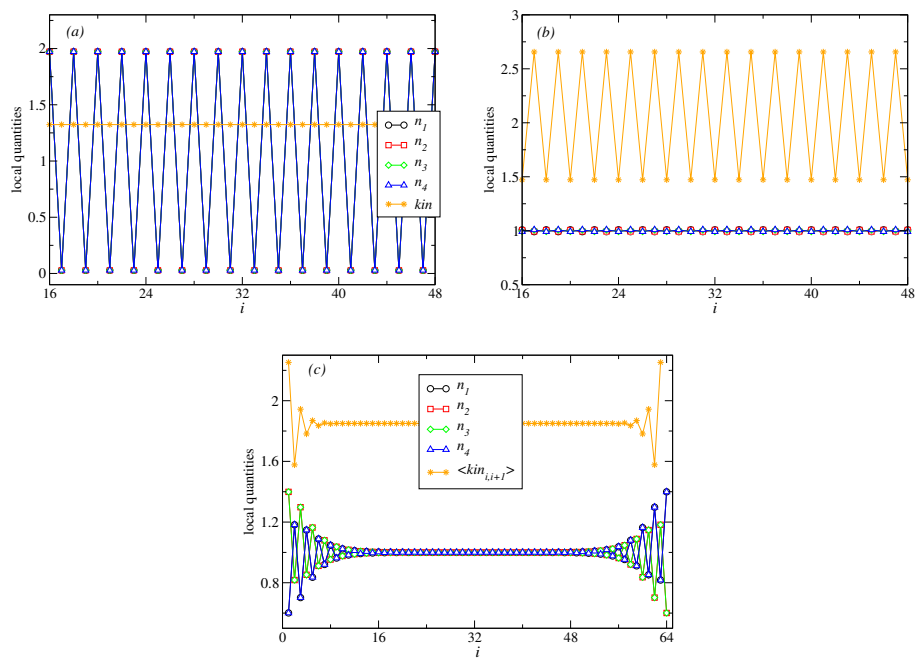


Fig. 20. (Color online) Local quantities for the  $p$ -band model at half-filling with  $N = 4$  obtained on  $L = 64$  chain using DMRG. The three panels correspond to several points relevant for harmonic trapping: (a)  $(U_1/t, U_2/t) = (-3, -1)$  corresponding to a CDW phase; (b)  $(U_1/t, U_2/t) = (3, 1)$  exhibits strong dimerization, as expected for a SP phase; (c)  $(U_1/t, U_2/t) = (9, 3)$  shows non-trivial edge states characteristics of the topological  $SU(4)$  phase. Note that in the first two panels, we only plot data in the bulk of the chain for readability.

#### 4. Concluding remarks

Alkaline-earth and ytterbium cold atomic gases allow the realization of fermionic cold gases with  $SU(N)$  symmetric interactions in a very controlled way. On top of almost perfect  $SU(N)$  symmetry, one has the advantage of being able to use two orbital levels so that we can play with spin-orbital coherent exchange interactions, as demonstrated experimentally [23–25]. Both ingredients are expected to lead to a variety of states of matter and phenomena depending on the microscopic parameters, the dimensionality and so on [14]. In such a context, our review has focused on the one-dimensional case, where powerful analytical and numerical techniques are available. Moreover, when discussing the two-orbital models, we have assumed that both orbitals play a symmetric role, i.e., atoms have identical hoppings and chemical potentials, as can be achieved experimentally using, for instance, the  $p$ -band levels discussed in Sec. 3.1.2. Therefore, we have not touched upon, e.g., the fascinating physical properties of the Kondo lattice models in the context of ultracold alkaline-earth atoms [171–173].

Our review has covered, in depth, the case of single-band  $SU(N)$  Fermi-Hubbard model which ultracold alkaline-earth fermions loaded into a one-dimensional optical lattice can simulate up to  $N$  as large as 10. The physics of the single-band Fermi-Hubbard model with a single contact interaction  $U$  is very rich for general fillings and turns out to be very different between  $N = 2$  and  $N \geq 3$ . One fascinating aspect of the model is the possible occurrence of the (finite- $U$ ) Mott transition for commensurate fillings when  $N > 2$  in sharp contrast to the  $N = 2$  where the critical value is  $U_c = 0$  and additional nearest-neighbor interactions are necessary to have a finite  $U_c$ . For one atom per site, a filling at which we have least three-body losses, the Mott-insulating phase is described by the integrable Sutherland model with  $N - 1$  gapless relativistic modes. For incommensurate fillings and in the low-density regime, a new Luther-Emery liquid with a spin gap and one gapless bosonic (charge) mode emerges in the attractive  $U < 0$  case. The instability toward a paired fermionic superfluid (an analogue of the BCS superconductivity) is completely suppressed in this phase and the dominant superconducting instability occurs in the  $N$ -particle channel, e.g., trionic or quartetting instability when  $N = 3$  and  $N = 4$ . Finally,  $N > 2$  systems support fully gapped Mott-insulating phases for special commensurate fillings; these phases display a bond-ordering with ground-state degeneracies as in a SP phase at half filling.

All these results obtained for the single-band case clearly imply a rich

variety of physics when  $N > 2$  which cannot be realized in the  $SU(2)$  two-component Fermi gas with a contact interaction. However, as already seen, the fully gapped  $SU(N)$  Mott-insulating phases occurring in the single-band model spontaneously break the translation symmetry. In this respect, many interesting SPT fermionic or bosonic phases are beyond the scope of the single-band  $SU(N)$  Fermi-Hubbard model. The realization of these important phases calls for generalization of the model by introducing, for instance, additional degrees of freedom. To this end, we have presented two microscopic models which describe the low-energy physics of the short-range interacting two-orbital  $SU(N)$  cold fermions on a lattice, namely the  $g$ - $e$  model and the  $p$ -band one. Both models can be realized with ultracold alkaline-earth or ytterbium atoms. The zero-temperature phase diagrams of these models are very rich and harbor very different Mott-insulating phases. On the basis of low-energy field-theory approaches as well as rigorous constructions of the ground states in some strong-coupling regime, a variety of phases have been found that are either degenerate (ODW or CDW, SP etc.) or non-degenerate (trivial singlet, various Haldane-like phases, as well as other SPT phases). All these results can be confirmed numerically by mapping out various phase diagrams, as we have presented for even  $N = 2$  and 4 at half-filling for both models.

Let us emphasize that in SPT phases, the edge states are protected (and thus cannot be removed without closing a gap) as long as a given symmetry is present. This is precisely the case, for instance, for the  $SU(N)$ -protected topological phase that we have discussed and corresponds to one microscopic realization among  $N - 1$  possible SPT phases [112]. Therefore, its experimental observation using for instance polarization measurements [175, 176] or spin-selective detection [177] looks like an exciting possibility, although the edge states may be suppressed or even absent if one takes into account a harmonic trap [96, 97]. An interesting framework would be to use a box trapping scheme [165] where presumably edge states should be more visible.

Recently, it has also been proposed that using synthetic gauge field on one-dimensional  $SU(N)$  cold atoms with contact interactions may be related to 2D Chern insulators [178] or quantum Hall phases [179], which also paves the way to realize exotic phases of matter with these systems. In the light of the recent experimental achievements with alkaline-earth cold fermionic gases, we hope that it will be possible in the future to unveil part of the richness that we highlighted in this review.

## Acknowledgements

The authors are very grateful to P. Azaria, V. Bois, A. Bolens, E. Boulat, P. Fromholz, T. Koffel, M. Moliner, H. Nonne, G. Roux, K. Tanimoto, A. M. Tsvelik, and S. R. White for collaborations on this topic over the years. Numerical simulations have been performed using HPC resources from GENCI–TGCC, GENCI–IDRIS (Grant 2015050225) and CALMIP. The authors would like to thank CNRS for financial support (PICS grant). One of the authors (K.T.) was supported in part by JSPS KAKENHI Grant No. 24540402 and No. 15K05211.

## References

- [1] A. J. Keller, S. Amasha, I. Weymann, C. P. Moca, I. G. Rau, J. A. Kantine, H. Shtrikman, G. Zaránd, and D. Goldhaber-Gordon, Emergent  $SU(4)$  Kondo physics in a spin-charge-entangled double quantum dot, *Nat. Phys.* **10**, 145 (2014). doi: 10.1038/nphys2844. URL <http://www.nature.com/nphys/journal/v10/n2/full/nphys2844.html>.
- [2] K. I. Kugel, D. I. Khomskii, A. O. Sboychakov, and S. V. Streltsov, Spin-orbital interaction for face-sharing octahedra: Realization of a highly symmetric  $SU(4)$  model, *Phys. Rev. B* **91**, 155125 (2015). doi: 10.1103/PhysRevB.91.155125. URL <http://link.aps.org/doi/10.1103/PhysRevB.91.155125>.
- [3] F. Wu, I. Sodemann, Y. Araki, A. H. MacDonald, and T. Jolicoeur,  $SO(5)$  symmetry in the quantum Hall effect in graphene, *Phys. Rev. B* **90**, 235432 (2014). doi: 10.1103/PhysRevB.90.235432. URL <http://link.aps.org/doi/10.1103/PhysRevB.90.235432>.
- [4] I. Bloch, J. Dalibard, and W. Zwerger, Many-body physics with ultracold gases, *Rev. Mod. Phys.* **80**(3), 885–80 (July, 2008). URL <http://link.aps.org/abstract/RMP/v80/p885>.
- [5] I. Bloch, J. Dalibard, and S. Nascimbène, Quantum simulations with ultracold quantum gases, *Nat. Phys.* **8**, 267–276 (2012). ISSN 1745-2473. URL <http://dx.doi.org/10.1038/nphys2259>.
- [6] M. Lewenstein, A. Sanpera, and V. Ahufinger, *Ultracold Atoms in Optical Lattices: Simulating quantum many-body systems* (2012).
- [7] C. Wu, J.-P. Hu, and S.-C. Zhang, Exact  $SO(5)$  symmetry in the spin-3/2 fermionic system, *Phys. Rev. Lett.* **91**, 186402 (2003). doi: 10.1103/PhysRevLett.91.186402. URL <http://link.aps.org/doi/10.1103/PhysRevLett.91.186402>.
- [8] C. Honerkamp and W. Hofstetter, Ultracold fermions and the  $SU(N)$  Hubbard models, *Phys. Rev. Lett.* **92**, 170403 (2004). doi: 10.1103/PhysRevLett.92.170403. URL <http://link.aps.org/doi/10.1103/PhysRevLett.92.170403>.
- [9] P. Lecheminant, E. Boulat, and P. Azaria, Confinement and superfluidity

- in one-dimensional degenerate fermionic cold atoms, *Phys. Rev. Lett.* **95**, 240402 (2005). doi: 10.1103/PhysRevLett.95.240402. URL <http://link.aps.org/doi/10.1103/PhysRevLett.95.240402>.
- [10] C. Wu, Hidden symmetry and quantum phases in spin-3/2 cold atomic systems, *Mod. Phys. Lett. B.* **20**, 1707 (2006). doi: 10.1142/S0217984906012213. URL <http://www.worldscientific.com/doi/abs/10.1142/S0217984906012213>.
- [11] A. Rapp, G. Zaránd, C. Honerkamp, and W. Hofstetter, Color superfluidity and “Baryon” formation in ultracold fermions, *Phys. Rev. Lett.* **98**, 160405 (2007). doi: 10.1103/PhysRevLett.98.160405. URL <http://link.aps.org/doi/10.1103/PhysRevLett.98.160405>.
- [12] P. Azaria, S. Capponi, and P. Lecheminant, Three-component fermi gas in a one-dimensional optical lattice, *Phys. Rev. A.* **80**, 041604 (R) (2009). doi: 10.1103/PhysRevA.80.041604. URL <http://link.aps.org/doi/10.1103/PhysRevA.80.041604>.
- [13] M. A. Cazalilla, A. F. Ho, and M. Ueda, Ultracold gases of ytterbium: ferromagnetism and Mott states in an SU(6) Fermi system, *New J. Phys.* **11**, 103033 (2009). URL <http://stacks.iop.org/1367-2630/11/i=10/a=103033>.
- [14] A. V. Gorshkov, M. Hermele, V. Gurarie, C. Xu, P. S. Julienne, J. Ye, P. Zoller, E. Demler, M. D. Lukin, and A. M. Rey, Two-orbital SU( $N$ ) magnetism with ultracold alkaline-earth atoms, *Nat. Phys.* **6**, 289–295 (2010). ISSN 1745-2473. URL <http://dx.doi.org/10.1038/nphys1535>.
- [15] M. A. Cazalilla and A. M. Rey, Ultracold fermi gases with emergent SU( $N$ ) symmetry, *Rep. Prog. Phys.* **77**, 124401 (2014). URL <http://arxiv.org/abs/1403.2792>.
- [16] B. J. DeSalvo, M. Yan, P. G. Mickelson, Y. N. Martinez de Escobar, and T. C. Killian, Degenerate fermi gas of  $^{87}\text{Sr}$ , *Phys. Rev. Lett.* **105**, 030402– (2010). URL <http://link.aps.org/doi/10.1103/PhysRevLett.105.030402>.
- [17] M. K. Tey, S. Stellmer, R. Grimm, and F. Schreck, Double-degenerate Bose-Fermi mixture of strontium, *Phys. Rev. A.* **82**, 011608(R) (2010). doi: 10.1103/PhysRevA.82.011608. URL <http://link.aps.org/doi/10.1103/PhysRevA.82.011608>.
- [18] S. Stellmer, F. Schreck, and T. C. Killian. Degenerate quantum gases of strontium. In *Annual Review of Cold Atoms and Molecules*, vol. 2, pp. 1–80. World Scientific (2014). doi: 10.1142/9789814590174\_0001. URL [http://dx.doi.org/10.1142/9789814590174\\_0001](http://dx.doi.org/10.1142/9789814590174_0001). arXiv:1307.0601.
- [19] T. Fukuhara, Y. Takasu, M. Kumakura, and Y. Takahashi, Degenerate Fermi Gases of Ytterbium, *Phys. Rev. Lett.* **98**, 030401 (2007). doi: 10.1103/PhysRevLett.98.030401. URL <http://link.aps.org/abstract/PRL/v98/e030401>.
- [20] S. Taie, Y. Takasu, S. Sugawa, R. Yamazaki, T. Tsujimoto, R. Murakami, and Y. Takahashi, Realization of a SU(2)×SU(6) system of fermions in a cold atomic gas, *Phys. Rev. Lett.* **105**, 190401– (2010). URL <http://link.aps.org/doi/10.1103/PhysRevLett.105.190401>.

- [21] S. Sugawa, Y. Takasu, K. Enomoto, and Y. Takahashi, *Ultracold ytterbium: Generation, many-body physics, and molecules*, In *Annual Review of Cold Atoms and Molecules*, chapter 1, pp. 3–51. World Scientific (2013). doi: 10.1142/9789814440400\_0001. URL [http://www.worldscientific.com/doi/abs/10.1142/9789814440400\\_0001](http://www.worldscientific.com/doi/abs/10.1142/9789814440400_0001).
- [22] S. Taie, R. Yamazaki, S. Sugawa, and Y. Takahashi, An  $SU(6)$  Mott insulator of an atomic Fermi gas realized by large-spin Pomeranchuk cooling, *Nat. Phys.* **8**, 825–830 (2012). ISSN 1745-2473.
- [23] X. Zhang, M. Bishof, S. L. Bromley, C. V. Kraus, M. S. Safronova, P. Zoller, A. M. Rey, and J. Ye, Spectroscopic observation of  $SU(N)$ -symmetric interactions in Sr orbital magnetism, *Science*. **345**(6203), 1467–1473 (Sept., 2014). URL <http://www.sciencemag.org/content/345/6203/1467.abstract?sid=78634a45-297e-4208-85e8-3f16fcde3b34>.
- [24] F. Scazza, C. Hofrichter, M. Hofer, P. C. De Groot, I. Bloch, and S. Folling, Observation of two-orbital spin-exchange interactions with ultracold  $SU(N)$ -symmetric fermions, *Nat. Phys.* **10**, 779–784 (2014). ISSN 1745-2473. URL <http://dx.doi.org/10.1038/nphys3061>.
- [25] G. Cappellini, M. Mancini, G. Pagano, P. Lombardi, L. Livi, M. Siciliani de Cumis, P. Cancio, M. Pizzocaro, D. Calonico, F. Levi, C. Sias, J. Catani, M. Inguscio, and L. Fallani, Direct observation of coherent interorbital spin-exchange dynamics, *Phys. Rev. Lett.* **113**, 120402 (2014). doi: 10.1103/PhysRevLett.113.120402. URL <http://link.aps.org/doi/10.1103/PhysRevLett.113.120402>.
- [26] G. Pagano, M. Mancini, G. Cappellini, P. Lombardi, F. Schafer, H. Hu, X.-J. Liu, J. Catani, C. Sias, M. Inguscio, and L. Fallani, A one-dimensional liquid of fermions with tunable spin, *Nat. Phys.* **10**, 198–201 (2014). ISSN 1745-2473. URL <http://dx.doi.org/10.1038/nphys2878>.
- [27] B. Sutherland, Model for a multicomponent quantum system, *Phys. Rev. B.* **12**, 3795 (1975). URL <http://link.aps.org/doi/10.1103/PhysRevB.12.3795>.
- [28] I. Affleck, Exact critical exponents for quantum spin chains, non-linear  $\sigma$ -models at  $\theta = \pi$  and the quantum Hall effect, *Nucl. Phys. B.* **265**, 409 (1986). ISSN 0550-3213. doi: [http://dx.doi.org/10.1016/0550-3213\(86\)90167-7](http://dx.doi.org/10.1016/0550-3213(86)90167-7). URL <http://www.sciencedirect.com/science/article/pii/0550321386901677>.
- [29] I. Affleck, Critical behaviour of  $SU(n)$  quantum chains and topological non-linear  $\sigma$ -models, *Nucl. Phys. B.* **305**, 582–596 (1988). URL <http://www.sciencedirect.com/science/article/B6TVC-4718MMW-12C/2/04da87f9aa53d2aaa48342141fc9be83>.
- [30] F. C. Alcaraz and M. J. Martins, Conformal anomaly for the exactly integrable  $SU(N)$  magnets, *Journal of Physics A: Mathematical and General.* **22**(18), L865 (1989). URL <http://stacks.iop.org/0305-4470/22/i=18/a=002>.
- [31] L. Bonnes, K. R. A. Hazzard, S. R. Manmana, A. M. Rey, and S. Wessel, Adiabatic loading of one-dimensional  $SU(N)$  alkaline-earth-atom fermions in optical lattices, *Phys. Rev. Lett.* **109**, 205305 (2012).

- doi: 10.1103/PhysRevLett.109.205305. URL <http://link.aps.org/doi/10.1103/PhysRevLett.109.205305>.
- [32] L. Messio and F. Mila, Entropy dependence of correlations in one-dimensional  $SU(N)$  antiferromagnets, *Phys. Rev. Lett.* **109**, 205306 (2012). URL <http://link.aps.org/doi/10.1103/PhysRevLett.109.205306>.
- [33] Z. Cai, H.-h. Hung, L. Wang, D. Zheng, and C. Wu, Pomeranchuk cooling of  $SU(2n)$  ultracold fermions in optical lattices, *Phys. Rev. Lett.* **110**, 220401 (2013). doi: 10.1103/PhysRevLett.110.220401. URL <http://link.aps.org/doi/10.1103/PhysRevLett.110.220401>.
- [34] Z.-C. Gu and X.-G. Wen, Tensor-entanglement-filtering renormalization approach and symmetry-protected topological order, *Phys. Rev. B.* **80**, 155131–23 (2009). URL <http://link.aps.org/abstract/PRB/v80/e155131>.
- [35] X. Chen, Z.-C. Gu, Z.-X. Liu, and X.-G. Wen, Symmetry-protected topological orders in interacting bosonic systems, *Science*. **338**, 1604 (2012). URL <http://www.sciencemag.org/content/338/6114/1604>.
- [36] X. Chen, Z.-C. Gu, and X.-G. Wen, Local unitary transformation, long-range quantum entanglement, wave function renormalization, and topological order, *Phys. Rev. B.* **82**, 155138– (2010). URL <http://link.aps.org/doi/10.1103/PhysRevB.82.155138>.
- [37] A. Gogolin, A. Nersisyan, and A. Tsvelik, *Bosonization and Strongly Correlated Systems*. Cambridge University Press (1998).
- [38] T. Giamarchi, *Quantum Physics in One Dimension*. Clarendon Press (Oxford) (2004).
- [39] T.-L. Ho, Spinor Bose Condensates in Optical Traps, *Phys. Rev. Lett.* **81** (4), 742–745 (1998). URL <http://link.aps.org/abstract/PRL/v81/p742>.
- [40] T.-L. Ho and S. Yip, Pairing of fermions with arbitrary spin, *Phys. Rev. Lett.* **82**, 247 (1999). doi: 10.1103/PhysRevLett.82.247. URL <http://link.aps.org/doi/10.1103/PhysRevLett.82.247>.
- [41] H. Nonne, P. Lecheminant, S. Capponi, G. Roux, and E. Boulat, Competing orders in one-dimensional half-filled multicomponent fermionic cold atoms: The Haldane-charge conjecture, *Phys. Rev. B.* **84**, 125123 (2011). doi: 10.1103/PhysRevB.84.125123. URL <http://link.aps.org/doi/10.1103/PhysRevB.84.125123>.
- [42] C. Wu, Competing orders in one-dimensional spin-3/2 fermionic systems, *Phys. Rev. Lett.* **95**(26):266404 (2005). doi: 10.1103/PhysRevLett.95.266404. URL <http://link.aps.org/abstract/PRL/v95/e266404>.
- [43] D. Controzzi and A. M. Tsvelik, Excitation spectrum of doped two-leg ladders: A field theory analysis, *Phys. Rev. B.* **72**, 035110 (2005). doi: 10.1103/PhysRevB.72.035110. URL <http://link.aps.org/doi/10.1103/PhysRevB.72.035110>.
- [44] S. Capponi, G. Roux, P. Azaria, E. Boulat, and P. Lecheminant, Confinement versus deconfinement of Cooper pairs in one-dimensional spin-3/2 fermionic cold atoms, *Phys. Rev. B.* **75**, 100503 (2007). doi: 10.1103/PhysRevB.75.100503. URL <http://link.aps.org/doi/10.1103/PhysRevB.75.100503>.



- [45] P. Lecheminant, P. Azaria, and E. Boulat, Competing orders in one-dimensional half-integer fermionic cold atoms: A conformal field theory approach, *Nucl. Phys. B.* **798**, 443 – 469 (2008). ISSN 0550-3213. doi: <http://dx.doi.org/10.1016/j.nuclphysb.2007.12.034>. URL <http://www.sciencedirect.com/science/article/pii/S0550321308000382>.
- [46] G. Roux, S. Capponi, P. Lecheminant, and P. Azaria, Spin 3/2 fermions with attractive interactions in a one-dimensional optical lattice: phase diagrams, entanglement entropy, and the effect of the trap, *Eur. Phys. J. B.* **68**, 293 (2009). doi: 10.1140/epjb/e2008-00374-7.
- [47] H. Nonne, P. Lecheminant, S. Capponi, G. Roux, and E. Boulat, Haldane charge conjecture in one-dimensional multicomponent fermionic cold atoms, *Phys. Rev. B.* **81**, 020408 (2010). URL <http://link.aps.org/doi/10.1103/PhysRevB.81.020408>.
- [48] K. Rodríguez, A. Argüelles, M. Colomé-Tatché, T. Vekua, and L. Santos, Mott-insulator phases of spin-3/2 fermions in the presence of quadratic Zeeman coupling, *Phys. Rev. Lett.* **105**, 050402 (2010). doi: 10.1103/PhysRevLett.105.050402. URL <http://link.aps.org/doi/10.1103/PhysRevLett.105.050402>.
- [49] G. Barcza, E. Szirmai, Ö. Legeza, and J. Sólyom, Emergence of mixed quintet superfluidity in the chain of partially polarized spin-3/2 ultracold atoms, *Phys. Rev. A.* **86**, 061602 (2012). doi: 10.1103/PhysRevA.86.061602. URL <http://link.aps.org/doi/10.1103/PhysRevA.86.061602>.
- [50] E. Szirmai and H. Nonne, Competing valence-bond states of spin- $\frac{3}{2}$  fermions on a strongly coupled ladder, *Phys. Rev. B.* **90**, 245135 (2014). doi: 10.1103/PhysRevB.90.245135. URL <http://link.aps.org/doi/10.1103/PhysRevB.90.245135>.
- [51] G. Barcza, E. Szirmai, J. Sólyom, and Ö. Legeza, Phase separation of superfluids in the chain of four-component ultracold atoms, *Eur. Phys. J. Special Topics.* **224**, 533 (2015). doi: 10.1140/epjst/e2015-02383-1.
- [52] Y. Jiang, X. Guan, J. Cao, and H.-Q. Lin, Exotic pairing in 1D spin-3/2 atomic gases with  $SO(4)$  symmetry, *Nucl. Phys. B.* **895**, 206 (2015).
- [53] A. Auerbach, *Interacting Electrons and Quantum Magnetism*. Springer, Berlin (1994).
- [54] D. Jaksch and P. Zoller, The cold atom Hubbard toolbox, *Ann. Phys.* **315**, 52–79 (2005). URL <http://www.sciencedirect.com/science/article/B6WB1-4F29SKJ-1/2/786ef052020301a290a1c76a16ebd711>.
- [55] E. H. Lieb and F. Y. Wu, Absence of Mott transition in an exact solution of the short-range, one-band model in one dimension, *Phys. Rev. Lett.* **20**, 1445 (1968). doi: 10.1103/PhysRevLett.20.1445. URL <http://link.aps.org/doi/10.1103/PhysRevLett.20.1445>.
- [56] F. H. L. Essler, H. Frahm, F. Gohmann, A. Klümper, and V. E. Korepin, *The One-Dimensional Hubbard Model*. Cambridge University Press, Cambridge, England (2010).
- [57] P. Schlottmann, Exact results for highly correlated electron systems in one dimension, *Int. J. Mod. Phys. B.* **11**, 355 (1997). doi: 10.1142/S0217979297000368.

- [58] X.-W. Guan, M. T. Batchelor, and C. Lee, Fermi gases in one dimension: From Bethe ansatz to experiments, *Rev. Mod. Phys.* **85**, 1633 (2013). doi: 10.1103/RevModPhys.85.1633. URL <http://link.aps.org/doi/10.1103/RevModPhys.85.1633>.
- [59] H. Georgi, *Lie Algebras in Particle Physics*. Perseus Books (1999).
- [60] S. R. Manmana, K. R. A. Hazzard, G. Chen, A. E. Feiguin, and A. M. Rey,  $SU(N)$  magnetism in chains of ultracold alkaline-earth-metal atoms: Mott transitions and quantum correlations, *Phys. Rev. A* **84**, 043601 (2011). doi: 10.1103/PhysRevA.84.043601. URL <http://link.aps.org/doi/10.1103/PhysRevA.84.043601>.
- [61] V. G. Knizhnik and A. B. Zamolodchikov, Current algebra and Wess-Zumino model in two dimensions, *Nucl. Phys. B* **247**, 83 (1984). URL <http://www.sciencedirect.com/science/article/B6TVC-4718WH6-11C/2/78488410cf4d8d21de2be2fb78354edb>.
- [62] E. Witten, Nonabelian bosonization in two dimensions, *Commun. Math. Phys.* **92**, 455 (1984).
- [63] P. Di Francesco, P. Mathieu, and D. Sénéchal, *Conformal Field Theory*. Springer Verlag (1996).
- [64] I. Affleck, Universal term in the free energy at a critical point and the conformal anomaly, *Phys. Rev. Lett.* **56**, 746 (1986). doi: 10.1103/PhysRevLett.56.746. URL <http://link.aps.org/doi/10.1103/PhysRevLett.56.746>.
- [65] H. W. J. Blöte, J. L. Cardy, and M. P. Nightingale, Conformal invariance, the central charge, and universal finite-size amplitudes at criticality, *Phys. Rev. Lett.* **56**, 742 (1986). doi: 10.1103/PhysRevLett.56.742. URL <http://link.aps.org/doi/10.1103/PhysRevLett.56.742>.
- [66] K. Lee, Low-temperature specific heat of the generalized antiferromagnetic  $SU(N)$  Heisenberg model with and without a field, *Physics Letters A* **187**(1), 112 – 118 (1994). ISSN 0375-9601. doi: [http://dx.doi.org/10.1016/0375-9601\(94\)90875-3](http://dx.doi.org/10.1016/0375-9601(94)90875-3). URL <http://www.sciencedirect.com/science/article/pii/0375960194908753>.
- [67] B. Frischmuth, F. Mila, and M. Troyer, Thermodynamics of the one-dimensional  $SU(4)$  symmetric spin-orbital model, *Phys. Rev. Lett.* **82**, 835–838 (1999). doi: 10.1103/PhysRevLett.82.835. URL <http://link.aps.org/doi/10.1103/PhysRevLett.82.835>.
- [68] C. Itoi and M.-H. Kato, Extended massless phase and the Haldane phase in a spin-1 isotropic antiferromagnetic chain, *Phys. Rev. B* **55**, 8295 (1997). doi: 10.1103/PhysRevB.55.8295. URL <http://link.aps.org/doi/10.1103/PhysRevB.55.8295>.
- [69] K. Majumdar and M. Mukherjee, Logarithmic corrections to finite-size spectrum of  $SU(N)$  symmetric quantum chains, *J. Phys. A: Math. Gen.* **35**, L543 (2002). URL <http://iopscience.iop.org/0305-4470/35/38/101/fulltext/>.
- [70] R. Assaraf, P. Azaria, M. Caffarel, and P. Lecheminant, Metal-insulator transition in the one-dimensional  $SU(N)$  Hubbard model, *Phys. Rev. B* **60**, 2299–2318 (1999). doi: 10.1103/PhysRevB.60.2299. URL <http://link.aps.org/doi/10.1103/PhysRevB.60.2299>.

- [//link.aps.org/doi/10.1103/PhysRevB.60.2299](http://link.aps.org/doi/10.1103/PhysRevB.60.2299).
- [71] A. Luther and V. J. Emery, Backward scattering in the one-dimensional electron gas, *Phys. Rev. Lett.* **33**, 589–592 (Sep, 1974). doi: 10.1103/PhysRevLett.33.589. URL <http://link.aps.org/doi/10.1103/PhysRevLett.33.589>.
- [72] S. Capponi, G. Roux, P. Lecheminant, P. Azaria, E. Boulat, and S. R. White, Molecular superfluid phase in systems of one-dimensional multi-component fermionic cold atoms, *Phys. Rev. A* **77**, 013624 (2008). doi: 10.1103/PhysRevA.77.013624. URL <http://link.aps.org/doi/10.1103/PhysRevA.77.013624>.
- [73] E. Szirmai, Ö. Legeza, and J. Sólyom, Spatially nonuniform phases in the one-dimensional  $SU(N)$  Hubbard model for commensurate fillings, *Phys. Rev. B* **77**, 045106– (2008). URL <http://link.aps.org/doi/10.1103/PhysRevB.77.045106>.
- [74] E. Szirmai and J. Sólyom, Mott transition in the one-dimensional  $SU(n)$  Hubbard model, *Phys. Rev. B* **71**, 205108 (2005). URL <http://link.aps.org/abstract/PRB/v71/e205108>.
- [75] K. Buchta, Ö. Legeza, E. Szirmai, and J. Sólyom, Mott transition and dimerization in the one-dimensional  $SU(N)$  Hubbard model, *Phys. Rev. B* **75**, 155108 (2007). doi: 10.1103/PhysRevB.75.155108. URL <http://link.aps.org/doi/10.1103/PhysRevB.75.155108>.
- [76] S. R. White, Density matrix formulation for quantum renormalization groups, *Phys. Rev. Lett.* **69**(19), 2863 (1992). URL <http://link.aps.org/doi/10.1103/PhysRevLett.69.2863>.
- [77] V. Berezinskii, Destruction of long-range order in one-dimensional and two-dimensional systems having a continuous symmetry group. I. classical systems, *Soviet Phys. JETP* **32**, 493 (1971).
- [78] J. M. Kosterlitz and D. J. Thouless, Ordering, metastability and phase transitions in two-dimensional systems, *Journal of Physics C: Solid State Physics* **6**(7), 1181 (1973). URL <http://stacks.iop.org/0022-3719/6/i=7/a=010>.
- [79] H. Shiba, Thermodynamic properties of the one-dimensional half-filled-band Hubbard model. II, *Prog. Theor. Phys.* **48**, 2171 (1972). URL <http://ptp.oxfordjournals.org/content/48/6/2171>.
- [80] V. J. Emery, Theory of the quasi-one-dimensional electron gas with strong "on-site" interactions, *Phys. Rev. B* **14**, 2989–2994 (1976). doi: 10.1103/PhysRevB.14.2989. URL <http://link.aps.org/doi/10.1103/PhysRevB.14.2989>.
- [81] J. Zhao, K. Ueda, and X. Wang, Low-energy excitations of the one-dimensional half-filled  $SU(4)$  Hubbard model with an attractive on-site interaction: Density-matrix renormalization-group calculations and perturbation theory, *Phys. Rev. B* **74**, 233102 (2006). doi: 10.1103/PhysRevB.74.233102. URL <http://link.aps.org/doi/10.1103/PhysRevB.74.233102>.
- [82] J. Zhao, K. Ueda, and X. Wang, Insulating charge density wave for a half-filled  $SU(N)$  Hubbard model with an attractive on-site interaction in one dimension, *J. Phys. Soc. Jpn.* **76**, 114711 (2007). doi: 10.1143/JPSJ.76.

- 114711.
- [83] R. Assaraf, P. Azaria, E. Boulat, M. Caffarel, and P. Lecheminant, Dynamical Symmetry Enlargement versus Spin-Charge Decoupling in the One-Dimensional SU(4) Hubbard Model, *Phys. Rev. Lett.* **93**, 016407 (2004). URL <http://link.aps.org/abstract/PRL/v93/e016407>.
  - [84] J. B. Marston and I. Affleck, Large- $n$  limit of the Hubbard-Heisenberg model, *Phys. Rev. B.* **39**, 11538–11558 (1989). URL <http://link.aps.org/doi/10.1103/PhysRevB.39.11538>.
  - [85] A. V. Onufriev and J. B. Marston, Enlarged symmetry and coherence in arrays of quantum dots, *Phys. Rev. B.* **59**, 12573–12578 (1999). doi: 10.1103/PhysRevB.59.12573. URL <http://link.aps.org/doi/10.1103/PhysRevB.59.12573>.
  - [86] A. Paramekanti and J. B. Marston, SU( $N$ ) quantum spin models: A variational wavefunction, *J. Phys. Cond. Matt.* **19**, 125215 (2007).
  - [87] P. Lecheminant and A. M. Tsvelik, Two-leg SU( $2n$ ) spin ladder: A low-energy effective field theory approach, *Phys. Rev. B.* **91**, 174407 (2015). doi: 10.1103/PhysRevB.91.174407. URL <http://link.aps.org/doi/10.1103/PhysRevB.91.174407>.
  - [88] J. Dufour, P. Nataf, and F. Mila, Variational Monte-Carlo investigation of SU( $N$ ) Heisenberg chains, *Phys. Rev. B.* **91**, 174427 (2015).
  - [89] S. Rachel, R. Thomale, M. Führinger, P. Schmitteckert, and M. Greiter, Spinon confinement and the Haldane gap in SU( $n$ ) spin chains, *Phys. Rev. B.* **80**(18), 180420 (2009). URL <http://link.aps.org/doi/10.1103/PhysRevB.80.180420>.
  - [90] M. Kitagawa, K. Enomoto, K. Kasa, Y. Takahashi, R. Ciuryło, P. Naidon, and P. S. Julienne, Two-color photoassociation spectroscopy of ytterbium atoms and the precise determinations of  $s$ -wave scattering lengths, *Phys. Rev. A.* **77**, 012719 (2008). doi: 10.1103/PhysRevA.77.012719. URL <http://link.aps.org/doi/10.1103/PhysRevA.77.012719>.
  - [91] Y. N. Martinez de Escobar, P. G. Mickelson, P. Pellegrini, S. B. Nagel, A. Traverso, M. Yan, R. Côté, and T. C. Killian, Two-photon photoassociative spectroscopy of ultracold  $^{88}\text{Sr}$ , *Phys. Rev. A.* **78**, 062708 (Dec, 2008). doi: 10.1103/PhysRevA.78.062708. URL <http://link.aps.org/doi/10.1103/PhysRevA.78.062708>.
  - [92] A. Stein, H. Knöckel, and E. Tiemann, The  $^1\text{S}+^1\text{S}$  asymptote of  $\text{Sr}_2$  studied by Fourier-transform spectroscopy, *The European Physical Journal D.* **57**, 171 (2010). ISSN 1434-6060. doi: 10.1140/epjd/e2010-00058-y. URL <http://dx.doi.org/10.1140/epjd/e2010-00058-y>.
  - [93] V. Bois, S. Capponi, P. Lecheminant, M. Moliner, and K. Totsuka, Phase diagrams of one-dimensional half-filled two-orbital SU( $n$ ) cold fermion systems, *Phys. Rev. B.* **91**, 075121 (2015). doi: 10.1103/PhysRevB.91.075121. URL <http://link.aps.org/doi/10.1103/PhysRevB.91.075121>.
  - [94] H. Nonne, E. Boulat, S. Capponi, and P. Lecheminant, Competing orders in the generalized Hund chain model at half filling, *Phys. Rev. B.* **82**, 155134 (2010). URL <http://link.aps.org/doi/10.1103/PhysRevB.82.155134>.
  - [95] H. Nonne, E. Boulat, S. Capponi, and P. Lecheminant, Phase diagram of

- one-dimensional alkaline-earth cold fermionic atoms, *Mod. Phys. Lett. B.* **25**(12n13), 955–962 (2011). doi: 10.1142/S0217984911026668. URL <http://www.worldscientific.com/doi/abs/10.1142/S0217984911026668>.
- [96] K. Kobayashi, M. Okumura, Y. Ota, S. Yamada, and M. Machida, Non-trivial Haldane phase of an atomic two-component fermi gas trapped in a 1d optical lattice, *Phys. Rev. Lett.* **109**, 235302 (2012). URL <http://link.aps.org/doi/10.1103/PhysRevLett.109.235302>.
- [97] K. Kobayashi, Y. Ota, M. Okumura, S. Yamada, and M. Machida, Quantum phases in degenerate  $p$ -orbital attractive one-dimensional fermionic optical lattices, *Phys. Rev. A.* **89**, 023625 (2014). doi: 10.1103/PhysRevA.89.023625. URL <http://link.aps.org/doi/10.1103/PhysRevA.89.023625>.
- [98] C. N. Yang and S. Zhang,  $SO(4)$  symmetry in a Hubbard models, *Modern Physics Letters B.* **04**(11), 759–766 (1990). doi: 10.1142/S0217984990000933. URL <http://www.worldscientific.com/doi/abs/10.1142/S0217984990000933>.
- [99] C. Itzykson and M. Nauenberg, Unitary groups: Representations and decompositions, *Rev. Mod. Phys.* **38**, 95 (1966). URL <http://link.aps.org/doi/10.1103/RevModPhys.38.95>.
- [100] H. J. Schulz, Phase diagrams and correlation exponents for quantum spin chains of arbitrary spin quantum number, *Phys. Rev. B.* **34**, 6372–6385 (1986). URL <http://link.aps.org/doi/10.1103/PhysRevB.34.6372>.
- [101] W. Chen, K. Hida, and B. C. Sanctuary, Ground-state phase diagram of  $S=1$  XXZ chains with uniaxial single-ion-type anisotropy, *Phys. Rev. B.* **67**, 104401 (2003). doi: 10.1103/PhysRevB.67.104401. URL <http://link.aps.org/doi/10.1103/PhysRevB.67.104401>.
- [102] T. Tonegawa, K. Okamoto, H. Nakano, T. Sakai, K. Nomura, and M. Kaburagi, Haldane, large- $D$ , and intermediate- $D$  states in an  $S = 2$  quantum spin chain with on-site and XXZ anisotropies, *J. Phys. Soc. Jpn.* **80**(4), 043001 (2011). doi: 10.1143/JPSJ.80.043001.
- [103] F. D. M. Haldane,  $O(3)$  nonlinear  $\sigma$  model and the topological distinction between integer- and half-integer-spin antiferromagnets in two dimensions, *Phys. Rev. Lett.* **61**(8), 1029–1032 (1988). URL <http://link.aps.org/abstract/PRL/v61/p1029>.
- [104] N. Read and S. Sachdev, Valence-bond and spin-Peierls ground states of low-dimensional quantum antiferromagnets, *Phys. Rev. Lett.* **62**, 1694–1697 (Apr, 1989).
- [105] N. Read and S. Sachdev, Some features of the phase diagram of the square lattice  $SU(N)$  antiferromagnets, *Nucl. Phys. B.* **316**, 609 – 640 (1989). ISSN 0550-3213. doi: 10.1016/0550-3213(89)90061-8. URL <http://www.sciencedirect.com/science/article/pii/0550321389900618>.
- [106] N. Read and S. Sachdev, Spin-Peierls, valence-bond solid, and Néel ground states of low-dimensional quantum antiferromagnets, *Phys. Rev. B.* **42**, 4568–4589 (1990). doi: 10.1103/PhysRevB.42.4568. URL <http://link.aps.org/doi/10.1103/PhysRevB.42.4568>.
- [107] S. Chakravarty, B. I. Halperin, and D. R. Nelson, Two-dimensional quantum Heisenberg antiferromagnet at low temperatures, *Phys. Rev. B.* **39**

- (4), 2344–2371 (Feb., 1989). URL <http://link.aps.org/doi/10.1103/PhysRevB.39.2344>.
- [108] F. D. M. Haldane, Continuum dynamics of the 1-D Heisenberg antiferromagnet: Identification with the  $O(3)$  nonlinear sigma model, *Phys. Lett. A.* **93**, 464 – 468 (1983). ISSN 0375-9601. doi: 10.1016/0375-9601(83)90631-X. URL <http://www.sciencedirect.com/science/article/pii/037596018390631X>.
- [109] F. D. M. Haldane, Nonlinear field theory of large-spin Heisenberg antiferromagnets: Semiclassically quantized solitons of the one-dimensional easy-axis Néel state, *Phys. Rev. Lett.* **50**, 1153–1156 (1983). URL <http://link.aps.org/doi/10.1103/PhysRevLett.50.1153>.
- [110] E. Lieb, T. Schultz, and D. Mattis, Two soluble models of an antiferromagnetic chain, *Annals of Physics.* **16**(3), 407 – 466 (1961). ISSN 0003-4916. doi: DOI:10.1016/0003-4916(61)90115-4. URL <http://www.sciencedirect.com/science/article/B6WB1-4DF520B-1J6/2/9fa7a2285d82e7db7386ac37243f0d77>.
- [111] I. Affleck and E. H. Lieb, A proof of part of Haldane’s conjecture on spin chains, *Lett. Math. Phys.* **12**, 57 (1986). URL <http://dx.doi.org/10.1007/BF00400304>.
- [112] K. Duivendoorn and T. Quella, Topological phases of spin chains, *Phys. Rev. B.* **87**, 125145 (2013). URL <http://link.aps.org/doi/10.1103/PhysRevB.87.125145>.
- [113] I. Affleck, D. Arovas, J. B. Marston, and D. Rabson,  $SU(2n)$  quantum antiferromagnets with exact  $C$ -breaking ground states, *Nucl. Phys. B.* **366**, 467 (1991). doi: 10.1016/0550-3213(91)90027-U. URL <http://www.sciencedirect.com/science/article/pii/055032139190027U>.
- [114] M. B. Hastings, Lieb-Schultz-Mattis in higher dimensions, *Phys. Rev. B.* **69**(10), 104431– (Mar., 2004). URL <http://link.aps.org/abstract/PRB/v69/e104431>.
- [115] B. Nachtergaele and R. Sims, A multi-dimensional Lieb-Schultz-Mattis theorem, *Comm. Math. Phys.* **276**, 437–472 (2007). doi: 10.1007/s00220-007-0342-z. URL <http://www.springerlink.com/content/n52175k8n68015v1/?p=9c9b88090b6b448b8cb43217a355301e&pi=5>.
- [116] M. Hermele, V. Gurarie, and A. M. Rey, Mott insulators of ultracold fermionic alkaline earth atoms: Underconstrained magnetism and chiral spin liquid, *Phys. Rev. Lett.* **103**(13), 135301– (Sept., 2009). URL <http://link.aps.org/doi/10.1103/PhysRevLett.103.135301>.
- [117] M. Hermele and V. Gurarie, Topological liquids and valence cluster states in two-dimensional  $su(n)$  magnets, *Phys. Rev. B.* **84**, 174441 (2011). doi: 10.1103/PhysRevB.84.174441. URL <http://link.aps.org/doi/10.1103/PhysRevB.84.174441>.
- [118] M. Greiter and S. Rachel, Valence bond solids for  $SU(n)$  spin chains: Exact models, spinon confinement, and the Haldane gap, *Phys. Rev. B.* **75**, 184441 (2007). URL <http://link.aps.org/doi/10.1103/PhysRevB.75.184441>.
- [119] M. Z. Hasan and C. L. Kane, Colloquium: Topological insulators, *Rev. Mod. Phys.* **82**(4), 3045– (Nov., 2010). URL <http://link.aps.org/doi/>

- [10.1103/RevModPhys.82.3045](https://doi.org/10.1103/RevModPhys.82.3045).
- [120] Y. Nishiyama, K. Totsuka, N. Hatano, and M. Suzuki, Real-space renormalization-group analysis of the  $s = 2$  antiferromagnetic heisenberg chain, *J. Phys. Soc. Jpn.* **64**, 414 (1995). doi: 10.1143/JPSJ.64.414. URL <http://jpsj.ipap.jp/link?JPSJ/64/414/>.
- [121] S. Qin, T.-K. Ng, and Z.-B. Su, Edge states in open antiferromagnetic heisenberg chains, *Phys. Rev. B.* **52**(17), 12844–12848 (Nov., 1995). URL <http://link.aps.org/doi/10.1103/PhysRevB.52.12844>.
- [122] H. Li and F. D. M. Haldane, Entanglement spectrum as a generalization of entanglement entropy: Identification of topological order in non-Abelian fractional quantum Hall effect states, *Phys. Rev. Lett.* **101**, 010504– (2008). URL <http://link.aps.org/doi/10.1103/PhysRevLett.101.010504>.
- [123] F. Pollmann, A. M. Turner, E. Berg, and M. Oshikawa, Entanglement spectrum of a topological phase in one dimension, *Phys. Rev. B.* **81**, 064439– (2010). URL <http://link.aps.org/doi/10.1103/PhysRevB.81.064439>.
- [124] F. Pollmann, E. Berg, A. M. Turner, and M. Oshikawa, Symmetry protection of topological phases in one-dimensional quantum spin systems, *Phys. Rev. B.* **85**, 075125 (2012). URL <http://link.aps.org/doi/10.1103/PhysRevB.85.075125>.
- [125] L. Fidkowski and A. Kitaev, Topological phases of fermions in one dimension, *Phys. Rev. B.* **83**, 075103– (2011). URL <http://link.aps.org/doi/10.1103/PhysRevB.83.075103>.
- [126] A. M. Turner, F. Pollmann, and E. Berg, Topological phases of one-dimensional fermions: An entanglement point of view, *Phys. Rev. B.* **83**, 075102– (2011). URL <http://link.aps.org/doi/10.1103/PhysRevB.83.075102>.
- [127] D. Zheng, G.-M. Zhang, T. Xiang, and D.-H. Lee, Continuous quantum phase transition between two topologically distinct valence bond solid states associated with the same spin value, *Phys. Rev. B.* **83**, 014409– (2011). URL <http://link.aps.org/doi/10.1103/PhysRevB.83.014409>.
- [128] H.-H. Tu and R. Orús, Intermediate Haldane phase in spin-2 quantum chains with uniaxial anisotropy, *Phys. Rev. B.* **84**(14), 140407 (2011). doi: 10.1103/PhysRevB.84.140407. URL <http://link.aps.org/doi/10.1103/PhysRevB.84.140407>.
- [129] S. Takayoshi, K. Totsuka, and A. Tanaka, Symmetry-protected topological order in magnetization plateau states of quantum spin chains, *Phys. Rev. B.* **91**, 155136 (Apr, 2015). doi: 10.1103/PhysRevB.91.155136. URL <http://link.aps.org/doi/10.1103/PhysRevB.91.155136>.
- [130] I. Affleck, T. Kennedy, E. H. Lieb, and H. Tasaki, Rigorous results on valence-bond ground states in antiferromagnets, *Phys. Rev. Lett.* **59**, 799 (1987). URL <http://link.aps.org/doi/10.1103/PhysRevLett.59.799>.
- [131] I. Affleck, T. Kennedy, E. H. Lieb, and H. Tasaki, Valence bond ground states in isotropic quantum antiferromagnets, *Comm. Math. Phys.* **115**, 477 (1988). ISSN 0010-3616. URL <http://dx.doi.org/10.1007/BF01218021>.
- [132] S. R. White and D. A. Huse, Numerical renormalization-group study of low-lying eigenstates of the antiferromagnetic  $S=1$  Heisenberg chains, *Phys.*

- Rev. B.* **48**(6), 3844–3852 (Aug., 1993). URL <http://link.aps.org/doi/10.1103/PhysRevB.48.3844>.
- [133] U. Schollwöck, O. Golinelli, and T. Jolicœur,  $S=2$  antiferromagnetic quantum spin chains, *Phys. Rev. B.* **54**(6), 4038– (Aug., 1996). URL <http://link.aps.org/doi/10.1103/PhysRevB.54.4038>.
- [134] S. Todo and K. Kato, Cluster algorithms for general- $S$  quantum spin systems, *Phys. Rev. Lett.* **87**, 047203 (Jul, 2001). doi: 10.1103/PhysRevLett.87.047203. URL <http://link.aps.org/doi/10.1103/PhysRevLett.87.047203>.
- [135] M. den Nijs and K. Rommelse, Preroughening transitions in crystal surfaces and valence-bond phases in quantum spin chains, *Phys. Rev. B.* **40**, 4709 (1989). URL <http://link.aps.org/doi/10.1103/PhysRevB.40.4709>.
- [136] S. M. Girvin and D. P. Arovas, Hidden topological order in integer quantum spin chains, *Phys. Scr.* **T 27**, 156 (1989). doi: <http://dx.doi.org/10.1088/0031-8949/1989/T27/027>. URL <http://iopscience.iop.org/1402-4896/1989/T27/027/>.
- [137] T. Kennedy and H. Tasaki, Hidden  $Z_2 \times Z_2$  symmetry breaking in Haldane-gap antiferromagnets, *Phys. Rev. B.* **45**, 304– (1992). URL <http://link.aps.org/doi/10.1103/PhysRevB.45.304>.
- [138] T. Kennedy and H. Tasaki, Hidden symmetry breaking and the Haldane phase in  $S=1$  quantum spin chains, *Comm. Math. Phys.* **147**, 431–484 (1992). ISSN 0010-3616. doi: 10.1007/BF02097239. URL <http://dx.doi.org/10.1007/BF02097239>.
- [139] M. Oshikawa, Hidden  $Z_2 \times Z_2$  symmetry in quantum spin chains with arbitrary integer spin, *J. Phys.: Condensed Matter.* **4**, 7469 (1992). ISSN 0953-8984. doi: 10.1088/0953-8984/4/36/019. URL <http://iopscience.iop.org/0953-8984/4/36/019>.
- [140] F. Verstraete, V. Murg, and J. I. Cirac, Matrix product states, projected entangled pair states, and variational renormalization group methods for quantum spin systems., *Advances in Physics.* **57**(2), 143 – 224 (2008). ISSN 00018732. URL <http://search.ebscohost.com/login.aspx?direct=true&db=a9h&AN=32990557&site=ehost-live>.
- [141] U. Schollwöck, The density-matrix renormalization group in the age of matrix product states, *Annals of Physics.* **326**(1), 96 (2011). ISSN 0003-4916. doi: 10.1016/j.aop.2010.09.012. URL <http://www.sciencedirect.com/science/article/pii/S0003491610001752>.  $\text{\textasciitilde{ce:title}}$ January 2011 Special Issue $\text{\textasciitilde{ce:title}}$ .
- [142] R. Orús, A practical introduction to tensor networks: Matrix product states and projected entangled pair states, *Annals of Physics.* **349**, 117 – 158 (2014). ISSN 0003-4916. doi: <http://dx.doi.org/10.1016/j.aop.2014.06.013>. URL <http://www.sciencedirect.com/science/article/pii/S0003491614001596>.
- [143] X. Chen, Z.-C. Gu, and X.-G. Wen, Classification of gapped symmetric phases in one-dimensional spin systems, *Phys. Rev. B.* **83**, 035107– (2011). URL <http://link.aps.org/doi/10.1103/PhysRevB.83.035107>.
- [144] X. Chen, Z.-C. Gu, Z.-X. Liu, and X.-G. Wen, Symmetry protected topo-



- logical orders and the group cohomology of their symmetry group, *Phys. Rev. B.* **87**, 155114 (2013). URL <http://link.aps.org/doi/10.1103/PhysRevB.87.155114>.
- [145] D. Pérez-García, F. Verstraete, M. Wolf, and J. Cirac, Matrix product state representations, *Quantum Inf. Comput.* **7**, 401 (2007). URL <http://arxiv.org/abs/quant-ph/0608197>.
- [146] D. Pérez-García, M. M. Wolf, M. Sanz, F. Verstraete, and J. I. Cirac, String order and symmetries in quantum spin lattices, *Phys. Rev. Lett.* **100**(16), 167202– (2008). URL <http://link.aps.org/doi/10.1103/PhysRevLett.100.167202>.
- [147] H. Nonne, M. Moliner, S. Capponi, P. Lecheminant, and K. Totsuka, Symmetry-protected topological phases of alkaline-earth cold fermionic atoms in one dimension, *Europhys. Lett.* **102**(3), 37008 (2013). doi: <http://dx.doi.org/10.1209/0295-5075/102/37008>. URL <http://stacks.iop.org/0295-5075/102/i=3/a=37008>.
- [148] K. Tanimoto and K. Totsuka. Symmetry-protected topological order in  $SU(N)$  Heisenberg magnets –quantum entanglement and non-local order parameters. URL <http://arxiv.org/abs/1508.07601>. preprint arXiv:1508.07601 .
- [149] T. Quella. private communications .
- [150] G. Vidal, Classical simulation of infinite-size quantum lattice systems in one spatial dimension, *Phys. Rev. Lett.* **98**(7), 070201– (2007). URL <http://link.aps.org/doi/10.1103/PhysRevLett.98.070201>.
- [151] R. Orús and G. Vidal, Infinite time-evolving block decimation algorithm beyond unitary evolution, *Phys. Rev. B.* **78**, 155117– (2008). URL <http://link.aps.org/doi/10.1103/PhysRevB.78.155117>.
- [152] H. Katsura, T. Hirano, and V. E. Korepin, Entanglement in an  $SU(n)$  valence-bond-solid states, *Journal of Physics A: Mathematical and Theoretical.* **41**(13), 135304 (2008). URL <http://stacks.iop.org/1751-8121/41/i=13/a=135304>.
- [153] V. E. Korepin and Y. Xu, Entanglement in valence-bond-solid states, *Int. J. Mod. Phys. B.* **24**, 1361–1440 (2010). doi: 10.1142/S0217979210055676. URL <http://www.worldscientific.com/doi/abs/10.1142/S0217979210055676>.
- [154] R. Orús and H.-H. Tu, Entanglement and  $SU(N)$  symmetry in one-dimensional valence-bond solid states, *Phys. Rev. B.* **83**, 201101 (2011). URL <http://link.aps.org/doi/10.1103/PhysRevB.83.201101>.
- [155] T. Morimoto, H. Ueda, T. Momoi, and A. Furusaki,  $Z_3$  symmetry-protected topological phases in  $SU(3)$  AKLT model, *Phys. Rev. B.* **90**, 235111 (2014). doi: 10.1103/PhysRevB.90.235111.
- [156] K. Totsuka and M. Suzuki, Matrix formalism for the VBS-type models and hidden order, *J. Phys.: Condensed Matter.* **7**, 1639 (1995). URL <http://iopscience.iop.org/0953-8984/7/8/012/>.
- [157] F. Pollmann and A. M. Turner, Detection of symmetry-protected topological phases in one dimension, *Phys. Rev. B.* **86**, 125441– (2012). URL <http://link.aps.org/doi/10.1103/PhysRevB.86.125441>.

- [158] K. Hasebe and K. Totsuka, Quantum entanglement and topological order in hole-doped valence-bond solid states, *Phys. Rev. B.* **87**, 045115 (2013). URL <http://link.aps.org/doi/10.1103/PhysRevB.87.045115>.
- [159] K. Duivenvoorden and T. Quella, Discriminating string order parameter for topological phases of gapped  $SU(N)$  spin chains, *Phys. Rev. B.* **86**, 235142 (2012). URL <http://link.aps.org/doi/10.1103/PhysRevB.86.235142>.
- [160] D. V. Else, S. D. Bartlett, and A. C. Doherty, Hidden symmetry-breaking picture of symmetry-protected topological order, *Phys. Rev. B.* **88**, 085114 (2013). doi: 10.1103/PhysRevB.88.085114. URL <http://link.aps.org/doi/10.1103/PhysRevB.88.085114>.
- [161] K. Duivenvoorden and T. Quella, From symmetry-protected topological order to Landau order, *Phys. Rev. B.* **88**, 125115 (2013). doi: 10.1103/PhysRevB.88.125115. URL <http://link.aps.org/doi/10.1103/PhysRevB.88.125115>.
- [162] M. Endres, M. Cheneau, T. Fukuhara, C. Weitenberg, P. Schauß, C. Gross, L. Mazza, M. C. Bañuls, L. Pollet, I. Bloch, and S. Kuhr, Observation of correlated particle-hole pairs and string order in low-dimensional Mott insulators, *Science.* **334**, 200 (2011). doi: 10.1126/science.1209284. URL <http://www.sciencemag.org/content/334/6053/200.abstract>.
- [163] M. Rigol, A. Muramatsu, G. G. Batrouni, and R. T. Scalettar, Local quantum criticality in confined fermions on optical lattices, *Phys. Rev. Lett.* **91**, 130403 (Sep, 2003). doi: 10.1103/PhysRevLett.91.130403. URL <http://link.aps.org/doi/10.1103/PhysRevLett.91.130403>.
- [164] U. Schneider, L. Hackermöller, S. Will, T. Best, I. Bloch, T. A. Costi, R. W. Helmes, D. Rasch, and A. Rosch, Metallic and insulating phases of repulsively interacting fermions in a 3D optical lattices, *Science.* **322**(5907), 1520–1525 (Dec., 2008). URL <http://www.sciencemag.org/content/322/5907/1520>.
- [165] A. L. Gaunt, T. F. Schmidutz, I. Gotlibovych, R. P. Smith, and Z. Hadzibabic, Bose-Einstein condensation of atoms in a uniform potential, *Phys. Rev. Lett.* **110**, 200406 (2013). doi: 10.1103/PhysRevLett.110.200406. URL <http://link.aps.org/doi/10.1103/PhysRevLett.110.200406>.
- [166] C. Gross and I. Bloch. Microscopy of many-body states in optical lattices. arXiv:1409.8501 (2014).
- [167] A. Weichselbaum, Non-abelian symmetries in tensor networks: A quantum symmetry space approach, *Ann. Phys.* **327**, 2972 (2012).
- [168] E. Szirmai, Two-orbital physics of high-spin fermionic alkaline-earth atoms confined in a one-dimensional chain, *Phys. Rev. B.* **88**, 195432 (2013). doi: 10.1103/PhysRevB.88.195432. URL <http://link.aps.org/doi/10.1103/PhysRevB.88.195432>.
- [169] V. Bois, S. Capponi, P. Lecheminant, and M. Moliner, Competing superconducting instabilities in the one-dimensional  $p$ -band degenerate cold fermionic system, *arXiv:1505.06715* (2015). URL <http://arxiv.org/abs/1505.06715>.
- [170] P. Coleman,  $1/N$  expansion for the Kondo lattice, *Phys. Rev. B.* **28**, 5255 (1983). doi: 10.1103/PhysRevB.28.5255. URL <http://link.aps.org/doi/>

- [10.1103/PhysRevB.28.5255](https://doi.org/10.1103/PhysRevB.28.5255).
- [171] M. Foss-Feig, M. Hermele, and A. M. Rey, Probing the Kondo lattice model with alkaline-earth-metal atoms, *Phys. Rev. A* **81**, 051603 (2010). doi: [10.1103/PhysRevA.81.051603](https://doi.org/10.1103/PhysRevA.81.051603). URL <http://link.aps.org/doi/10.1103/PhysRevA.81.051603>.
- [172] M. Foss-Feig, M. Hermele, V. Gurarie, and A. M. Rey, Heavy fermions in an optical lattice, *Phys. Rev. A* **82**, 053624 (2010). doi: [10.1103/PhysRevA.82.053624](https://doi.org/10.1103/PhysRevA.82.053624). URL <http://link.aps.org/doi/10.1103/PhysRevA.82.053624>.
- [173] L. Isaev and A. M. Rey, Heavy-fermion valence-bond liquids in ultra-cold atoms: Cooperation of Kondo effect and geometric frustration, *arXiv:1505.06271* (2015). URL <http://arxiv.org/abs/1505.06271>.
- [174] E. G. Dalla Torre, E. Berg, and E. Altman, Hidden order in 1D Bose insulators, *Phys. Rev. Lett.* **97**, 260401– (2006). URL <http://link.aps.org/doi/10.1103/PhysRevLett.97.260401>.
- [175] G. Partridge, W. Li, R. I. Kamar, Y.-A. Liao, and R. G. Hulet, Pairing and phase separation in a polarized fermi gas, *Science* **311**, 503 (2006). doi: [10.1126/science.1122876](https://doi.org/10.1126/science.1122876).
- [176] Y.-a. Liao, A. S. C. Rittner, T. Paprotta, W. Li, G. B. Partridge, R. G. Hulet, S. K. Baur, and E. J. Mueller, Spin-imbalance in a one-dimensional Fermi gas, *Nature* **467**, 567 (2010). doi: [10.1038/nature09393](https://doi.org/10.1038/nature09393).
- [177] C. Weitenberg, P. Schauß, T. Fukuhara, M. Cheneau, M. Endres, I. Bloch, and S. Kuhr, Coherent light scattering from a two-dimensional Mott insulator, *Phys. Rev. Lett.* **106**, 215301 (2011). doi: [10.1103/PhysRevLett.106.215301](https://doi.org/10.1103/PhysRevLett.106.215301). URL <http://link.aps.org/doi/10.1103/PhysRevLett.106.215301>.
- [178] N. Goldman, F. Gerbier, and M. Lewenstein, Realizing non-Abelian gauge potentials in optical square lattices: an application to atomic Chern insulators, *J. Phys. B: At. Mol. Opt. Phys.* **46**, 134010 (2013). doi: [10.1088/0953-4075/46/13/134010](https://doi.org/10.1088/0953-4075/46/13/134010).
- [179] S. Barbarino, L. Taddia, D. Rossini, L. Mazza, and R. Fazio, Magnetic crystals and helical liquids in alkaline-earth fermionic gases, *arXiv:1504.00164* (2015).